Mechanisms underlying the adverse impact of mitochondrial dysfunction and its prevention on the ubiquitin/proteasome pathway: relevance to Parkinson disease

by

Hu Wang

A dissertation proposal submitted to the Graduate Faculty in Biology in partial fulfillment of the requirements for the degree of Doctor of Philosophy

The City University of New York
2013

This Manuscript has been read and accepted by the Graduate Faculty in Biology in satisfaction of the dissertation requirement for the degree of Doctor of Philosophy

Date	**Dr. MARIA E. FIGUEIREDO-PEREIRA** (Hunter College, Chair of Examining Committee)
Date	**Dr. LAUREL A. ECKHARDT** Executive Officer
Date	**Dr. THOMAS SCHMIDT-GLENEWINKEL** (Hunter College)
Date	**Dr. MITCHELL GOLDFARB** (Hunter College)
Date	**Dr. YULING CHI** (Albert Einstein College of Medicine)
Date	**Dr. CHRISTOPHER CARDOZO** (Mount Sinai School of Medicine)

Supervisory Committee

THE CITY UNIVERSITY OF NEW YORK

ABSTRACT

Mechanisms underlying the adverse impact of mitochondrial dysfunction and its prevention on the ubiquitin/proteasome pathway: relevance to Parkinson disease

By

Hu Wang

Advisor: Dr. Maria E. Figueiredo-Pereira

Neuroinflammation has long been accepted as a probable factor in Parkinson disease(PD)(3,4). Besides neuroinflammation, mitochondrial impairment (5,6) and ubiquitin/proteasome pathway (UPP) dysfunction (7,8) have also been recognized as important contributors to the pathogenesis of PD.

Parkin, which plays a central role in the link between mitochondria and the UPP, is mutated in both familial and sporadic forms of PD (9). The function of Parkin was first described as an E3 ubiquitin ligase that delivers its substrates to the proteasome to be degraded. However, recent findings discovered another important role for Parkin, which is its

involvement in mitochondrial quality control (10) and mitochondrial dynamics (11).

Since neuroinflammation, mitochondrial impairment, UPP dysfunction and Parkin are all involved in PD pathogenesis, it is of great interest and importance to investigate the interaction among these pathogenic elements. Therefore, the MAJOR AIMS of these studies were to:

(1) Investigate whether Parkin is affected by neuroinflammation, mitochondrial and UPP dysfunction, and assess approaches to protect from these insults.

(2) Determine the mechanisms by which mitochondrial impairment disturbs the UPP.

Rat E18 midbrain and cerebral cortical neuronal cultures were used to carry-out our specific aims.

We used a pharmacological approach to mimic neuroinflammation, as well as mitochondrial and proteasomal dysfunction. The neuronal cultures were treated with:

(1) Prostaglandin J2 (PGJ2), an endogenous product of inflammation, which inhibits mitochondrial complex I and impairs proteasomal function.

(2) Mitochondrial toxins that target the electron transport chain (ETC): a) Oligomycin, which inhibits ATP synthase (complex

V); b) Antimycin, which inhibits complex III; c) Rotenone, which inhibits complex I;

(3) Epoxomicin, a specific and irreversible proteasomal inhibitor.

The results from the first aim reveal that:

(1) Upon mitochondrial dysfunction a new form of Parkin (newParkin) is detected that is generated by calpain cleavage of full length Parkin. To our knowledge, we are the first to report this new form of Parkin.

(2) NewParkin generated upon mitochondrial impairment translocates to mitochondria, and dissociates from the 26S proteasome.

(3) Phosphorylation attenuates Parkin cleavage induced by mitochondrial impairment.

(4) The endogenous product of inflammation PGJ2 and the proteasomal inhibitor epoxomicin, also lead to Parkin cleavage but under these conditions, cleavage is mediated by caspase and not calpain activation.

(5) Increasing intracellular cAMP with the lipophilic peptide PACAP27 mitigates some of the adverse effects of the product of inflammation PGJ2, including caspase activation, caspase-mediated cleavage of Parkin, and loss of neuronal viability.

(6) Partially replenishing intracellular ATP with the nearly planar creatine analog cyclocreatine, diminishes Parkin cleavage triggered by mitochondrial impairment.

The results from the second aim reveal that:

(1) Mitochondrial toxins which deplete intracellular ATP levels, lead to the downregulation of protein ubiquitination, by adversely affecting the first step of the ubiquitination cascade, i.e. E1-mediated ubiquitin activation, which is ATP-dependent.

(2) Mitochondrial toxins downregulate 26S proteasome assembly via selective processing of the Rpn 10 subunit of the 26S proteasome by calpain cleavage. To our knowledge, we are the first to identify this unique calpain substrate.

(3) The 26S proteasome deficit induced by the mitochondrial toxins is accompanied by a rise in 20S proteasome levels.

(4) These events were induced by acute (16h) and long term (up to seven days) mitochondrial impairment.

In summary, our results addressed the complex relationship among neuroinflammation, mitochondrial impairment, proteasomal dysfunction and Parkin, all of which are relevant to Parkinson Disease (PD). We identified the PARKIN-mitochondria-UPP link as

highly vulnerable to stress conditions, revealing a relevant mechanistic pathway to exploit for protecting against the progressive nature of PD. We identified two pharmacological approaches to diminish the adverse effects of an impaired PARKIN-mitochondria-UPP link, by increasing intracellular cAMP as well as ATP levels with PACAP27 and cyclocreatine, respectively. Our findings provide a new basis for the development of novel and more effective therapeutic strategies that prevent/stop neurodegeneration in PD.

ACKNOWLEDGEMENTS

Firstly, I would like to express my deepest gratitude to my mentor, Dr. Maria Figueiredo-Pereira, for her continuous guidance, patience, motivation, enthusiasm and constructive criticism during the whole journey of my Ph.D. study.

Secondly, I am also grateful to my current lab colleagues, Magdalena Kiprowska, Teneka Jean-Louis and previous lab colleagues: Qian Huang, Kai Shivers, Maria Jose Metcalfe, Natura Myeku, Lisette Arnaud for their generous help, technical support and useful suggestions.

I would like to extend my sincere gratitude to my thesis advisory committee members, for their insightful comments and challenging questions.

Special thanks to all my friends and classmates at the City University of New York, who have been spiritually and academically supportive throughout my Ph.D. study.

Last but not the least, I offer my deepest thanks and blessings to my whole family members including my one-year old daughter Cindy Wang, for their endless love and persistent encouragement and support during the entire period of my study.

Hu Wang

Table of Contents

LIST OF FIGURES

Chapter I

Chapter II

Chapter III

LIST OF ABBREVIATIONS

15d-PGJ2: 15-deoxy-$\Delta^{12,14}$-prostaglandin J2

ASN: α-synuclein

ATP: adenosine triphosphate

COX: cyclooxygenase

CNS: central nervous system

CSF: cerebrospinal fluid

DAPI: 4',6-diamidino-2-phenylindole

DMSO: dimethyl sulfoxide

DNA: Deoxyribonucleotide acid

E18: embryonic day 18

FBS: fetal bovine serum

GAD: glutamate decarboxylase

GFP: green fluorescent protein

LPS: lipopolysaccharide

MMP: mitochondrial membrane potential

MTT: (3-(4,5-dimethylthiazol-2-yl)-2,5-diphenyl tetrazolium bromide

MPTP: 1-methyl-4phenyl-1,2,3,6-tetrahydropyridine

NF-κB: nuclear factor kappa-light-chain-enhancer of activated B cells

Nrf2: nuclear factor-erythroid 2-related factor 2

PARP: Poly ADP-ribose polymerase

PBS: phosphate buffer saline

PD: Parkinson Disease

PGJ2: prostaglandin J2

PINK1: phosphatase and tensin homolog (PTEN)--induced putative kinase 1

PKA: protease kinase A

PSI: proteasome inhibitor

PVDF: polyvinylidene difluoride

RNAi: RNA interference

ROS: reactive oxygen species

SDS-PAGE: sodium dodecyl sulfate-polyacrylamide gel electrophoresis

SN: *substantia nigra*

SNpc: *Substantia nigra pars compacta*

TH: tyrosine hydroxylase

Ub: Ubiquitin

UCH-L1: Ubiquitin C-terminal hydrolase-L1

PACAP: Pituitary adenylate cyclase-activating peptide

UPP: ubiquitin/proteasome pathway

CHAPTER I

Introduction

1.1. Parkinson disease and Neuroinflammation

Parkinson disease (PD) was first described by James Parkinson in 1817 in his essay 'An Essay of the Shaking Palsy' (12). Since then, many more cases have been reported. PD is currently the second most common neurodegenerative disorder afflicting 1-2% of the population over 50 (13). Among the most characteristic pathological PD hallmarks are the gradual loss of dopaminergic (DA) neurons in the midbrain *substantia nigra pars compacta* (SNpc) and the presence of DA cytoplasmic inclusion bodies (Lewy bodies). The appearance of Lewy bodies has long been suggested to be involved in the death of DA neurons (14). Traditionally, the etiology of PD focused on *(1)* genetic mutations (familiar cases) in proteins such as α-synuclein, PINK1 and Parkin, and *(2)* non-familiar cases associated with environmental toxins such as rotetone, paraquat, and MPTP (1-methyl-4phenyl-1,2,3,6-tetrahydropyridine). However, more recent studies support the notion that familiar as well as non-familiar cases of PD share an important pathogenic mechanism: chronic neuroinflammation.

Exposing the brain to prolonged neuroinflammation for months,

and even years, will inevitably lead to neuronal damage. Glia and neuronal interactions during inflammation are thus particularly critical to neurodegeneration in PD [reviewed in (15)]. Glia activation involved in the neuroinflammation process could be one of the major contributors to the initiation and or progression of PD (16). At the histological level, the main actors of CNS inflammation are the activated microglia (17), the astrocytes and, to a lesser extent, the neurons themselves (18). Current studies are still assessing the degree of inflammation in the brain of PD patients. CSF markers fail to reflect exactly the situation of the brain, highlighting the difficulty of determining the real degree of inflammation in the PD brain (19-21).

The question persists regarding the role of inflammation in PD: Is it a driving force, a bystander or a beneficial response (22)? If inflammation cannot be ruled as the initiator of the disease, its systematic presence in the pathological areas of the brain and the decreased pathology observed after treatment with anti-inflammatory drugs, links inflammation to the development of the disease. If the acute activation of microglia might be beneficial for the brain after injury, its chronic activation might not. Chronic inflammation may induce the release of toxic inflammatory products suspected to worsened the pathology and prevent the proper removal of waste products, emphasizing the

necessity of a close control of inflammation. Microglia activation into phagocytic glia might be beneficial for the removal of toxic aggregates or dying cells. However, neurotoxic inflammatory factors released by chronically activated glia can fuel the toxic course of events leading to neuronal death.

Cyclooxygenases are key players in inflammation. They mediate the conversion of arachidonic acid into an assortment of prostanoids. Arachidonic acid signaling through the cyclooxygenase pathway yields an enormous variety of products, some of them with pro-survival, while others with pro-death effects. For instance, prostaglandins are known to be pro-inflammatory under certain conditions and anti-inflammatory under others [reviewed in (23)]. The dual role of prostaglandins is quite complex as a single prostaglandin can bind to multiple receptors. For example, two receptors (DP1 and DP2) were identified for PGD2 the most abundant prostaglandin in the CNS. DP1 activation increases cAMP, activates protein kinase A and is linked to an anti-inflammatory response, while DP2 activation decreases cAMP, increases the cellular influx of calcium and triggers a pro-inflammatory response [reviewed in (24)]. PGD2-mediated activation of DP1 was found to be neuroprotective while DP2 activation was neurotoxic (25). Besides binding to different receptors some prostaglandins such as PGD2, are spontaneously metabolized by non-enzymatic dehydration to cyclopentenone

prostaglandins of the J2 series. These cyclopentenone prostaglandins may have an anti-inflammatory effect by inhibiting the NFκB pathway or a neurotoxic effect by inducing apoptosis [reviewed in (26)]. [The prostaglandin D2 conversion scheme on the left is from (27)].

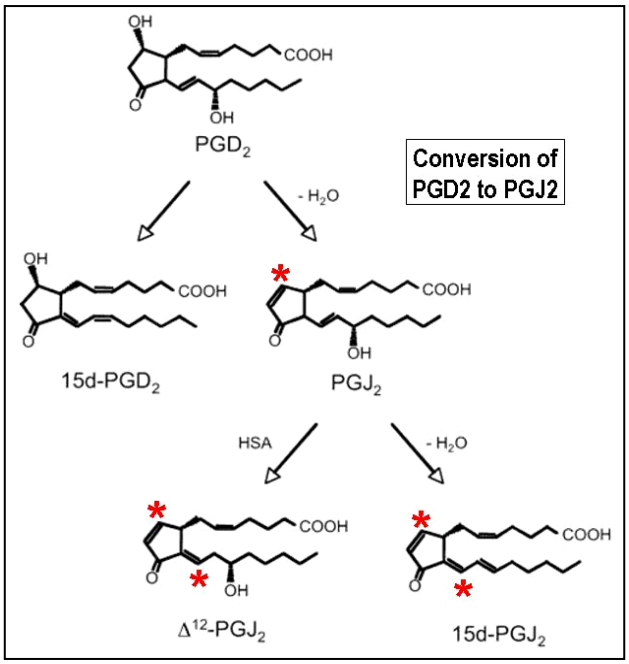

Clearly, the effects of different prostaglandins are variable and may depend on factors such as intracellular concentrations, receptor types, cell types and timing of activation of downstream targets that participate in the inflammatory response. Rather than inhibiting COX, modulating the effects of PG through more specific interference with their selective synthases and/or their receptors may be more effective, as prostaglandins can play different roles in recovery or degeneration. Much more needs to be learned about the functions of inflammation in the normal and diseased CNS. The challenge resides in dissecting the dual nature of neuroinflammation as it has both positive and negative effects differing spatially and temporally in the CNS.

1.2. Why investigate the role of prostaglandin J2 (PGJ2) in PD

Although it is generally accepted that chronic inflammation plays a major role in PD, the mechanistic understanding of how prostaglandins affect and/or participate in the progressive nature of this disease is still unclear. We propose that the endogenous and bioactive product of inflammation PGJ2 is implicated in PD, as the effects of PGJ2 recapitulate molecular, cellular and behavioral pathological processes in PD. There is strong data supporting this role for PGJ2:

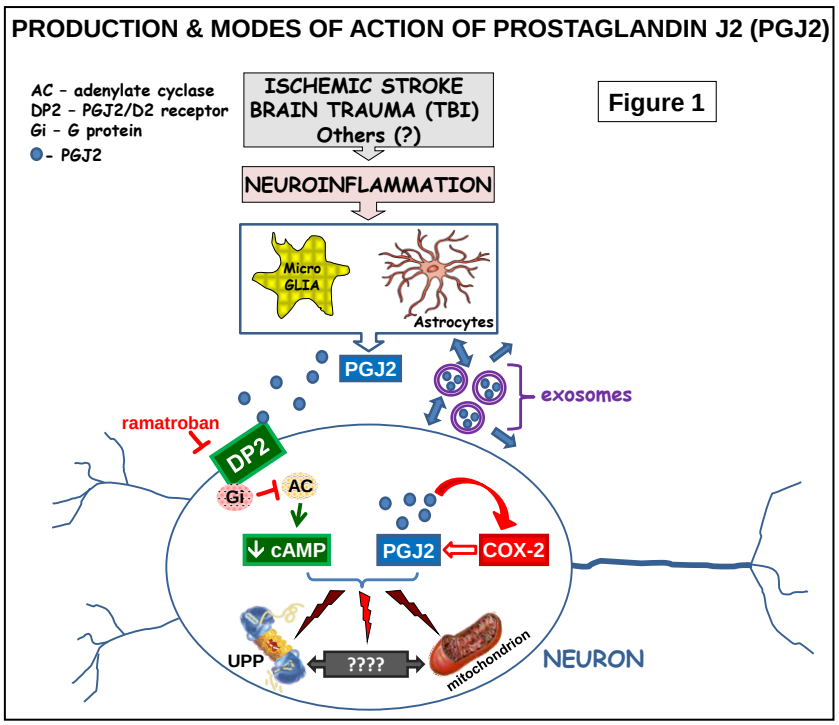

(1) *In vitro.* We and others showed that PGJ2 is highly neurotoxic (28), impairs the ubiquitin/proteasome pathway (UPP) (28-31) and mitochondrial function (32-34) (Fig. 1), potentiates dopamine toxicity (35), and up-regulates COX-2 (36), most likely leading to a positive feedback loop (Fig. 1, red). Moreover, PGJ2 signals via the DP2 receptor for PGD2(37,38) (Fig. 1, green). DP2 is negatively coupled to cAMP and potentiates

neuronal injury (38,39). We established that the DP2 antagonist ramatroban (Fig. 1) mitigates PGJ2 neurotoxicity (*data not shown here*).

(2) *In vivo.* The levels of PGJ2 are highly induced *in vivo* upon stroke (cerebral ischemia) (40,41) and traumatic brain injury (TBI) (42,43), both of which increase the long-term risk for PD (44-48) (Fig. 1, top). Thus, PGJ2 will have a major effect on the development of PD. In fact, we showed that microinfusing *PGJ2 alone* into the *substantia nigra* of mice is sufficient to induce molecular, cellular and behavioral traits similar to PD (49).

One potential mechanism for PGJ2 involves mediating the transition from acute to chronic inflammation via a positive feedback loop, as shown for other prostaglandins (50). Another potential mechanism shown in non-neuronal cells, is that PGJ2 and other prostaglandins can be transferred from cell to cell via exosomes (51) (Fig. 1, violet). These latter data are important, as exosomes are being considered as propagation vehicles for disease progression in PD (52).

These exciting and important studies support the notion that PGJ2 causes neuronal injury critical to PD, and emphasize the need to investigate PGJ2-dependent neurotoxic mechanisms and how to prevent them in order to develop novel and more effective neuroprotective therapeutic strategies for PD neurodegeneration.

1.3. PD and UPP impairment

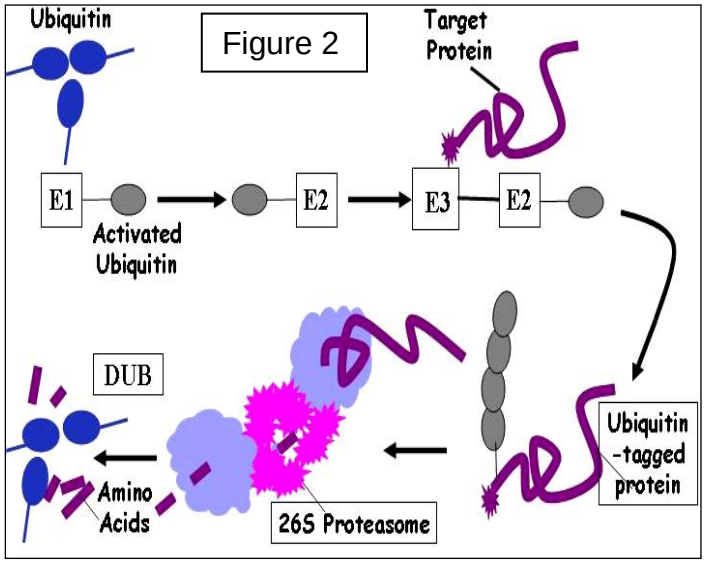

Figure 2. Ubiquitination and degradation of proteins by the ubiquitin/proteasome pathway (UPP). Protein ubiquitination is a complex ATP-dependent process in which ubiquitin (Ub) is sequentially activated by ubiquitin-activating enzymes (E1), transferred to ubiquitin-conjugating enzymes (E2) and ligated to protein substrates by ubiquitin ligases (E3). Most polyubiquitin chains are formed by isopeptide bonds between Gly76 and Lys48 on adjacent ubiquitin molecules. Once a protein is polyubiquitinated, it is degraded rapidly by the 26S proteasome. De-ubiquitinating enzymes (DUB) remove and disassemble polyubiquitin chains.

Protein aggregation as a result of misfolding is implicated in PD. Protein aggregates in PD are known as Lewy bodies and contain among other proteins, α-synuclein and ubiquitinated proteins (53). In order to survive under various stress and mutational conditions that lead to protein misfolding, cells have a repertoire of mechanisms that they can activate or inhibit according to their needs. Neuronal survival demands a dynamic, effective and safe capacity to deal with this abnormal protein burden. The ubiquitin/proteasome pathway (UPP, Figure 2) is the ultimate mechanism that cells use to ensure the selective destruction of misfolded or damaged proteins (54,55).

Besides α-synuclein and ubiquitinated proteins, other proteins such as Parkin and UCH-L1 support a role for UPP in PD. Parkin is an E3 ubiquitin ligase, an enzyme that catalyzes the addition

of ubiquitin to target proteins to be degraded by the proteasome. Parkin mutations account for approximately 50% of early-onset (<45 years) familial cases of PD (56) and are also associated with late-onset (≥60 years) PD cases (57). The gene *uch-l1* encodes for PGP 9.5, a de-ubiquitinating enzyme which is also a susceptible locus in familial PD (58).

Proteasome activity is reduced by approximately 44-55% in the SNpc of PD patients compared to age-matched controls. However, proteasome activity remains unchanged in other brain regions of PD patients such as cortex, striatum and hippocampus (59-62). Besides its activity, proteasome levels are also changed in the SNpc of PD patients: there is a 40% reduction in the content of proteasome α-subunits in PD patients compared to age-matched controls (63). Furthermore, the levels of PA28, a proteasome activator, are significantly decreased in the SNpc compared to frontal cortex and striatum (64). These findings support UPP changes in both familial and sporadic cases of PD thus singling out the UPP as a potential target for drug therapy.

Some PD models were developed based on UPP impairment. McNaught et al (65) reported that rats systemically injected with proteasome inhibitors exhibited PD-like clinical symptoms and pathology. However this model has not been consistently replicated, and remains controversial. Recently, Matsui and colleagues (66) injected lactacystin or epoxomicin into the CSF

of Medaka fish and detected selective DA neuronal loss, formation of inclusion bodies resembling Lewy bodies and reduced spontaneous movement, which mimics some of the PD pathology. Xie and colleagues (67) established another PD model by injecting the proteasome inhibitors lactacystin, PSI or MG-132 into the medial forebrain bundle (iMFB) of C57/BL mice. DA neurons in the SN degenerated preferentially and α-synuclein positive inclusion-like granules as well as decreased motor activities were observed. Together, these findings support the role of UPP impairment in PD pathology.

1.4. PD and mitochondrial impairment

Mitochondria have long been suggested to play a critical role in PD pathogenesis. MPTP, a mitochondrial complex I inhibitor, was the first drug to provide a link between mitochondrial impairment and idiopathic PD (68). The findings that mitochondrial complex I is deficient in the *substantia nigra* of PD patients (69) and that other mitochondrial complex I inhibitors, such as rotenone, induce PD-like symptoms in animals (70) later confirmed the link between mitochondrial dysfunction and PD pathogenesis. Besides mitochondrial complex I inhibition, the levels of ROS which are mainly produced in mitochondria were also found to be increased in PD patients (71). In familial PD, *α-synuclein, pink1, parkin and dj-1* are the most common mutated

genes and they all interact with mitochondria (72,73). α-Synuclein accumulates in mitochondria during PD pathogenesis (74,75). PINK1 and Parkin regulate mitochondrial dynamics and function (76). Translocation of DJ-1 to mitochondria protects them from oxidative stress (77). Overall, these findings support a role for mitochondrial dysfunction in neurodegeneration in PD.

1.5. Parkin

Parkin was first mapped to human chromosome 6q25.2-27 in 1997 (78). This gene was named *parkin* because point mutations and several exon deletions were identified in a number of families with Autosomal Recessive Juvenile Parkinsonism (AR-JP) (79). It is estimated that 50% of AR-JP patients have *parkin* mutations (80). However, a series of reports revealed that *parkin* mutations also occur in sporadic PD patients (81-83). Having one normal and one mutant form of *parkin* increases the risk of late-onset PD, reflecting the dosage effect of *parkin* mutations (84). Further evidence supports the notion that Parkin is relevant to PD: (1) a recent Positron Emission Tomography (PET) study showed that patients with *parkin* mutations exhibit striatal dysfunction that is similar to that of sporadic PD patients (85). (2) Animal models expressing mutant *parkin* exhibit hallmarks of PD. Mice which carry Q311X *parkin* exhibit age-dependent motor deficits, dopaminergic neuron degeneration, and accumulation of

protein K-resistant α-synuclein (86). (3) Parkin was found to co-localize with inclusion bodies in PD patients (87,88).

1.5.1. Parkin Structure

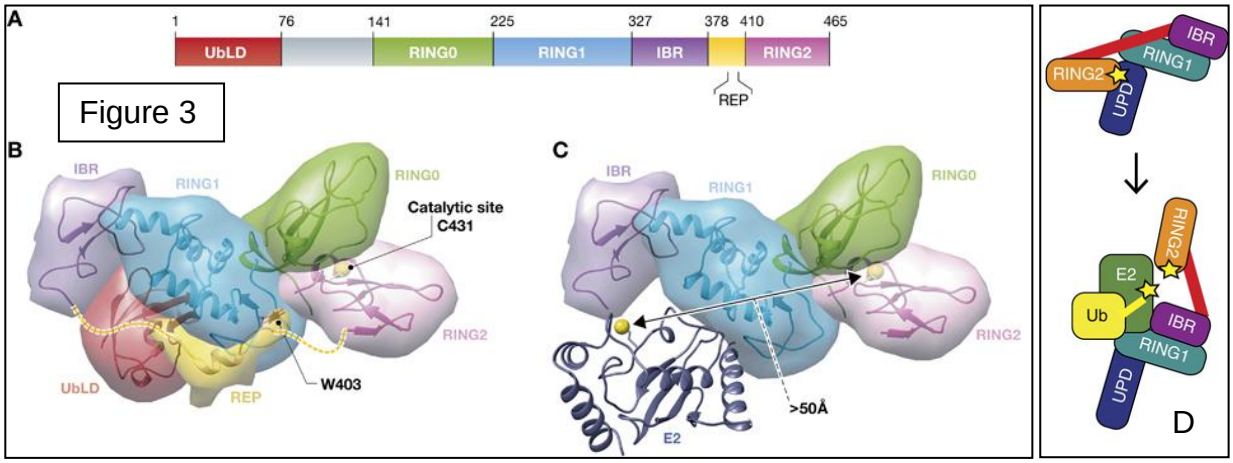

Figure 3 – The structure of PARKIN. A – Primary structure and domains, REP = repressor element. B – Spatial representation highlighting domain interactions in the 3D structure, the C431 catalytic cysteine, and W403 which stabilizes autoinhibited parkin. C – Model showing the E2 UbxH5B/Ube2D2 bound to parkin. D – Proposed model for parkin activation requiring relieving the inhibitory interaction between RING1 and RING2. Stars – active site cysteines in parkin and E2. A, B and C from (1); D from (2).

Parkin is a 465 amino acid protein which is conserved in evolution. Rat Parkin has strikingly 85% similarity with human Parkin in amino acid sequence and 95% with mouse. Parkin is composed of 5 known different domains (Figure 3): an N-terminal UBL (ubiquitin-like) domain (1-76 a.a), two C-terminal RING (Really Interesting New Gene) domains (RING1, 236-293 a.a; RING2, 413-450 a.a respectively), one IBR (In Between RING) domain (327-380 a.a) between the RING domains, and a newly identified RING0 domain (145-215 a.a) (89). The UBL domain binds to the 26S proteasome through its subunit Rpn10 to deliver substrates

to be degraded (90). The RING0 domain has a cysteine at position 212 that when mutated (C212Y) leads to the formation of cellular inclusions and to defective ubiquitination (91). The other two RING domains and the IBR domain are critical for substrate recognition and E2 enzyme binding. The RING2 domain plays a role in transferring the ubiquitin from the E2 to the substrate, preparing the substrate for degradation by the 26S proteasome. The RING domain is a type of Zn^{2+} finger domain, and the three RING domains as well as the IBR domain of Parkin each bind to two Zn^{2+}. The binding directly affects Parkin structure in its stability and proper folding and the removal of Zn^{2+} leads to the near complete unfolding of Parkin (92,93). Interestingly, mutations in the RING1 domain increase Parkin aggregation and the formation of inclusions (94). The UBL and RING-IBR-RING domains are highly conserved among human, rat and mouse (95).

Parkin contains 35 cysteines which not only promote Zn^{2+} binding, but also play an important role in the protective function of Parkin. Oxidative stress and other stress conditions induce modifications of the cysteines located within and outside the RING-IBR-RING domain, changing the solubility of Parkin, increasing Parkin aggregation, and perturbing its E3 ligase activity (96,97). Moreover, a recent study revealed that under physiological conditions, sulfhydration of these cysteines by hydrogen sulfide enhances the catalytic activity of Parkin and

its neuroprotective function (98). This is in agreement with the finding that Parkin sulfhydration is depleted in the brains of PD patients (98). The cysteine at position 431 within the RING2 domain is the active site, since its mutation to serine (C431S) disrupts the E3 ligase activity of Parkin, as well as its translocation to mitochondria (99).

1.5.2. Alternative splicing of Parkin

In human, rat and mouse there are 12 different Parkin transcripts generated by alternative splicing (100): TV1 to TV12. These variant transcripts (TV) contain different numbers of exons suggesting that their functions differ from normal Parkin. Alterations in the isoform profile of Parkin in the frontal cortex of normal individuals compared to PD patients, suggests that Parkin isoform profiles are relevant to LB pathogenesis and the development of PD (101,102). Parkin isoform expression also changes during development, as the 55kDa isoform is present in adult mouse brain while the 22kDa and 50kDa isoforms are detected in the fetal and adult mouse brain (103).

1.5.3. Parkin Cleavage products

Parkin can be cleaved by several proteases. During apoptosis caspase-1, caspase-3 and caspase-8 cleave Parkin at Asp126 into a 38kDa and a 12kDa fragment (104). Caspase-1 and caspase-8 are

directly responsible for Parkin inactivation. The serine protease HtrA2/Omi, which is located in the mitochondrial intermembrane space(105), cleaves Parkin between the RING1 and IBR domains generating 17kDa and 19kDa fragments (106). The HtrA2/Omi cleavage inactivates the E3 ligase ability of Parkin to ubiquinate syniphilin-1. Uncharacterized Parkin cleavage fragments are detected in PD patients (107).

1.5.4. Parkin Tissue distribution and subcellular localization

In primates, Parkin is expressed ubiquitously in the brain, being detected mostly in neurons, but also in glia and blood vessels (108). Parkin is present not only in the SN, but also in other regions of the brain such as cerebellum and caudate-putamen, a region of the brain that receives dopaminergic neuronal projections (109-111). Human autopsy studies confirmed the same tissue distribution: Parkin is identified in the substantia nigra of sporadic PD, as well as in familial PD patients (112). There is one single report claiming that Parkin protein is missing in the adult mouse midbrain SN *pars compacta*, while Parkin mRNA was detected (113).

Concerning subcellular localization, Parkin is enriched in the cytoplasm (114-116), while it is also localized in neurites (117), postsynaptic fractions (118), Golgi apparatus (119), endoplasmic reticulum (120), and nucleus (94). Parkin

localization changes upon stress. When the proteasome is inhibited, Parkin is recruited to centrosomes via binding to γ-tubulin, and locally ubiquitinates misfolded substrates (121). DNA damage induces Parkin nuclear translocation to promote DNA repair (122). When mitochondrial membrane potential is dissipated, Parkin translocates to mitochondria to promote the degradation of mitochondrial substrates as well as mitophagy (123,124). However, that Parkin translocates to mitochondria is a controversial issue, as the majority of the supporting studies include cell lines (125,126). Currently, only a few studies confirmed the translocation of Parkin to the mitochondrion in neurons (127,128), while most studies with primary neuronal cultures dispute this finding (129-131).

1.5.5. Parkin Function

1.5.5.1 Parkin E3-ligase related function

As an E3 ligase, Parkin ubiquitinates its substrates and targets them to proteasomes to be degraded. So far, multiple potential substrates are reported to be ubiquitinated by Parkin (9,94,132). However, whether these substrates represent "true" Parkin substrates is still controversial (9). Aminoacyl-tRNA synthetase-Interacting Multifuncational Protein type 2 (AIMP2)

(133) and Far up stream element Binding Protein-1 (FBP-1) (134) are proposed to be true Parkin substrates.

Changes in the expression of Parkin cause a number of cellular dysfunctions related to its E3 ligase activity. For example, Parkin knock-out with overexpression of Pael-R induces progressive and selective catecholaminergic neuronal loss (135). Pael-R, which is an ER stress-induced protein, is one of reported Parkin substrates. Parkin regulates cellular cytoskeleton homeostasis through ubiquitination and degradation of α/β tubulin (136). The cell cycle is also regulated by Parkin via its substrates: β-catenin (137), cyclin E (138) and RanBP2 (139). Mitophagy and mitochondrial fission and fusion are also controlled by Parkin. The translocation of Parkin to mitochondria leads to the recruitment of 26S proteasomes to mitochondria resulting in the degradation of a range of mitochondrial outer membrane proteins, such as Mitofusin 1/2 and Drp-1, thus inducing mitophagy (140,141). General and neuron-specific overexpression of Parkin in adult *Drosophila* increases their lifespan and physical activity, reduces protein aggregation during aging, changes mitochondrial morphology, and increases mitochondrial activity (142). Parkin can also regulate metal transport via ubiquitination followed by degradation of a divalent metal transporter (143). Moreover, Parkin directly

modulates proteasome activity when it binds to Rpn10, a subunit of the 26S proteasome (144).

1.5.5.2. Alternate functions of Parkin

Parkin exhibits a number of E3 ligase independent functions. Parkin acts as a repressor of p53 expression by physically interacting with its promoter to exhibit anti-apoptotic properties (145). In contrast to its anti-apoptotic function, Parkin expression in TNF-α-treated HeLa cells induces apoptotic cell death (146). Moreover, Parkin regulates fat uptake in mice and human cells (147). Finally, Parkin suppresses stress-activated protein kinase pathways including c-Jun and p38 pathway, to protect against tyrosine-mediated dopamine neurotoxicity in SH-SY5Y cells (148). The latter reveals a potential neuroprotective mechanism for Parkin, against 6-OHDA (149), MPTP (150) and α-synuclein overexpression (151), in models of PD.

1.6. PACAP and PD (from ***Cell Biochem Biophys***. 2013 May 18. (Epub ahead of print). Copyright was obtained from Springer.

PACAP (pituitary adenylate cyclase-activating peptide) exists in two bioactive molecular forms, one with 38 residues (PACAP38) and a shorter form corresponding to the N-terminal 27 residues of PACAP38 (PACAP27) (152). PACAP is a 38-amino acid peptide and

a member of the vasoactive intestinal polypeptide (VIP)-secretin-growth hormone-releasing hormone-glucagon superfamily. This superfamily of peptides binds to two types of receptors: *(a)* type I receptor (PAC1-R), which has a much higher affinity for PACAP than for VIP and activates both adenylate cyclase (AC) and phospholipase C (PLC); *(b)* type II receptors (VPAC1-R and VPAC2-R), which have a similar affinity for PACAP and VIP, and activate primarily AC (152). Gene expression profiles of the three different PACAP receptors by real time PCR, revealed that PAC1-R expression declines during later stages of development, while VPAC1-R and VPAC2-R expression increases from newborn to the later stages of development (153).

PACAP regulated genes involved in neuritogenesis, cell morphology modulation, and cell survival have been screened in both PC12 cells and *in vivo* (154). A recent proteomics study conducted upon PACAP administration further explored the mechanisms by which PACAP exerts its neurotrophic and neuroprotective effects in the brain (155).

The neuroprotective effects of PACAP are mediated by both the canonical cAMP/PKA pathway and the non-canonical cAMP/ERK1/2 pathway (156). These two downstream PACAP-mediated pathways seem to be activated in a concentration-dependent manner, as the effects of subpicomolar PACAP38 levels are mainly mediated by ERK type MAPK, whereas those of nanomolar PACAP38 levels result

from activation of the cAMP/PKA pathway (157).

PACAP was found to have neuroprotective effects in several *in vivo* and *in vitro* models of neurodegenerative disorders including PD, Huntington disease (HD) and Alzheimer disease (AD) (158). *In vivo*, PACAP protects against MPTP (159), 6-OHDA (160) and paraquat (161) neurotoxicity in rodent models of PD. Moreover, PACAP deficiency sensitizes dopaminergic neurons to toxic insults, and regulates central and peripheral inflammatory activation (162). *In vitro*, PACAP protects neurons against salsolinol (163), MPP+ (164), 6-OHDA (165) and rotenone (166) neurotoxicity.

Overall, these studies reveal that proteins with expression profiles altered by PACAP treatment are involved in many cellular processes including cytoskeleton modulation, synaptic plasticity, cellular differentiation, neuroprotection, neurodegeneration and apoptosis, supporting that PACAP is a promising therapeutic peptide for treatment of multiple neural disorders (155).

CHAPTER II

New form of Parkin generated by calpain cleavage upon mitochondrial dysfunction in rat midbrain cultures: relevance to Parkinson disease

2.1. ABSTRACT

Parkin is an E3 ubiquitin ligase that plays a role in the ubiquitin/proteasome pathway. Parkin is suggested to also regulate mitophagy as well as nuclear gene transcription through mechanisms that are not fully characterized. In our current studies, we identified a new form of cleaved Parkin (newParkin) in rat midbrain cultures undergoing mitochondrial impairment. In rat cerebral cortical cultures, we detected full length Parkin in mitochondrial and cytoplasmic fractions regardless of cellular conditions, while newParkin was detected mostly in mitochondrial fractions. NewParkin is generated by calpain cleavage, as it is blocked by a calpain inhibitor and is refractory to a caspase inhibitor. The size of newParkin differs from a caspase-dependent cleaved fragment of Parkin, and newParkin appears as a doublet potentially resulting from its phosphorylation and/or cleavage. Phosphorylation of full length Parkin protects its cleavage by calpain. We demonstrate that stabilizing intracellular ATP levels with the nearly planar creatine analog cyclocreatine prevents the cleavage of full length Parkin by calpain. Increasing cAMP levels with the lipophilic peptide PACP27 prevents caspase-mediated Parkin cleavage. Delineating mechanisms to stabilize Parkin integrity provide novel therapeutic strategies for Parkinson disease.

2.2. MATERIALS AND METHODS

2.2.1. Materials – Inhibitors: oligomycin A, antimycin A, and rotenone (Sigma-Aldrich, St. Louis, MO); epoxomicin (Peptides International Inc., Louisville, KY); calpain inhibitor III and calpeptin (Calbiochem/EMD Bioscience, Gibbstown, NJ); caspase-3 inhibitor (Z-DEVD-FMK) and the proteasome substrate Suc-LLVY-AMC (BACHEM Bioscience Inc., King of Prussia, PA); PGJ2 and okadaic acid (Cayman Chemical, Ann Arbor, MI). Activators: PACAP27 (BACHEM Bioscience Inc., King of Prussia, PA) and cyclocreatine (Sigma, St. Louis, MO). Primary antibodies: rabbit polyclonal anti-Parkin (1:1000, cat#2132); rabbit polyclonal anti-caspase 3 (1:1000, cat# 9662)(both from Cell Signaling Technology, Danvers, MA); rabbit polyclonal anti-ubiquitinated proteins (1:1,500, cat# Z0458, Dako North America, Carpinteria, CA); rabbit polyclonal anti-β5 (1:5,000, cat# PW8895), mouse monoclonal anti-Rpt6 (1:2,000, cat# PW9265), anti-Rpn10 (1:2000, cat# PW9250), anti-α5 (1:2,000, cat# PW8125), (all from ENZO Life Sciences, Inc., Farmingdale, NY); mouse monoclonal anti-β-actin (1:10,000, cat# A-2228, Sigma, St. Louis, MO); rabbit polyclonal anti-caspase-3 (1:1000, cat# 9662)(Cell Signaling Technology, Danvers, MA); mouse monoclonal anti-spectrin α chain (clone AA6, cat# MAB1622, Millipore, Billerica, MA); mouse monoclonal anti-βIII-tubulin (1:10,000, cat# MMS-435P, Covance, Oakland, CA); rabbit polyclonal anti-HSP90 (1:2000, cat# PA3-013, Thermo

Scientific, Rockford, IL); Rabbit polyclonal heme oxygenase 1 (HO-1) antibody (1:2000,cat#sc-10789), rabbit polyclonal TOM20 antibody (1:1000, cat#sc-11415) (Santa Cruz biotechnology Inc, Santa Cruz, CA); Mouse monoclonal fibrillarin antibody (1:1000, cat#ab4566, Abcam, Cambridge, MA); Rabbit polyclonal VDAC antibody(1:1000, cat#PC548, Calbiochem, Gibbstown, NJ) Secondary antibodies with HRP conjugate (1:10,000, Bio-Rad Laboratories, Hercules, CA).

2.2.2. Primary neuronal cultures – These studies include two different types of primary neuronal cultures obtained from Sprague Dawley rat embryonic (E18, both sexes) midbrain and cerebral cortical neurons.

1) Rat E18 ventral midbrain cultures: These cells, routinely prepared in our laboratory as in (167), are ideal to use in our studies. The proteins that we study, including Parkin, calpain, caspases, ubiquitinated (Ub)-proteins, and others, are endogenously expressed and detectable in these cultures. These ventral midbrain neuronal cultures contain dopaminergic and other types of neurons, providing for the simultaneous analysis of multiple cell types. Taking this heterogeneity into account, besides biochemical analyses, the cell cultures were analyzed by immunofluorescence to specifically identify dopaminergic (tyrosine hydroxylase, TH+) neurons as described in (168).

Studies with these cells will address the biological functions of wild type Parkin, as relevant to "sporadic" PD.

2) Rat E18 cerebral cortical neuronal cultures: In assays that require large numbers of cells, cortical cultures were used, as they express Parkin that in terms of "calpain cleavage" responds in a manner similar to the midbrain cultures.

3) Culture preparation: Dissociated cultures from midbrain and cerebral cortical neurons were prepared as follows: The isolated midbrain and cortices free of meninges were digested with papain (0.5mg/ml from Worthington Biochemical Corp., Lakewood, NJ) in Hibernate E without calcium (BrainBits LLC., Springfield, IL) at 37°C for 30min in a humidified atmosphere containing 5% CO_2. After removal of the enzymatic solution, the tissues were gently dissociated in Neurobasal media (Invitrogen, Carlsbad, CA). Dissociated tissues were centrifuged at 300X*g* for 2min. The pellet was resuspended in Neurobasal media without antibiotics and plated on 10cm dishes pre-coated with 50µg/mL poly-D-lysine (Sigma, Saint Louis, MO). Cells were plated at a density of $6X10^6$ cells per 10cm dish, or $2.5X10^5$ cells per well on 24-well plates (cell viability only). Cultures were maintained in Neurobasal media supplemented with 2% B27 and 0.5mM L-Glutamax (all from Invitrogen) at 37°C in a humidified atmosphere containing 5% CO_2. Half of the medium was changed every 4 days. Experiments were run upon 8-11 DIV. According to manufacturer's specifications,

Neurobasal medium contains several proprietary factors that ensure a mostly pure (>95%) neuronal culture; glial growth is inhibited without a need for the anti-mitotic agent arabinofuranosyl cytidine (169,170).

Midbrain isolation was carried-out as in Dr. David Sulzer's lab (Columbia University, NY) and described in the Sulzer's lab protocol: *Postnatal ventral midbrain dopamine neuronal culture protocols* (Figures below).

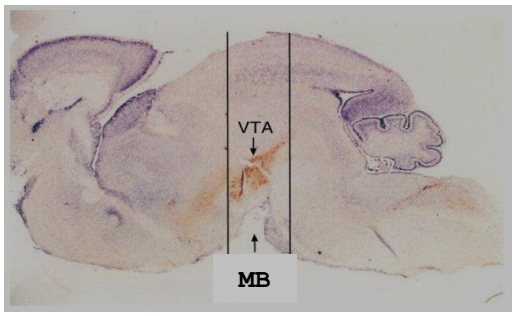

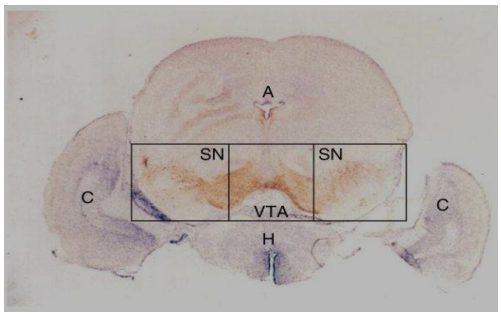

VTA: ventral tegmental area; MB: midbrain. Figure modified from Dr. David Sulzer's lab "*Postnatal ventral midbrain dopamine neuronal culture protocols".*

2.2.3. Culture treatments – Neurons were treated (1.5h to 16h) with DMSO or with the different drugs in DMSO added directly to Neurobasal supplemented with 0.5mM L-Glutamax (all from Invitrogen).

2.2.4. Mitochondrial fractionation – Mitochondrial fractionation was carried-out with a mitochondrial isolation kit cat# 89874 (Pierce, Rockford, IL). Cells were harvested with ice cold 1×PBS and centrifuged at 800×*g* for 2 min. The pellet was resuspended

with 800µl reagent A plus a protease inhibitor cocktail (Sigma, cat# P8340). Samples were vortexed (medium speed, 5s) and incubated on ice (2min). Upon addition of other reagents, an aliquot representing the total lysate was removed. The remaining sample was centrifuged (700X*g*, 10min, 4°C). The pellet (crude nuclear fraction) was separated from the supernatant, which was centrifuged again (12,000X*g*, 15min, 4°C). The resulting supernatant (cytosolic fraction) was separated from the pellet, which contained the enriched mitochondrial fraction. The mitochondrial pellet was washed with reagent C, centrifuged (12,000X*g*, 5min, 4°C) and the pellet resuspended in 1% SDS lysis buffer. Cold acetone (1:3 dilution) was added to the cytosolic fraction, stored at -20°C overnight, centrifuged (19,000*Xg*, 15min), and the pellet was air dried and resuspended in 1% SDS lysis buffer. All fractions were boiled (100°C) for 5min. Four fractions resulted from this procedure: total lysate, crude nuclear, cytosolic and enriched mitochondrial fractions. Protein concentration was determined with the bicinchoninic acid assay (BCA) kit (Pierce, Rockf., IL).

2.2.5. ATP assay – Steady state ATP content was measured with a kit using the sensitive luciferin/luciferase system (Molecular Probes, Carlsbad, CA). This assay is based on luciferase requiring ATP for light production using luciferin as a

substrate. Cells were harvested with 4% trichloroacetic acid followed by centrifugation (19,000X*g*, 15min at 4°C). ATP steady state levels were determined in cleared supernatants upon neutralizing the samples with 10mM Tris-HCl, pH 8.0. Samples were then added to the reaction buffer containing luciferin and assayed using a Luminoskan Ascent microplate luminometer (Thermo Electron Corporation, Waltham, MA). Protein concentration was determined with the bicinchoninic acid assay kit (Pierce, Rockf., IL) upon resuspending the pellet with buffer (10mM Tris-HCl, pH 8.0 and 1% SDS), and sonication. ATP levels were normalized for protein concentration.

2.2.6. Cell viability assay - Cells were treated under various conditions for 1h to 16h. Cell viability was assessed with the 3-(4,5-dimethylthiazol-2-yl)-2,5-diphenyl tetrazolium bromide (MTT) assay as described in (171).

2.2.7. Western blotting - After treatment, cells were rinsed twice with PBS and harvested by gently scraping into hot (100°C) SDS buffer (0.01M Tris-EDTA, pH 7.5 and 1% SDS) to make sure all intracellular proteins were included. Samples were subjected to a 5min boil at 100°C followed by brief sonication. After determination of the protein concentration with the bicinchoninic acid assay kit (Pierce, Rockf., IL) the following

was added to each sample (final concentrations): β-mercaptoethanol (4%), bromophenol blue (0.005%), and glycerol (4%). Following SDS-PAGE on 6%, 8%, 10% or 12% polyacrylamide gels, proteins were transferred to an Immobilon-P membrane (Millipore, Bedford, MA). The membranes were probed with the respective antibodies and antigens were visualized by a standard chemiluminescent horseradish peroxidase method with the ECL reagent.

2.2.8. In gel proteasome activity and levels - Upon treatment with vehicle (control, DMSO) or the respective drugs, cells were washed twice with PBS and harvested for the in gel assay as described in (172). The native gels loaded with 30µg protein/lane, were run at 150V for 120min. The in gel proteasome activity was detected by incubating the native gel on a rocker for 10min at 37°C with 15ml of 300µM Suc-LLVY-AMC followed by exposure to UV light (360nm). Gels were photographed with a NIKON Cool Pix 8700 camera with a 3-4219 fluorescent green filter (Peca Products, Inc). Proteins on the native gels were transferred (110mA) for 2h onto PVDF membranes. Immunoblotting was carried-out for detection of the 20S and 26S proteasomes with the anti-Rpt6 and anti-β5 antibodies, which react with subunits of the 19S or the 20S particles, respectively, thus detecting 26S and 20S proteasomes. Antigens were visualized by a

chemiluminescent horseradish peroxidase method with the ECL reagent.

2.2.9. Glycerol gradient sedimentation centrifugation – Cells were harvested in 25mM Tris-HCl, pH 7.5, 2mM ATP and 1mM DTT. Following homogenization and sonication the lysates were centrifuged (19,000xg for 15min) at 4°C. The cleared supernatants (one mg of protein/sample) were subjected to centrifugation (83,000xg for 24h) at 4°C in a Beckman SW41 rotor in a 10-40% glycerol gradient (fractions 1 to 24) made in the same lysis buffer. Following centrifugation 24 fractions (500µl each) were collected. Aliquots (50µl) of each fraction were assayed for chymotrypsin-like activity with the substrate Suc-LLVY-AMC. After 3h of incubation at 37°C samples were read with a spectrofluorometer. In addition, proteins were precipitated with acetone from 450µl of each fraction and subjected to western blot analysis (10% gels). The membranes were probed with the respective antibodies and antigens were visualized by a standard chemiluminescent horseradish peroxidase method with the ECL reagent.

2.2.10. Caspase-3 and calpain activation – Cell lysates were analyzed by standard western blotting with anti-caspase-3

(rabbit polyclonal antibody, 1:1000 from Cell Signaling, cat# 9662) to detect caspase-3 cleavage that are indicative of apoptosis. Calpain activation was assessed with the anti-α-spectrin antibody (mouse monoclonal antibody, 1:5000 from Millipore, cat# MAB1622). Calpain cleavage of α-spectrin generates a 150/145kDa doublet, while caspase cleavage generates a 120kDa fragment.

2.2.11. Mitochondrial membrane potential and ROS measurements – Upon treatment with the drugs, mitochondrial membrane potential ($\Delta\Psi_m$) was assessed with TMRE (Abcam Inc.), and ROS with H_2DCFDA (Invitrogen). At the designated time points, treatment medium (DMEM) with the drugs was removed, and fresh DMEM without drugs but with TMRE (200nM) or H_2DCFDA (20μM) was added to separate cultures. Following a 30-min dye-loading incubation that included Hoechst 33342 for nuclear staining for the last 5-min, the cultures were changed to fresh dye-free DMEM. The dyes were allowed to re-equilibrate in the fresh dye-free media, then TMRE and H_2DCFDA fluorescence were imaged on a Nikon Eclipse TE 200 inverted epifluorescence microscope. The following excitation/emission wavelengths were used for: TMRE (red) 549/575nm, ROS (green) 495/529nm, and Hoechst 33342 (blue) 350/461nm.

2.2.12. OXYBLOT – To detect carbonyl groups on proteins, the oxyblot assay was used (Oxyblot Protein Oxidation Detection Kit, Millipore, cat#S7150). Cells were harvested with RIPA buffer, stored at -80°C overnight for lyses, followed by centrifugation (19,000×g, 10min, 4°C). The protein concentration of the supernatant was determined with the BCA assay. Samples were normalized to 20µg of protein in 5µl per sample, the proteins were denatured by adding 5µl of 12% SDS, for a final 6% SDS concentration. Samples were derivatized by adding 10µl of 1X DNPH (2,4-dinitrophenylhydrazine) solution, and incubated at room temperature for 15min. Then 1.5 volumes of neutralization buffer and 2-mercaptoethanol (β-ME) were added to the sample mixture (β-ME final concentration: 5%v/v or 0.74M). Samples were run on 12% gels, followed by western blotting probed with primary rabbit anti-DNP antibody and secondary goat anti-rabbit IgG HRP-conjugated antibody.

2.2.13 Statistical analysis – Statistical significance was estimated using one-way ANOVA (Tukey-Kramer multiple comparison test) with the Instat 2.0, Graphpad Software (San Diego, CA).

2.3. RESULTS

2.3.1. Oligomycin, PGJ2, and epoxomicin induced cleavage of Parkin – To compare the effects of mitochondrial and proteasome impairment on Parkin, rat midbrain neuronal cultures were treated with *(1)* oligomycin (Oligo), which binds to a polypeptide in the F0 baseplate and blocks ATP synthesis by the F0/F1 mitochondrial ATP synthase (173); (2) epoxomicin (Epox), a specific and irreversible inhibitor of the proteasome, which forms a covalent adduct with the amino terminal Thr of the 20S proteasome catalytic subunits, generating irreversible morpholino adducts (174,175); and *(3)* prostaglandin J2 (PGJ2), an endogenous and bioactive product of inflammation known to inhibit the proteasome and to adversely affect mitochondria.

As shown in Fig. 4 (panels 2, next page), all three drugs induce the cleavage of Parkin in a time-dependent manner. However, the pattern of cleaved Parkin differs among the three drugs. While the size of the Parkin fragment(s) induced by PGJ2 and Epox are below 37kDa, the ones induced by Oligo are above 37kDa and appear as a clear doublet.

The three drugs also differed in relation to their effects on *(1)* the levels of ubiquitinated proteins, and *(2)* on activation of caspase 3 and calpain. Oligo decreased the levels of ubiquitinated (Ub) proteins to below basal levels (Fig. 4, panel

1), and activated calpain (Fig. 4, panel 4), indicated by cleavage of spectrin to the 145/150kDa calpain-specific fragments (Fig. 4, panel 4, α-spectrin CL1). PGJ2 and Epox increased Ub-proteins (Fig. 4, panels 1) and activated caspase 3 (Fig. 4, panels 3) established by its cleavage to a 17kDa fragment known to correspond to activated caspase 3. Note that Oligo also induces caspase 3 cleavage, but the generated fragment (~29kDa) reflects caspase 3 inactivation (Fig. 4, panel 3). These results clearly indicate that proteasome and mitochondrial impairment diverge on their impact *(1)* on the function of the ubiquitin/proteasome pathway (UPP), in particular on Parkin cleavage and Ub-protein levels, and *(2)* on cell death pathways represented by caspase 3 (apoptosis) or calpain (necrosis) activation.

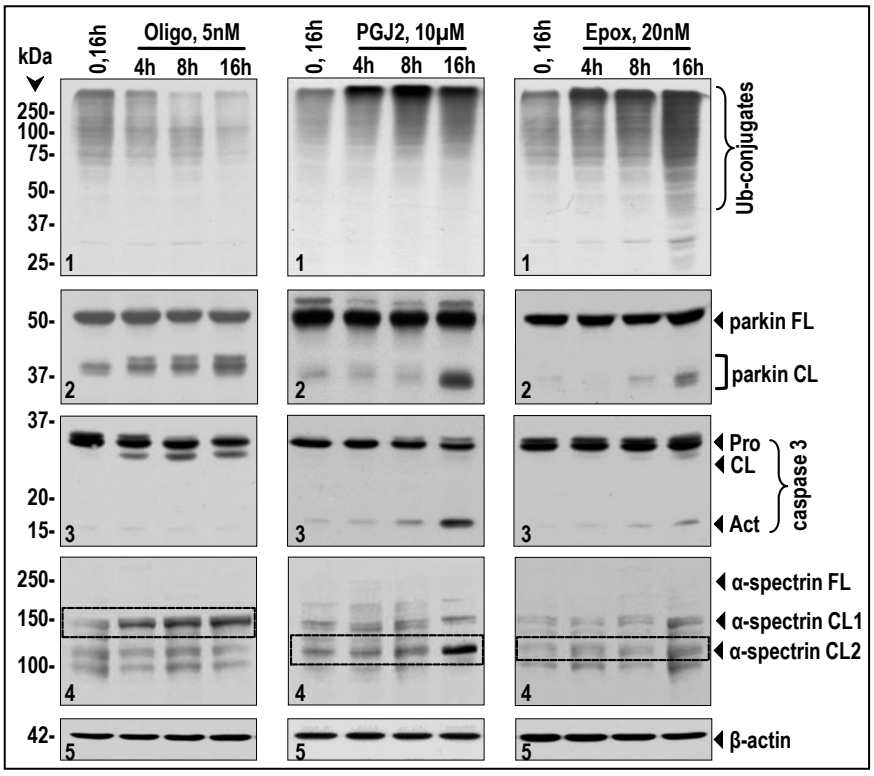

FIGURE 4. Effects of oligomycin (Oligo), PGJ2, and epoxomicin (Epox) on: ubiquitinated (Ub)-proteins (panels 1), and on the cleavage of Parkin (panels 2), caspase 3 (panels 3), and α-spectrin (panels 4). Rat midbrain neurons were treated as indicated. Total lysates were analyzed by western blotting (50 μg of protein/lane) probed with the respective antibodies. Actin (panels 5, loading control). Molecular mass markers in kDa are shown on the left. Data represent one of at least three experiments for each condition. FL, full length, CL, cleaved, Act, active.

2.3.2. Calpain and caspase-dependent cleavage of Parkin induced by oligomycin, PGJ2, or epoxomicin - It is known that Parkin is a substrate for caspases, as it is cleaved by caspase-1, caspase-3 and caspase-8 at Asp126, leading to its inactivation (176). To our knowledge, we are the first to report that in rat midbrain neuronal cultures proteasome inhibition (with epox), and the neurotoxic prostaglandin PGJ2 induce caspase-3 mediated Parkin cleavage. This notion is supported by inhibition of Parkin-cleavage with a caspase-3 specific inhibitor, under these conditions. Furthermore, we identified a new form of cleaved

Parkin (newParkin) detected upon mitochondrial impairment with Oligo in rat midbrain cultures (Fig. 5, panels 1).

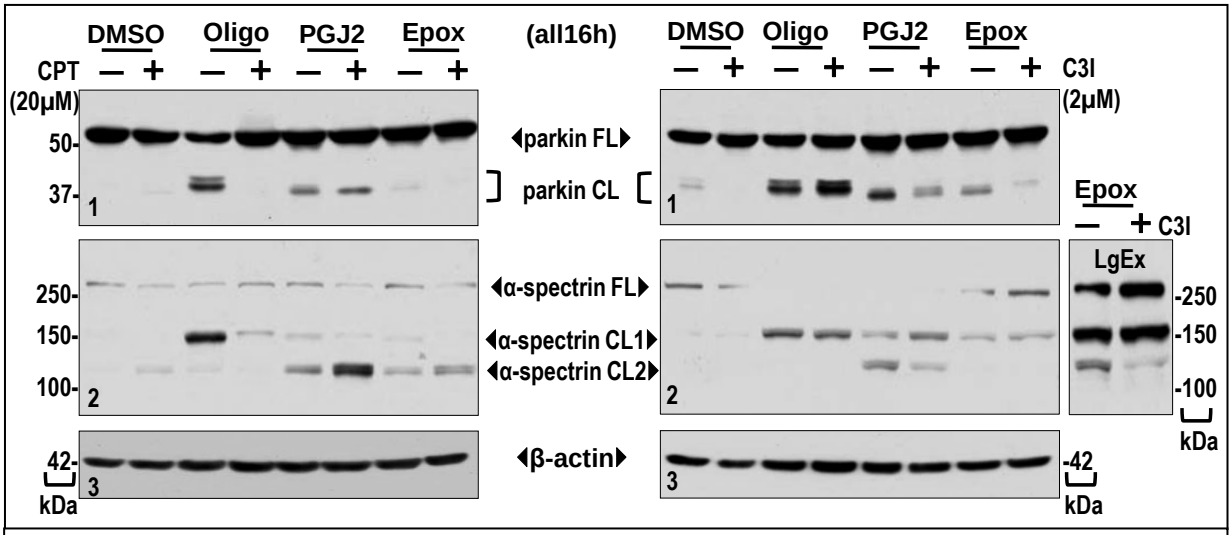

FIGURE 5. Oligomycin (Oligo, 5nM) induces calpain-dependent cleavage of PARKIN (CL) that is blocked by pre-treatment with the calpain inhibitor calpeptin (CPT, *left*) but not by the caspase 3 inhibitor (C3I, Z-DEVD-FMK, *right*). PGJ2 (10μM) and epoxomicin (Epox, 20nM) trigger caspase-dependent cleavage of PARKIN. Cleaved α-spectrin (panels 2) depicts calpain (CL1) or caspase (CL2) activation/inhibition. Actin (panels 3, loading control). Rat midbrain neurons were treated as indicated. Total lysates were analyzed by western blotting (50 μg of protein/lane) probed with the respective antibodies. Molecular mass markers in kDa are shown on the left and on the right. Data represent one of at least three experiments for each condition. FL, full length, CL, cleaved, LgEx, long exposure.

NewParkin is generated by calpain cleavage, as it is blocked by a calpain inhibitor (Fig. 5, panel 1, left), and is refractory to a caspase inhibitor (Fig. 5, panel 1, right). NewParkin migrates at a size that differs from the caspase-cleaved fragment triggered by PGJ2 and, to a lesser extent, by epoxomicin (Fig. 5).

2.3.3. The effect of oligomycin on Parkin is mimicked by other mitochondrial inhibitors – To tested if other mitochondrial inhibitors recapitulate the effect of Oligo on Parkin, rat midbrain neuronal cultures were treated with two different mitochondrial toxins that affect different elements of the electron transport chain: *(1)* rotenone that binds to ND1 and inhibits NADH–ubiquinone reductase activity of complex I (177), and *(2)* antimycin A that binds to the quinone reduction site of complex III (ubiquinol-cytochrome c oxidoreductase), inhibiting the reduction of cytochrome c. Rotenone is particularly relevant to PD, as its effects mimic some of its pathological features (178). Like Oligo, the two other mitochondrial inhibitors induced calpain-dependent cleavage of Parkin (Fig. 6A, panel 1, next page), caspase 3 to an inactive form (Fig. 6A, panel 2 and 3), and α-spectrin (Fig. 6A, panel 4). From the three mitochondrial drugs tested, rotenone caused the weakest changes as it required the highest concentrations to generate detectable levels of newParkin with our western blot analysis (Fig. 6B). Thus, we show that three mitochondrial toxins, which inhibit oxidative phosphorylation at different steps, lead to the generation of a calpain-cleaved form of Parkin.

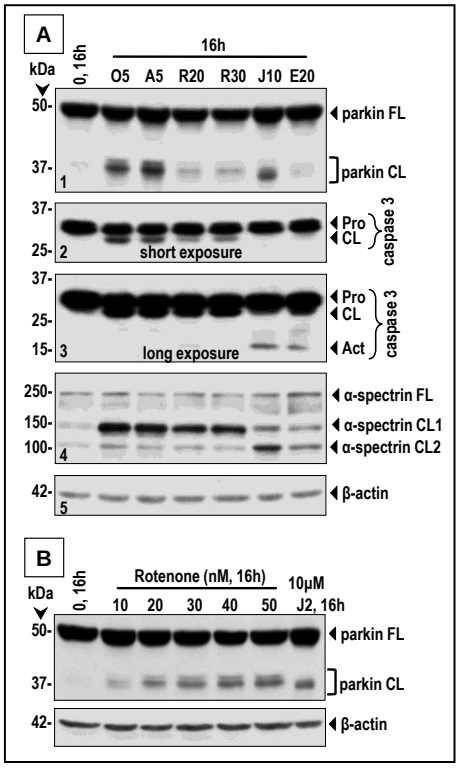

FIGURE 6. A - Oligomycin (O, 5nM), antimycin A (A, 5nM), and rotenone (R, 20nM and 30nM) induce calpain-dependent cleavage of PARKIN (CL) (panel 1). PGJ2 (J, 10μM) and epoxomicin (E, 20nM) trigger caspase-dependent cleavage of PARKIN (panel 1). Cleaved caspase 3 indicates calpain activation (panel 2), and caspase activation (panel 3). Cleaved α-spectrin (panel 4) also depicts calpain (CL1) or caspase (CL2) activation. Actin (panel 5) is the loading control). **B** – Rotenone triggers the generation of newParkin (calpain-cleaved) in a concentration-dependent manner. Actin is the loading control. Rat midbrain neurons were treated as indicated. Total lysates were analyzed by western blotting (50 μg of protein/lane) probed with the respective antibodies. Molecular mass markers in kDa are shown on the left. Data represent one of at least three experiments for each condition. FL, full length, CL, cleaved.

2.3.4. Subcellular localization and phosphorylation of newParkin

- Parkin is an E3 ubiquitin ligase that (a) regulates mitochondrial dysfunction via mitophagy, and (b) targets some mitochondrial as well as cytoplasmic substrates for proteasomal mediated degradation. We thus investigated the subcellular localization of cleaved Parkin in rat cerebral cortical cultures treated with Oligo (5nM), PGJ2 (10μM), and Epox (20nM). We carried-out these studies with cortical cultures instead of midbrain cultures, because this study requires large numbers of cells that are easily prepared from the rat embryonic brains. As shown in Fig. 7A (panels 1 & 2), the cortical neurons respond to the three drugs in a manner that is similar to the midbrain

cultures. It is clear that full length (FL) Parkin is detected in nuclear, mitochondrial and cytoplasmic fractions regardless of cellular conditions as reported in (179). However, most of the newParkin fractionates with the mitochondria, while caspase-cleaved Parkin is distributed between the nuclear and mitochondrial fractions (Fig. 7A, panels 1 & 2). Subcellular markers are: nuclear – fibrillarin (Fig. 7A, panels 3 & 4), a nucleolar protein that is regulated by the UPP (180); mitochondrial – Tom20 (Fig. 7A, panel 5 & 6), a peripheral member of the TOM complex that is the primary receptor for import of mitochondrial precursor proteins (181), and VDAC (Fig. 7A, panel 7 & 8), the voltage-dependent anion channel located on the mitochondrial outer membrane (182); and cytosolic – Hsp90 (Fig. 7A, panel 9 & 10) a well established chaperone (183).

Very few studies address the phosphorylation of endogenous Parkin in primary neuronal cultures. We show in midbrain neuronal cultures that the phosphatase inhibitor okadaic acid (OA) stabilizes the phosphorylation state of full length (FL) Parkin indicating its transient phospho/dephospho cycle (Fig. 7B, compare lanes a/b with c/d). In addition, phosphorylation of FL Parkin decreases its susceptibility to calpain-cleavage induced by oligomycin (Fig. 7B, compare CL Parkin in lanes b and d).

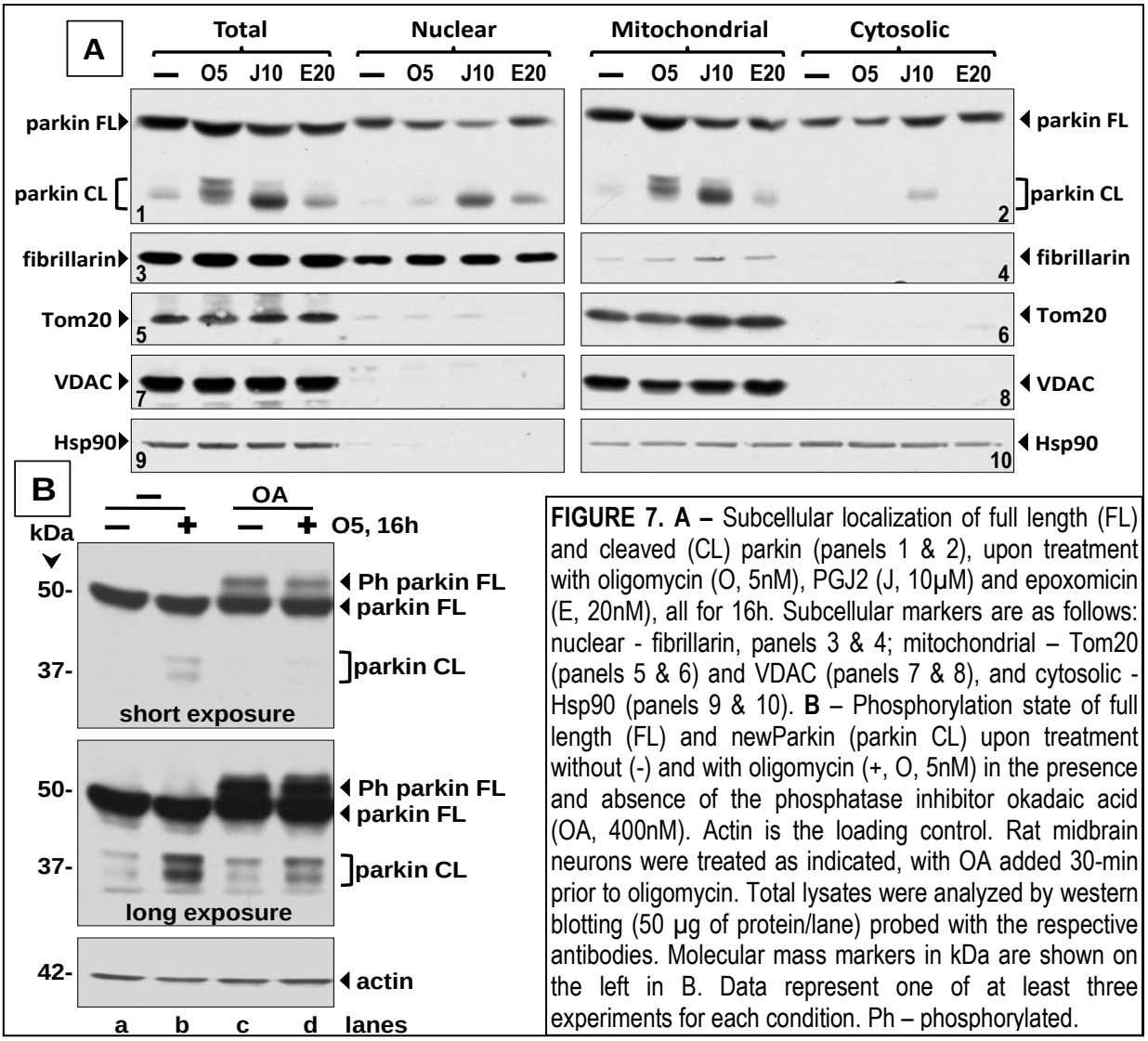

FIGURE 7. A – Subcellular localization of full length (FL) and cleaved (CL) parkin (panels 1 & 2), upon treatment with oligomycin (O, 5nM), PGJ2 (J, 10μM) and epoxomicin (E, 20nM), all for 16h. Subcellular markers are as follows: nuclear - fibrillarin, panels 3 & 4; mitochondrial – Tom20 (panels 5 & 6) and VDAC (panels 7 & 8), and cytosolic - Hsp90 (panels 9 & 10). **B** – Phosphorylation state of full length (FL) and newParkin (parkin CL) upon treatment without (-) and with oligomycin (+, O, 5nM) in the presence and absence of the phosphatase inhibitor okadaic acid (OA, 400nM). Actin is the loading control. Rat midbrain neurons were treated as indicated, with OA added 30-min prior to oligomycin. Total lysates were analyzed by western blotting (50 μg of protein/lane) probed with the respective antibodies. Molecular mass markers in kDa are shown on the left in B. Data represent one of at least three experiments for each condition. Ph – phosphorylated.

2.3.5. Parkin association with the 26S proteasome – We previously demonstrated in rat cortical neurons that, upon mitochondrial impairment, calpain activation leads to selective cleavage of the Rpn10 subunit of the 26S proteasome, as other proteasome subunits tested were not affected (184 and chapter 3). Thus, like Parkin, Rpn10 is cleaved by calpain upon mitochondrial impairment. Based on these data, we determined

whether calpain cleavage of Parkin and Rpn10 affects the association of Parkin with the proteasome. For this purpose, total extracts from cells treated with vehicle (DMSO, control) or oligomycin (5nM, 8h) were fractionated by glycerol gradient sedimentation centrifugation. Fractions were analyzed for Suc-LLVY-AMC hydrolysis which reflects the chymotrypsin-like activity (Fig. 8, next page). As expected, the chymotrypsin-like activity of the 26S proteasome (white squares) was significantly lower than in controls (black squares, fraction 14, peak for 26S). The activity of 20S proteasomes, however, was increased in the oligomycin-treated cells (fraction 8, *peak for 20S*). The proteasome elution pattern was confirmed by western blot analyses of each fraction with the anti-Rpt6 antibody that reacts with an ATPase subunit of the 19S particle (rows 1 for control and oligomycin-treated), and the anti-α5 antibody that reacts with a subunit of the 20S core particle, (rows 2 for control and oligomycin-treated). The levels of the Rpn10 subunit were significantly reduced upon oligomycin treatment (rows 3 for control and oligomycin-treated). Finally, under control conditions, FL Parkin eluted slightly to the left (row 4, peak fractions 8-10) of the 26S proteasome peak (fraction 14). Oligomycin-treatment not only induced Parkin cleavage, but also exacerbated the gap between the Parkin peak (row 4, fractions 6-8) and the 26S proteasome peak (fraction 14), suggesting

dissociation of Parkin from the 26S proteasome.

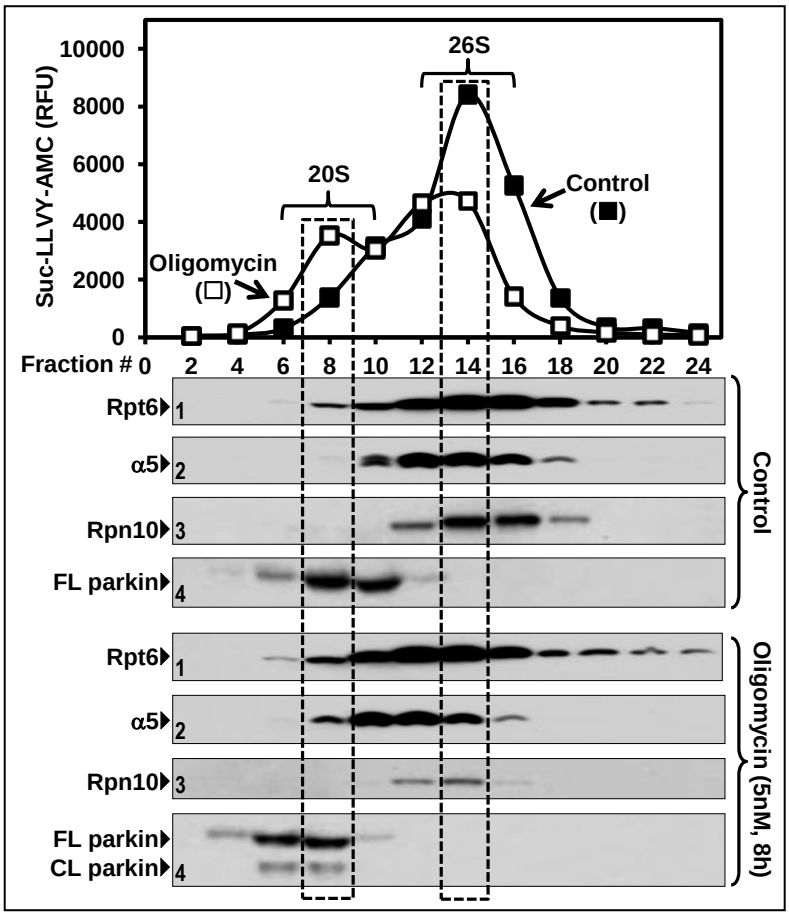

FIGURE 8. Sedimentation velocity of proteasomes and parkin in rat cerebral cortical neurons. Total lysates (one mg protein/sample) were fractionated by glycerol density gradient centrifugation (10-40% glycerol corresponding to fractions 1 to 24). For analysis every two fractions were combined. Aliquots (50μl) of the combined fractions obtained from control (*black squares*), and oligomycin (5nM, 8h, *white squares*) treated cells were assayed for chymotrypsin-like activity with Suc-LLVY-AMC (*top graph*). Immunoblot analyses of the combined fractions probed with antibodies that react with Rpt6 and Rpn10 (19S regulatory particle, *panels 1 and 3, respectively*) or α5, (core particle, *panels 2*). Fractions were also probed for parkin (*panels 4*). Proteins were precipitated with acetone from 450μl of the combined fractions. Similar results were obtained in duplicate experiments.

2.3.6. Effects of oligomycin, PGJ2 and epoxomicin on the proteasome – We assessed with the native in-gel assay, the effects of the three drugs on proteasome activity and levels in the midbrain neurons as described in (184). The in-gel assay detects the three assembled forms of the proteasome: 26S proteasomes with either two regulatory caps [26S (2)] or one cap [26S(1)], and the 20S core particle alone (20S). The three drugs decreased 26S proteasome activity with epoxomicin being the most efficient of the three (Fig. 9). Oligomycin (O, 5nM) and PGJ2 (J,

10μM) also decreased the levels of the 26S proteasome while increasing those of the 20S proteasome. Epoxomicin however, did not increase 20S proteasome levels.

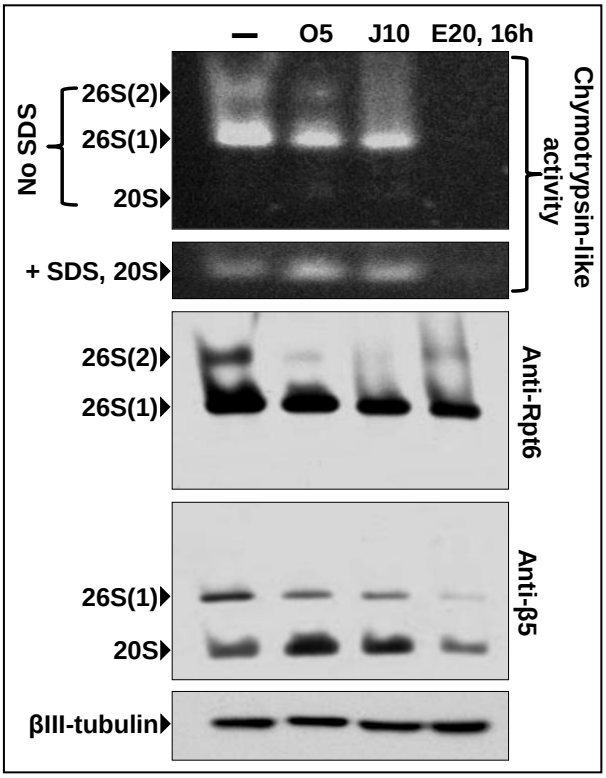

FIGURE 9. Effects of oligomycin, PGJ2 and epoxomicin on proteasome activity and levels in rat midbrain neurons. Cultures were treated for 16h with DMSO (—, control), oligomycin (O, 5nM), PGJ2 (J, 10μM), or epoxomicin (E, 20nM). Cleared lysates (25μg/sample) were subjected to non-denaturing gel electrophoresis. The chymotrypsin-like active of fully assembled 26S and 20S proteasomal (*indicated on the left by arrows*) were assessed with Suc-LLVY-AMC by the in-gel assay (*two top panels*). To improve detection of 20S proteasome activity, 0.04% SDS was added to the reaction buffer (*second panel*). Proteasome levels were detected by immunoblotting with anti-Rpt6 anti-β5 antibodies (*labeled on the right*).

2.3.7. Comparison of the effects of oligomycin, PGJ2 and epoxomicin on cell viability, ATP, oxidative stress, and mitochondrial membrane potential ($\Delta\Psi_m$) – Since the three drugs act via different mechanisms, we compared their effects on cell viability and mitochondrial function assessed by ATP levels, oxidative stress, and $\Delta\Psi_m$. At the concentrations and times tested, oligomycin (Oligo, 5nM) was the most neurotoxic, decreasing cell viability by ~50%, followed by PGJ2 (10μM, ~20%

decrease) and epoxomicin (Epox, 20nM, less than 4%, not significant), as shown in Fig. 10A, below. Oligo was the only one that decreased intracellular ATP levels, causing ~60% depletion (Fig. 10B).

Reactive oxygen species (ROS) are generated whenever electron transport through the ETC is slowed (185,186). Proteins are one of the major targets of ROS that introduce carbonyl groups (aldehydes and ketones) at lysine, arginine, proline or threonine residues in a site-specific manner, thus serving as markers of ROS-mediated protein damage (187). Using the oxyblot kit for immunodetection of carbonyl groups on proteins, we established that among the three drugs, PGJ2 most effectively increased the oxidation status of proteins in the midbrain cultures (Fig. 10C). This finding is further strengthened by the demonstration that hemeoxygenase-1 (HO-1) increases upon treatment with PGJ2 (Fig. 10C). Although HO-1 is maintained at low levels in the brain under normal conditions, its levels increase upon oxidative damage and inflammation (188). As expected ROS production was elevated the most in response to 1.5h treatment with PGJ2, followed by oligomycin, as measured by H_2DCFDA fluorescence (Fig. 11A, gain of green immunofluorescence).

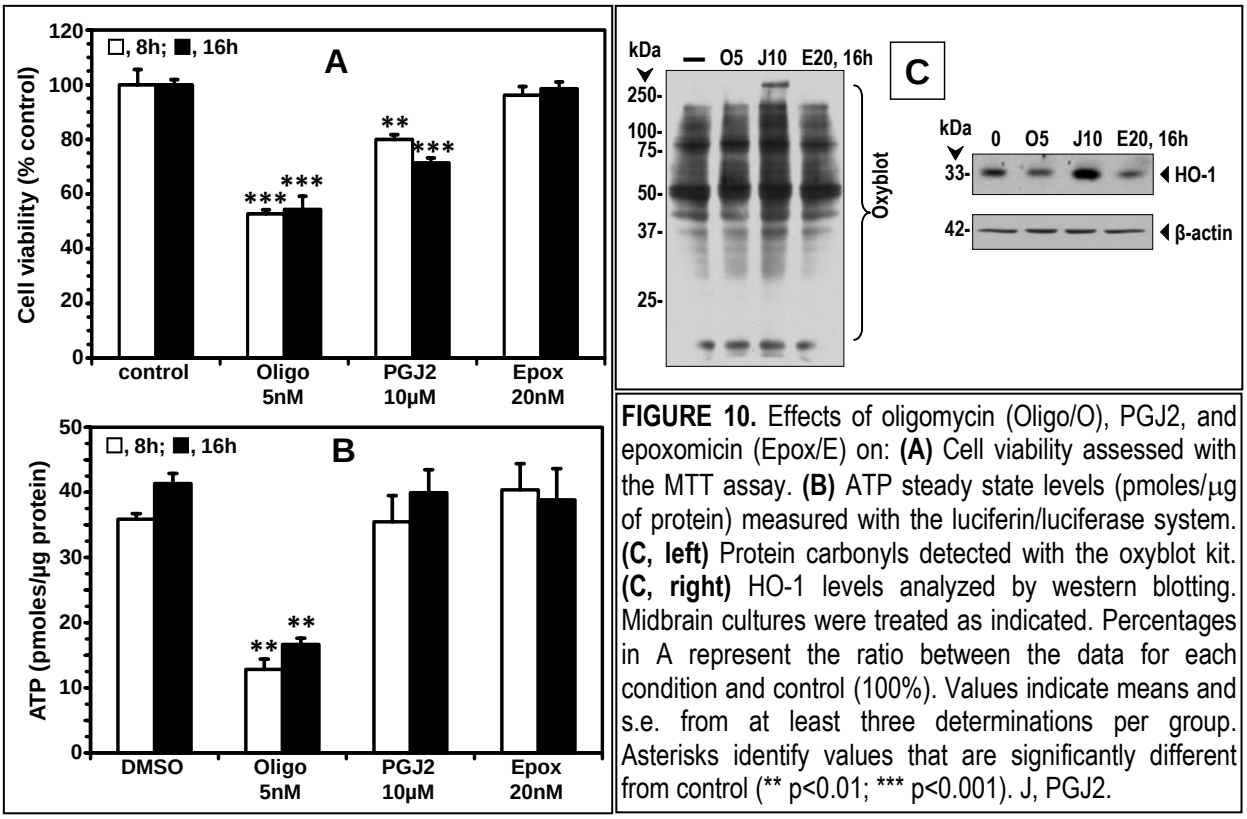

FIGURE 10. Effects of oligomycin (Oligo/O), PGJ2, and epoxomicin (Epox/E) on: **(A)** Cell viability assessed with the MTT assay. **(B)** ATP steady state levels (pmoles/μg of protein) measured with the luciferin/luciferase system. **(C, left)** Protein carbonyls detected with the oxyblot kit. **(C, right)** HO-1 levels analyzed by western blotting. Midbrain cultures were treated as indicated. Percentages in A represent the ratio between the data for each condition and control (100%). Values indicate means and s.e. from at least three determinations per group. Asterisks identify values that are significantly different from control (** p<0.01; *** p<0.001). J, PGJ2.

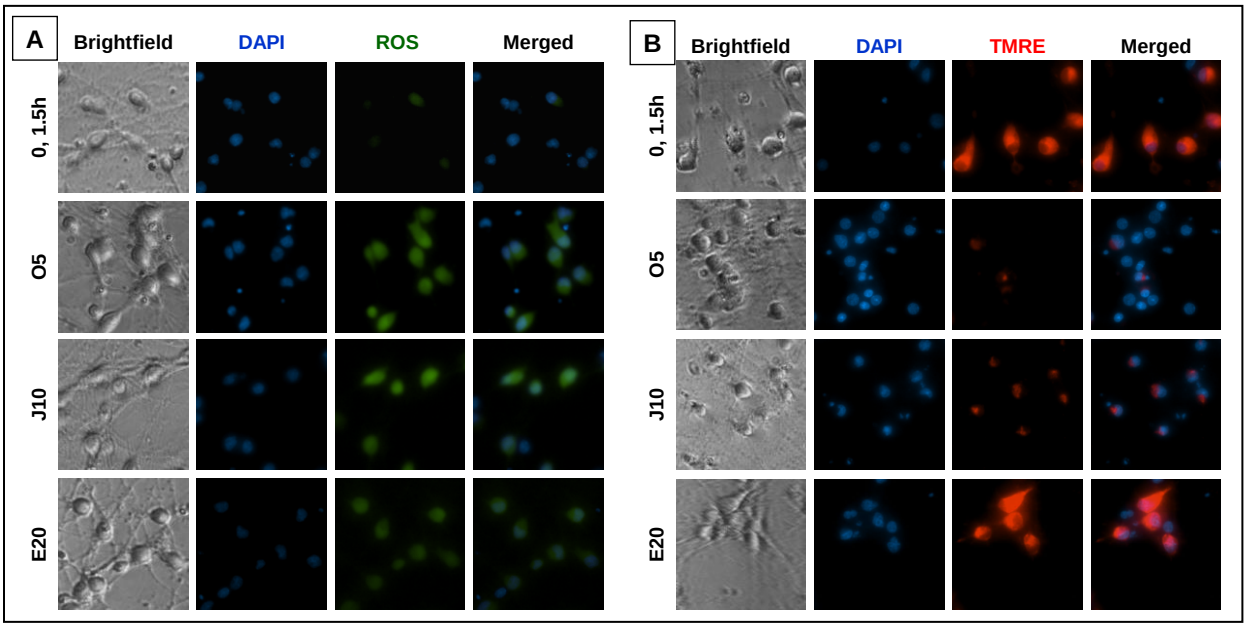

FIGURE 11. Effects of oligomycin (O, 5nM), PGJ2 (J, 10μM) and epoxomicin (E, 20nM) on **(A)** ROS assessed with H_2DCFDA (gain of green immunofluorescence), and **(B)** mitochondrial membrane potential ($\Delta\Psi_m$) assessed with TMRE (loss of red immunofluorescence) in rat midbrain cultures treated as indicated for 1.5h. Nuclei were counterstained with DAPI.

Oligomycin (O, 5nM) and PGJ2 (J, 10μM), but not epoxomicin (E, 20nM), decreased TMRE signal after 1.5h treatment, (Fig. 11B, loss of red immunofluorescence, previous page). This decline in TMRE signal by PGJ2 reflects a decrease in $\Delta\Psi_m$, that results, at least in part, from inhibiting complex I (34), and thus reducing proton efflux from the mitochondria. The decline in $\Delta\Psi_m$ caused by longer-term (not acute) oligomycin treatment is consistent with the overall loss of metabolic (i.e. namely NADH) activity (assessed by the MTT assay), and may also be caused by uncoupling proteins activated in response to prolonged elevation of $\Delta\Psi_m$ (189,190).

2.3.8. PACAP27 and cyclocreatine mitigate some of the effects of PGJ2 and oligomycin, respectively – cAMP-signaling has been shown to be neuroprotective(191). Particularly, we previously established that raising intracellular cAMP levels with the lipophilic peptide PACAP27 prevents the cleavage of TAU and caspase 3 activation induced by PGJ2 in rat cerebral cortical neuronal cultures (192). We now demonstrate in rat midbrain cultures (Fig. 12A, next page) that PACAP27 mitigates PGJ2-induced caspase activation (panel 2), caspase-dependent Parkin cleavage (panel 3), and loss in cell viability (panel 5). However, PACAP27 did not seem to cause a decline in the levels

of ubiquitinated proteins elevated by PGJ2 (Fig. 12A, panel 1).

PACAP27 failed to abolish the oligomycin effects that we analyzed in midbrain cultures (data not shown), thus we tested another protective approach. Since oligomycin inhibits ATP synthesis by mitochondria, we decided to increase ATP production by a different pathway, i.e. the phosphagen system. We did not consider activating glycolysis, since this approach can increase lactic acid production leading to pH changes. The phosphagen system involves phosphagen kinases, such as creatine kinase, that function to temporally buffer ATP levels in cells, including neurons, that display high and variable rates of aerobic energy production (193). To activate the creatine phosphate/creatine kinase (CP/CK) phosphagen system we treated rat midbrain cultures with cyclocreatine, as this compound is phosphorylated and dephosphorylated by CKs at the same rate as creatine, but has the advantage of crossing membranes due to its relatively planar structure(194). We show (Fig. 12B, next page) that cyclocreatine (CCr, 5mM) mitigated the oligomycin-induced ATP depletion (panel 6) and calpain-dependent cleavage of Parkin panel 2) and α-spectrin (panel 3), but did not affect the levels of ubiquitinated proteins (panel 1). Changes in cell viability are not apparent (panel 5), due to the short term treatment.

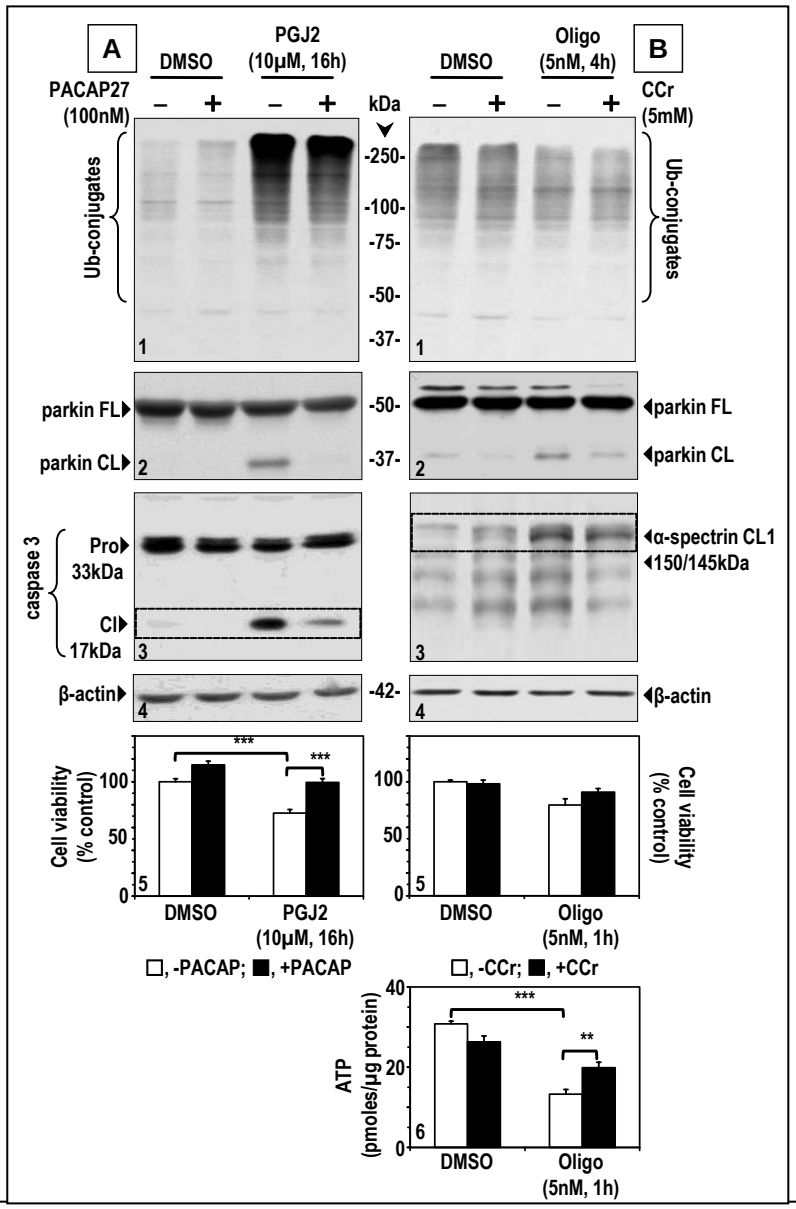

FIGURE 12. PACAP and cyclocreatine diminish the effects of PGJ2 or oligomycin (Oligo), respectively. Rat E18 midbrain cultures were treated with DMSO (0, control, vehicle), or: **(A)** PGJ2 (10μM, 16h) in conjunction with water (control, vehicle) or PACAP27 (100nM); in **(B)** Oligo [5nM, 1h (panels 5 & 6) or 4h (panels 1-4)] in conjunction with cyclocreatine (CCr, 5mM in medium). For the 4h Oligo treatment CCr was co-added and then added again two hours post-Oligo. Total lysates were analyzed by western blotting (50 μg of protein/lane) probed with the respective antibodies. Molecular mass markers in kDa are shown in the middle. Data represent one of at least three experiments for each condition. Cell viability (*panels 5*) was assessed with the MTT assay. Percentages represent the ratio between the data for each condition and control (100%). ATP steady state levels (pmoles/μg of protein) were measured with the luciferin/luciferase system. Values indicate means and s.e. from at least 4 determinations. *Asterisks* identify values that are significantly different as indicated, with $^{**}p<0.01$, $^{***}p<0.001$.

2.4. DISCUSSION

In this study we characterize the vulnerability of Parkin to proteasomal and mitochondrial impairment, and establish pharmacological approaches that maintain Parkin integrity. In particular, we address the effects of the endogenous product of inflammation PGJ2, the mitochondrial inhibitor oligomycin, and the proteasome inhibitor epoxomicin, on Parkin integrity in rat midbrain neuronal cultures.

We demonstrate that the three drugs induce Parkin cleavage to distinct fragments. Parkin cleavage triggered by PGJ2 and epoxomicin is mediated by caspase, while oligomycin provokes calpain-dependent Parkin cleavage. Caspase cleavage of Parkin was previously characterized in Parkin overexpressing cell lines treated with apoptotic inducers (195,196). The latter studies reported that caspase-1 and -8 directly cleave Parkin after Asp126 located within the linker region between its Ubl and RINGO domains, but the caspase-3 site remains unclear. The ubiquitin ligase activity of Parkin is abrogated by its caspase-cleavage, and this cleavage is not affected by the PD disease-causing mutations tested (195). PGJ2 is a product of inflammation postulated to activate the Fas/FasL death signaling pathway (33) and caspase 8 (192), thus linking inflammatory stress to caspase-mediated loss of Parkin ubiquitin ligase

activity and accumulation of its substrates. Furthermore, proteasome inhibition sensitizes cells to apoptosis mediated by the death signaling pathway via retardation of caspase-8 degradation (197,198), thus also linking proteasome impairment to loss of Parkin activity.

Upon ATP depletion, low ATP levels disable the plasma membrane Ca^{2+} pump (PMCA) and the sarcoplasmic/endoplasmic reticulum Ca^{2+}-ATPase (SERCA), which require ATP to pump cytosolic Ca^{2+} out of the cell or into the ER lumen, respectively (199). This disruption will cause an elevation of cytosolic Ca^{2+} leading to the activation of several Ca^{2+}–dependent proteases including calpain. We show that upon mitochondrial deficiency, calpain-cleavage of Parkin in midbrain neuronal cultures is induced by three mitochondrial toxins, olygomycin, antimycin and rotenone, which inhibit different elements of the electron transport chain. It is highly likely that this Parkin cleavage is due to calpain-dependent processing, as it is prevented by pre-treatment with a calpain inhibitor and not by a caspase inhibitor.

Calpains do not have a strict cleavage specificity, although some preferences for particular amino acid sequences, secondary structure (disordered regions) and PEST regions were suggested (200,201). To find a putative calpain cleavage site on Parkin, we used two computational programs [http://ccd.biocuckoo.org/ (202) and http://calpain.org (203)]. We predict two calpain

cleavage sites (P1 position) in human/rat full-length Parkin: (1) Gln71 within the following sequence in human: *IVHIV***Q**-*RPWRK* and in rat: *IVHIV***Q**-*RPQRK*, with a predicted molecular weight of 43.6, and located within the Ubl domain. (2) Ala134 within the following sequence in human: *KDSPP***A**-*GSPAG* and in rat: *SDSEA***A**-*RGPAA*, with a predicted molecular weight of 36.9, and located within the linker region between the Ubl and RINGO domains, close to the caspase-cleavage site.

From all reported Parkin alternative splicing variants [reviewed in (204)], transcript variant 3 (TV3) lacks exons 3-5 that encode for a.a. 58-206 of full-length Parkin (205). TV3 has a predicted molecular weight of ~36kDa (204) that is similar to the caspase- or calpain-cleaved forms of Parkin. However, since the latter Parkin forms are not detected in cells treated with caspase or calpain inhibitors, and TV3 lacks the caspase and calpain (predicted) cleavage sites, we conclude that the shorter Parkin forms detected in our studies are cleavage products of full-length Parkin.

One of the predicted Parkin calpain-cleavage sites (Ala134) is in close proximity to two Parkin phosphorylation sites (Ser131 and Ser136), identified in Parkin overexpressing cell lines upon treatment with the phosphatase inhibitor okadaic acid (206). The latter study established that Parkin is constitutively

phosphorylated at the N- and C-terminus, but its phospho/dephospho cycle is rapid as phosphatase inhibitors are necessary to detect phosphoparkin. In our current studies with rat midbrain cultures, we confirmed these findings, i.e. the stabilization of putative phosphoparkin upon treatment with okadaic acid. We also extend these results by predicting that phosphoparkin is less vulnerable to calpain-cleavage induced by oligomycin, as the levels of newParkin are decreased in the presence of okadaic acid. We speculate that phosphorylation at Ser131 and Ser134, in proximity to the calpain predicted cleavage site, protect Parkin from calpain cleavage. Furthermore, since okadaic acid exhibits selectivity for PP2A over PP1, the two most abundant serine/threonine phosphatases in mammalian cells (207), it is possible that PP2A curbs Parkin phosphorylation, just as it does for Tau hyperphosphorylation (208). These premises require verification in future studies.

The subcellular fractionation of Parkin with the midbrain cultures demonstrates that newParkin generated upon mitochondrial dysfunction localizes mostly to the mitochondrial fraction. In addition, the glycerol gradient sedimentation suggests that oligomycin treatment shifts the elution pattern of Parkin away from the 26S proteasome. Other studies showed that Parkin associates and regulates the 26S proteasome via binding of its Ubl domain to the Rpn10 subunit of the 26S proteasome

(90,144). Together, all of these findings suggest that upon mitochondrial impairment, calpain cleavage of Parkin promotes its dissociation from the 26S proteasome and its translocation to the mitochondria. We speculate that calpain-cleavage of Parkin at the putative Gln71 site located within its Ubl domain, could diminish the Parkin/Rpn10 interaction under conditions of ATP depletion when protein ubiquitination is limited by E1 inhibition as we previously demonstrated (184). This could free Parkin to translocate to mitochondria to promote mitophagy. Interestingly, the Arg to Pro mutation at position 42 of the Ubl domain of Parkin, identified in patients with autosomal-recessive juvenile parkinsonism (ARJP), disrupts the Rpn10-Parkin interaction(90). This disruption could mediate the "loss of function" of Parkin on the regulation of the 26S proteasome (144).

Overall, the above data support the notion that the Parkin-mitochondria-UPP link is affected by the product of inflammation PGJ2, and by mitochondrial as well as proteasomal impairment. Based on our observations, the mitochondrial deficit induced by PGJ2 increases ROS production without mitigating ATP levels, increases the levels of ubiquitinated proteins and caspase-mediated Parkin cleavage. These effects are replicated by proteasome inhibition with epoxomicin. In contrast, oligomycin significantly reduces mitochondrial production of ATP and

protein ubiquitination, and leads to calpain-mediated Parkin cleavage. Both of these situations are associated with PD pathogenesis, since both caspase and calpain activation are linked to PD (209). Two studies report the detection of Parkin processed to a ~41/42kDa form in human brains of a control (210) and a PD patient (211), but there is no discussion of the possible cleavage mechanisms. Potential neuroprotective strategies for PD should be aimed at targeting both apoptotic and nonapoptotic pathways. Since cAMP-signaling is considered to be neuroprotective(191), we tested the effects of raising intracellular cAMP levels with the lipophilic peptide PACAP in the rat midbrain cultures. PACAP27 mitigated the loss of cell viability, caspase 3 activation, and caspase-cleavage of Parkin induced by PGJ2, as well as epoxomicin-induced cleavage of Parkin (not shown here). Calpain-cleavage of Parkin induced by oligomycin, was diminished by cyclocreatine. The latter was used *in vivo* to improve cognition in mice with creatine transporter deficiency (194) and in other neurodegenerative conditions including PD (212). These data are highly significant to PD since Parkin dysfunction is associated with familial as well as sporadic forms of PD, thus it is of interest to develop means to prevent its cleavage and thus preserve its function.

CHAPTER III

Negative Regulation of 26S Proteasome Stability via Calpain-Mediated Cleavage of Rpn10 Upon Mitochondrial Dysfunction in Neurons

by

Qian Huang (黄倩)[1*], Hu Wang (王虎)[1*], Seth W. Perry[2], and Maria E. Figueiredo-Pereira[1]

[1]Department of Biological Sciences, Hunter College and Graduate Center, City University of New York, NY 10065, USA; [2]Department of Biomedical Engineering, University of Rochester, NY 14627, USA

***** - These authors contributed equally to this project and should be considered co-first authors

J Biol Chem. 2013 Apr 26;288(17):12161-74

NOTE: Hu Wang's data are identified under results

3.1. ABSTRACT

Proteasomal and mitochondrial dysfunction are implicated in chronic neurodegenerative diseases. To investigate the impact of mitochondrial impairment on the proteasome we treated rat cerebral cortical neurons with oligomycin, antimycin, or rotenone, which inhibit different elements of the electron transport chain. Firstly, we observed a reduction in ubiquitinated proteins and E1 activity. Secondly, we established that 26S proteasomes are disassembled with a decline in activity. Thirdly, we show to our knowledge for the first time, that calpain is activated triggering the selective processing of the 26S proteasome subunit Rpn10. Other proteasome subunits tested were not affected. Calpain also cleaved caspase 3 to an inactive fragment, thus preventing apoptosis that is an energy-dependent cell death pathway. In addition, calpain cleaved the microtubule associated protein TAU, a major component of neurofibrillary tangles in Alzheimer disease and other tauopathies. Fourthly, we detected a rise in 20S proteasome levels and activity. Finally, we show that both acute (16h) and long-term (up to seven days) mitochondrial impairment led to down-regulation of ubiquitinated-proteins, 26S proteasome disassembly, and a rise in 20S proteasomes. We postulate that upon mitochondrial dysfunction, ATP-depletion and calpain activation contribute to the demise of protein turnover by the ubiquitin/ proteasome

pathway. The concomitant rise in 20S proteasomes, which seem to degrade proteins in an unregulated and energy-independent manner, in the short term may carry out the turnover of randomly unfolded oxidized proteins. However, if chronic it could lead to neurodegeneration, as regulated protein degradation by the ubiquitin/proteasome pathway is essential for neuronal survival.

3.2. INTRODUCTION

Proteasome function is essential for neuronal homeostasis and survival. Neurons are also critically dependent on mitochondria for energy production necessary for maintaining homeostasis, neurotransmission and plasticity. There is a mutual dependence between mitochondrial and proteasomal function (213). Mitochondria provide ATP required for 26S proteasomal degradation of ubiquitinated proteins, some of which are mitochondrial proteins. Emerging evidence implicates proteasomal and mitochondrial dysfunction in ageing and neurodegenerative disorders such as Alzheimer disease (AD) (214,215). In neurons this is particularly important because, on the one hand neurons have a limited glycolytic capacity (216) thus are particularly sensitive to the ageing-associated decline in mitochondrial bioenergetics (217). On the other hand intraneuronal accumulation of ubiquitinated proteins, indicative of proteasome malfunction, is a hallmark of most chronic neurodegenerative

diseases including AD (218). Notably, the impact of mitochondrial impairment on proteasome function remains poorly defined.

One of the principal mechanisms by which mitochondrial dysfunction contributes to ageing and neurodegeneration is via the limitation in ATP production that can cause an energy crisis in neurons (219). Brain glucose hypometabolism is detected early in AD patients and is implicated in the initiation and progression of AD pathology (220). ATP loss in AD brains was estimated to reach as much as 50% in stable advanced dementia (221). This energy deficit may have a drastic impact on brain function. Degradation of proteins by the 26S proteasome is highly dependent on ATP binding and hydrolysis (222).

Another deleterious mechanism associated with mitochondrial dysfunction is a net increase in the production of reactive oxygen species (223). Oxidative stress induced by reactive oxygen species (ROS) alters the structure of cellular proteins (187) which, if not repaired, must be removed by proteolysis to prevent their accumulation and aggregation. One of the major roles of the proteasome is to degrade oxidatively modified proteins, but whether ubiquitination is required remains elusive (224). Some studies support the notion that oxidatively modified proteins in cells are removed by the 20S proteasome independently of ubiquitination (225). Others demonstrate that

upon oxidative stress there is an increase in the levels of ubiquitinated proteins, and in ubiquitin-activating and ubiquitin-conjugating enzyme activities, suggesting that the ubiquitination machinery is recruited to degrade oxidatively modified proteins (226). This is an important issue since there is ample evidence that neural tissue is especially vulnerable to oxidative stress, which plays an important role in many neurodegenerative disorders (227). Neurons exhibit a higher sensitivity to proteasome inhibition than astrocytes, mostly because they undergo increased levels of oxidized proteins (228). Impaired clearance of oxidatively modified proteins can cause their aggregation and directly promote progression of the neurodegenerative process (229). Both deleterious consequences of mitochondrial impairment, i.e. restricted ATP generating capacity and ROS production, are likely to contribute to impaired proteasome-dependent proteolysis in neurons (222,230,231).

It is postulated that in neurons even a modest restriction of ATP production by mitochondria far outweighs the negligible effects of ROS, although the underlying mechanisms are not clearly understood (219). In our current study with neurons, we demonstrate that low ATP levels caused by mitochondrial dysfunction, correlate with impairment of the ubiquitin/proteasome pathway (UPP): there is a decline in E1 and

26S proteasome activities, both of which are energy-dependent, with a concomitant rise in 20S proteasomes. This decline in UPP function occurs upon acute and long-term mitochondrial impairment. Notably, upon energy depletion, calpain activation leads to the selective cleavage of Rpn10, a 26S proteasome subunit. Other proteasome subunits tested were not affected. Rpn10 cleavage combined with ATP depletion, contribute to the demise of 26S proteasome function, a critical step in the UPP. We postulate that under acute mitochondrial stress conditions, unregulated and energy-independent protein degradation via 20S proteasomes could carry-out the degradation of randomly unfolded oxidized proteins. However, regulated and ATP-dependent protein degradation via the UPP is essential for long-term neuronal survival.

3.3. MATERIALS AND METHODS (THOSE THAT DIFFER FROM CHAPTER 2)

3.3.1. Materials – Primary antibodies: rabbit polyclonal anti-β5 (1:5000, cat# PW8895), mouse monoclonal anti-Rpt6 (1:2000, cat# PW9265), anti-Rpn10 (1:2000, cat# PW9250), anti-α5 (1:2000, cat# PW8125), anti-Rpn2 (1:2000, cat# PW9270), anti-Rpt5 (1:2000, cat# PW8770), all from ENZO Life Sciences, Inc.; rabbit polyclonal anti-UBE1a (1:1000, cat# 4890), and anti-E2-25K/Hip2 (1:1000, cat# 3847), all from Cell Signaling Technology; mouse

monoclonal TAU C5 (1:50000; detects all TAU isoforms; ep: a.a. 210–241), courtesy of Dr. L. Binder (Northwestern University, Chicago, IL).

3.3.2. Culture treatments –For long term (one day to 7 days) studies, neurons were maintained for the entire time in DMEM with 2% B27 supplemented with 0.5mM L-Glutamax and 1mM sodium pyruvate. Drugs were added once at the beginning of each experiment, following the same protocol as for the acute studies.

3.3.3. Cell viability assays – Cell viability with propidium iodide (Invitrogen) and 6-CFDA (Sigma) cell staining were carried out following the respective manufacturer's specifications.

3.3.4. Evaluation of endogenous E1- and E2-25k-ubiquitin thiol esters – Upon treatment with vehicle (control, DMSO) or with the respective drugs, cortical neurons were washed twice with PBS, harvested with a thiol stabilizing buffer [5mM Tris-HCl, pH 7.8, 8.7M urea, 1% Nonidet P-40, 20mM N-ethylmaleimide, 3mM EDTA, 2% protease inhibitor cocktail (Sigma)], and kept on ice for 15min for lysing, as described in (232). Samples were sonicated for 10s, centrifuged at 19,000X*g* for 15min at 4°C, mixed (30µg) 1:2 (volume) with thiol ester gel buffer (33mM Tris-HCl, pH 6.8,

2.7M urea, 2.5% SDS and 13% glycerol), and boiled for 5min. After determination of the protein concentration with the Bradford assay (Bio-Rad Laboratories), the normalized samples were separated into reducing (with 4% β-mercaptoethanol) and non-reducing (no β-mercaptoethanol) aliquots for SDS-PAGE, followed by western blotting with anti-E1 and anti-E2 antibodies, as described above.

3.4.RESULTS

3.4.1.Oligomycin, antimycin, and rotenone as mitochondrial inhibitors *(Hu Wang: antimycin and rotenone data)* –

To investigate the link between mitochondrial impairment and loss of neuronal viability, rat cerebral cortical neurons were treated with three mitochondrial inhibitors that affect different elements of the electron transport chain: *(1)* rotenone binds to ND1 and inhibits NADH–ubiquinone reductase activity of complex I (177), *(2)* antimycin A binds to the quinone reduction site of complex III (ubiquinol-cytochrome c oxidoreductase) inhibiting the reduction of cytochrome c (233), and *(3)* oligomycin binds to a polypeptide in the F0 baseplate and blocks ATP synthesis by the F0/F1 mitochondrial ATP synthase (173). As shown in Fig. 13A (next page), all three drugs decrease ATP levels in a concentration dependent manner. Oligomycin was the

most efficient, as 5nM of this drug lowered ATP levels by ~75%. The 25% ATP that remains upon oligomycin-treatment must be generated in a mitochondrial-independent manner by glycolysis. The decline in ATP levels induced a loss of neuronal viability (Fig. 13B) assessed with the MTT assay, which is reduced largely within the cytoplasm of most cells (234,235). From the three drugs tested, rotenone caused the weakest changes in all assays, except for ROS.

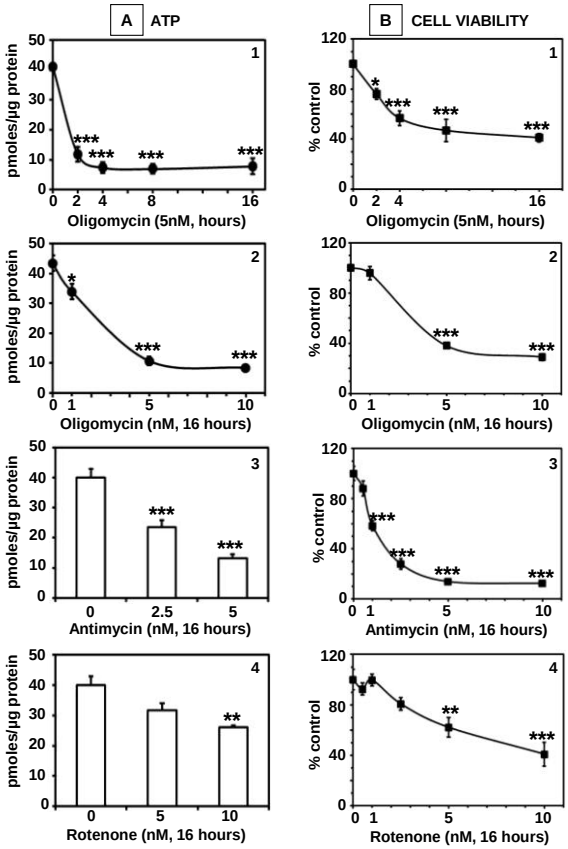

FIGURE 13. Effects of oligomycin, antimycin and rotenone on ATP levels and viability in rat cerebral cortical neurons. Neurons were treated with oligomycin (*panels 1 and 2*), antimycin (*panels 3*) and rotenone (*panels 4*) for the times and concentrations indicated. **(A)** ATP steady state levels (pmoles/µg of protein) were assessed with the luciferin/luciferase system. **(B)** Cell viability was assessed with the MTT assay. Percentages represent the ratio between the data for each condition and control (100%). Values indicate means and s.e. from at least three experiments per group. Asterisks identify values that are significantly different from control (* $p<0.05$; ** $p<0.01$; *** $p<0.001$).

3.4.2. Effect of oligomycin, antimycin, and rotenone on $\Delta\Psi_m$ and ROS ***(Hu Wang: all data)*** –

Oligomycin (5nM), antimycin (5nM), and rotenone (10nM) all decreased TMRE signal after 1.5h or 4h treatment, as did the protonophore FCCP (100 nM) (Fig. 14A, next page). This decline in TMRE signal is likely to reflect a decrease in $\Delta\Psi_m$. By inhibiting complex I and III respectively, and thus reducing proton efflux from the mitochondria, rotenone and antimycin are classically associated with decreased $\Delta\Psi_m$, as supported by our decline in TMRE signal. Under non-glycolytic conditions, acute oligomycin treatment is typically associated with increased $\Delta\Psi_m$ due to the oligomycin-induced blockade of proton influx through the ATP synthase. Oligomycin will decrease $\Delta\Psi_m$ when $\Delta\Psi_m$ is being maintained by reversal of the ATP synthase by hydrolyzing glycolysis derived ATP (236), but this scenario is not consistent with our oligomycin-induced decline in ATP levels at these same 1.5h and 4h time points (Fig. 13). Rather, a decline in $\Delta\Psi_m$ caused by longer-term oligomycin treatment would be consistent with the overall loss of metabolic (i.e. namely NADH) activity we observed by MTT assay at these same time points, and may also be caused by uncoupling proteins activated in response to prolonged elevation of $\Delta\Psi_m$ (189,190).

ROS are generated whenever electron transport through the ETC is slowed (185,186). As expected ROS production in response to 1.5h or 4h oligomcyin (5nM), antimycin (5nM), and rotenone (10nM) treatment was elevated as measured by H_2DCFDA fluorescence (Fig. 14B). For the TMRE and ROS measurements, only the 1.5h and 4h time points were quantified because quantification of later time points would be confounded by significant loss of cell integrity and thus not informative.

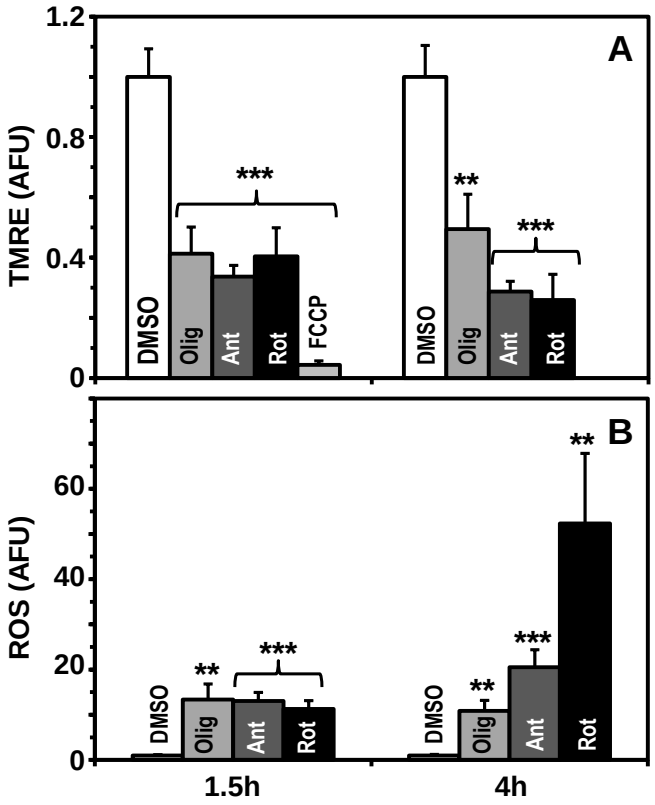

FIGURE 14. Effects of oligomycin (Olig), antimycin (Ant) and rotenone (Rot) on mitochondrial membrane potential $\Delta\Psi_m$ and ROS in rat cerebral cortical neurons. Neurons were treated with oligomycin (5nM), antimycin (5nM) and rotenone (10nM) for the times indicated. **(A)** Mitochondrial membrane potential ($\Delta\Psi_m$) was assessed with TMRE. The effect of the uncoupler FCCP (carbonylcyanide-p-trifluoromethoxyphenylhydrazone) is shown for comparison. **(B)** ROS was assessed with H_2DCFDA. Total fluorescence from cells was quantified in each image field using ImageJ. Values (AFU, arbitrary fluorescent units) indicate means and s.e. from 10-15 images per group pooled over two independent experiments for each group, and normalized to time-matched DMSO (vehicle) control = 1. Asterisks identify values that are significantly different from control (** p<0.01; *** p<0.001).

3.4.3. The decline in polyubiquitinated proteins induced by the three mitochondrial inhibitors is linked to E1 failure

(Hu Wang: antimycin and rotenone data) –

Chronic neurodegenerative disorders like AD, are linked to mitochondrial dysfunction and to accumulation/aggregation of ubiquitinated (Ub) proteins (237). We examined the effect of the three mitochondrial inhibitors on Ub-protein levels in the cortical neurons. Oligomycin and antimycin decreased Ub-proteins in a concentration (Fig. 15A and 15B, panels 1, below) and time (established for oligomycin, Fig 15C, panel 1) dependent manner. Only the highest concentration of rotenone tested (10nM) significantly lowered Ub-protein levels. In neurons treated with oligomycin, but not with antimycin or rotenone, the decline in Ub-proteins coincided with a rise in free mono ubiquitin, observed in a concentration (Fig. 15B, panel 2) and time (Fig. 15C, panel 2) dependent manner. The effect of prostaglandin J2 (J2) on Ub-proteins in neurons is shown for comparison in Fig. 15E. J2 is an endogenous product of inflammation (27) shown to increase the levels of Ub-proteins (238), in contrast to the mitochondria toxins.

To address a mechanism mediating the decline in Ub-proteins induced by oligomycin, we focused on the E1A ubiquitin activating enzyme, and on the E2 conjugating enzyme E2-25K. E1 activity requires ATP for formation of a thiol ester adduct with

ubiquitin, a process that is sensitive to reducing agents, such as β-mercaptoethanol (239). In principle, if E1 activity is impaired all protein ubiquitination including E1-E2 transthiolation, should be diminished. To assess E1- and E2-ubiquitin thiol ester levels, the samples were run on SDS-PAGE under reducing (with β-mercaptoethaol) and non-reducing (without β-mercaptoethaol) conditions. As shown in Fig. 15D (panels 1 and 4, left lanes), under non-reducing conditions E1-ubiquitin thiol ester (~126kDa) migrated ~9kDa above native E1 (117kDa), consistent with the additional mass of ubiquitin. Oligomycin- and antimycin-treatment abolished the E1-ubiquitin thiol ester, reflecting the loss of the ubiquitin monomer. The effect of rotenone on E1-ubiquitin thiol ester was very minor (undetectable). A similar pattern was observed for the E2 conjugating enzyme E2-25K. Its E2-ubiquitin thiol ester (~33kDa), which is dependent on E1 transthiolation activity, was eliminated in neurons treated with oligomycin (Fig. 15D, *panel 2*, *three left lanes*). Under reducing conditions (Fig. 15D, panel 1 and 4, right lanes) only native E1 and E2 were detected. Together these data demonstrate that due to mitochondrial impairment, ATP depletion in neurons prevents E1 from forming thiol ester intermediates with ubiquitin, resulting in an overall down-regulation of Ub-proteins.

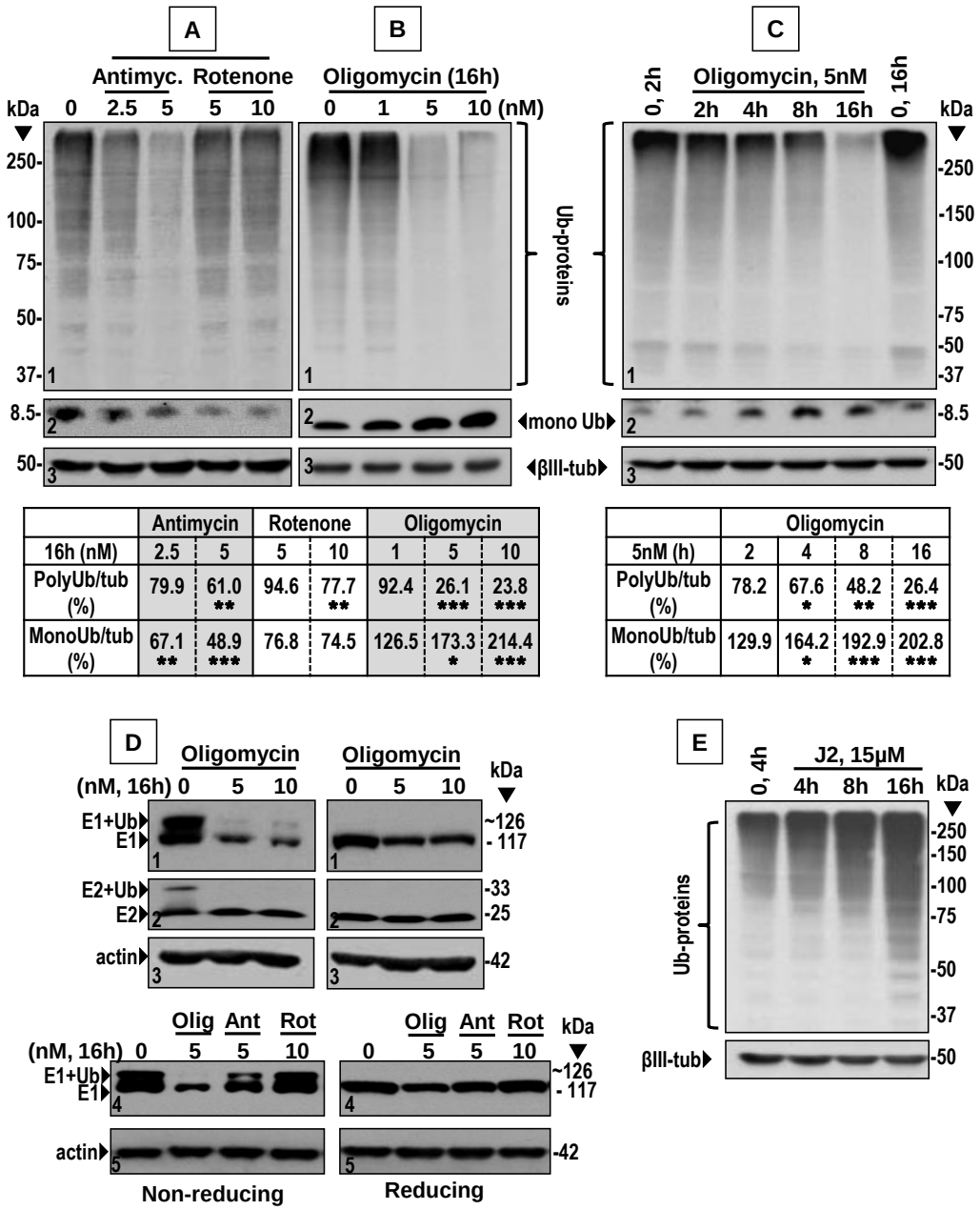

FIGURE 15. Effects of oligomycin, antimycin and rotenone on: ubiquitinated(Ub)-proteins and mono ubiquitin(Ub) in rat cerebral cortical neurons (A, B, and C), and on the levels of E1- and E2-ubiquitin thiol esters (D). Effect of prostaglandin J2 (15μM, J2) on ubiquitinated proteins (E). Rat cerebral cortical neurons were treated as indicated. Total lysates were analyzed by western blotting (30 μg of protein/lane) probed with the respective antibodies to detect in: **(A, B and C)** - Ub-proteins (*panels 1*), free mono ubiquitin (*panels 2*), and βIII-tubulin (βIII-tub, loading control, *panels 3*); **(D)** - E1-ubiquitin (Ub) and E2-Ub thiol esters (*upper bands*) and native E1 and E2 (*lower bands)* run under non-reducing conditions (*left side panels*), or reducing conditions with β-mercaptoethanol (*right side panels*); actin (loading control, *panels 3 and 5*); **(E)** - Ub-proteins and βIII-tub (loading control). Molecular mass markers in kDa are shown on the left and right. In A, B and C the levels of ubiquitinated proteins (polyUb/βIII-tub) and mono Ub, (monoUb/βIII-tub) were semi-quantified by densitometry (*values in tables*). Data represent the percentage of the pixel ratio for Ub-proteins and monoUb over the respective loading control for each condition compared to control (100%). Values are means from at least three experiments. Asterisks identify values that are significantly different from control (*p<0.05, **p<0.01, ***p<0.001).

3.4.4. Perturbing mitochondria in neurons causes a decline in 26S proteasomes and a concomitant increase in 20S proteasomes

(Hu Wang: antimycin and rotenone data) –

The activity and assembly of 26S proteasomes are highly dependent on ATP binding and hydrolysis (222,240). We thus assessed with the native in-gel assay, the effects of the three mitochondrial inhibitors on proteasome activity and levels in the cortical neurons. The in-gel assay detects the three assembled forms of the proteasome: 26S proteasomes with either two regulatory caps [26S (2)] or one cap [26S(1)], and the 20S core particle alone (20S). Proteasome activity was determined with the substrate Suc-LLVY-AMC, which assesses the chymotrypsin-like activity (Fig. 16A, B and C, panels 1). Under control conditions (lanes marked with "0"), the activity of the 20S proteasome is substantially lower than that of the 26S, because the 20S is a latent proteasome form (241). Proteasome levels were determined by immunoblotting with the anti-Rpt6 antibody that reacts with an ATPase subunit of the 19S particle (Fig. 16A, B and C, panels 2), and with the anti-β5 antibody (Fig. 16A, B and C, panels 3). The β5 subunit is a component of the 20S core, thus its antibody detects assembled 26S and 20S proteasomes. The three mitochondria inhibitors decreased 26S proteasome activity in a concentration (Fig. 16A and B, panels 1) and time (oligomycin, Fig. 16C, panel 1) dependent manner.

Furthermore, the three drugs caused the disassembly of the 26S proteasome, as its levels decreased while those of the 20S proteasome increased (Fig. 16A, B and C panels 2 and 3). Semi-quantification of proteasome activity and levels for each condition is listed in the respective tables shown in Fig. 16.

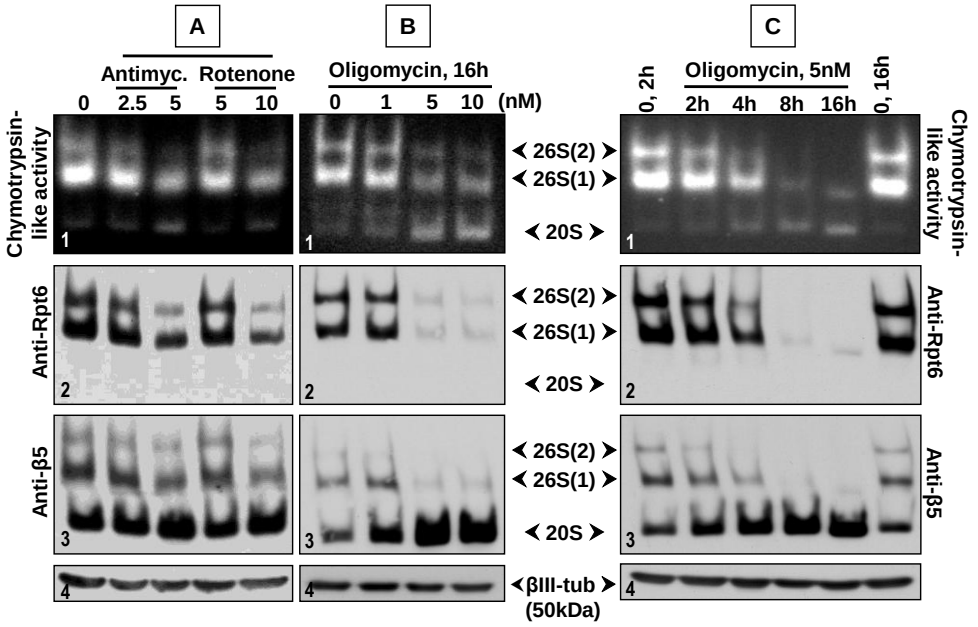

Proteasome activity

	Antimycin		Rotenone		Oligomycin		
16h (nM)	2.5	5	5	10	1	5	10
26S (2) (%)	64.5 ***	17.8 ***	74.3	42.1 **	87.2	20.6 ***	14.5 ***
26S (1) (%)	99.8	57.3 **	80.4	57.8 *	104.6	49.5 **	43.3 **
20S (%)	184.5	237.6 *	95.1	103.9	179.6	290.0 **	298.3 **

	Oligomycin			
5nM (h)	2	4	8	16
26S (2) (%)	87.4	57.7 **	16.4 ***	19.2 ***
26S (1) (%)	90.0	76.1	34.4 ***	43.8 **
20S (%)	146.4	225.4	357.5 ***	279.4 *

Proteasome levels

	Antimycin		Rotenone		Oligomycin		
16h (nM)	2.5	5	5	10	1	5	10
26S (2) (%)	63.2 *	13.2 ***	80.5	43.5 *	99.7	6.38 ***	5.11 ***
26S (1) (%)	100.4	63.6 *	93.6	74.1 **	118.6	25.1 ***	15.0 ***
20S (%)	137.2 *	165.3 ***	87.3	120.0	152.2	266.6 ***	290.8 ***

	Oligomycin			
5nM (h)	2	4	8	16
26S (2) (%)	84.9	63.0 ***	5.7 ***	3.3 ***
26S (1) (%)	89.6	76.2	23.6 ***	43.9 **
20S (%)	119.2	181.6	258.4 **	286.8 ***

FIGURE 16. Effects of oligomycin, antimycin and rotenone on proteasome activity and levels in rat cerebral cortical neurons. Neurons were treated for 16h with antimycin or rotenone **(A)** or oligomycin **(B),** or with 5nM oligomycin for different time points **(C)**. Cleared lysates (30µg/sample) were subjected to non-denaturing gel electrophoresis as described under "Experimental Procedures". Fully assembled 26S and 20S proteasomal (*indicated in the middle by arrows*) chymotrypsin-like activity was assessed with Suc-LLVY-AMC by the in-gel assay (*panels 1*). Proteasome levels were detected by immunoblotting with anti-Rpt6 (*panels 2*) and anti-β5 antibodies (*panels 3*). Proteasome chymotrypsin-like activity and levels were semi-quantified by densitometry (*values in tables*). Percentages represent the ratio between data for each condition and control (DMSO) considered to be 100%. Values are means from at least three experiments. Asterisks identify values that are significantly different from control (*p<0.05, **p<0.01, ***p<0.001).

We corroborated by glycerol gradient fractionation that mitochondrial dysfunction in neurons causes a shift from 26S to 20S proteasomes (Fig. 17, next page). Since oligomycin has the strongest effect, we only tested this drug here. Total extracts from cells treated with vehicle (DMSO, control) or oligomycin (5nM, 8h) were fractionated by glycerol density gradient centrifugation. Fractions were analyzed for Suc-LLVY-AMC hydrolysis which reflects the chymotrypsin-like activity (graph). Compared to control, the chymotrypsin-like activity of oligomycin-treated cells was significantly reduced in the fractions corresponding to the elution of the 26S proteasomes: fractions 12-16 (peak for 26S), compare oligomycin-treatment (*white squares*) with control (*black squares*). In contrast, the activity of 20S proteasomes (fractions 7-9, peak for 20S) was increased in the oligomycin-treated cells.

To confirm the proteasome elution pattern, aliquots from each fraction were subjected to western blot analyses with the anti-Rpt6 antibody that reacts with an ATPase subunit of the 19S particle (rows 1 and 3, control and oligomycin-treated, respectively), and the anti-α5 antibody that reacts with a subunit of the 20S core particle, (rows 2 and 4, control and oligomycin-treated, respectively). From these experiments we can conclude that an 8h treatment with 5nM oligomycin triggers the

disassembly of 26S proteasomes with a parallel increase in 20S proteasomes.

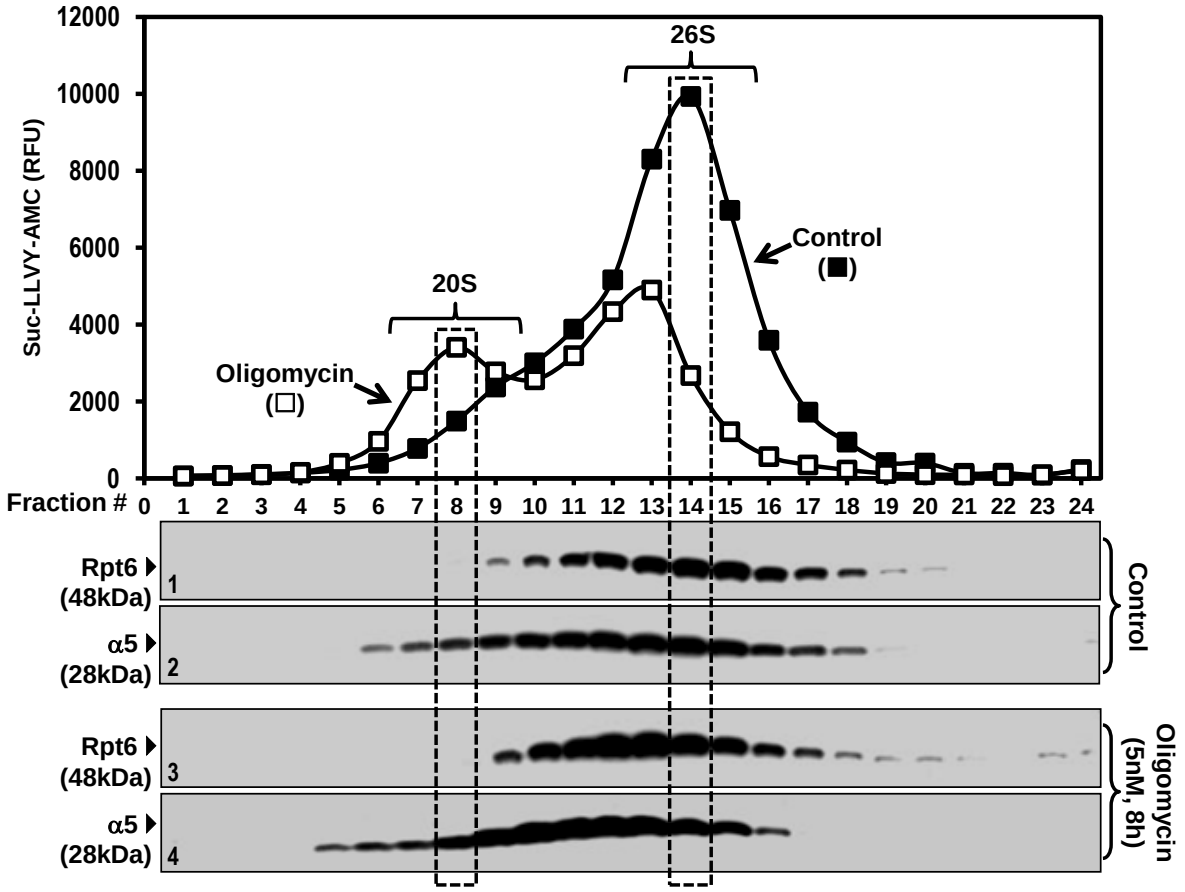

FIGURE 17. **Effects of oligomycin on the sedimentation velocity of proteasomes in rat cerebral cortical neurons.** Total lysates (one mg protein/sample) were fractionated by glycerol density gradient centrifugation (10-40% glycerol corresponding to fractions 1 to 24). Aliquots (50μl) of each fraction obtained from control (*black squares*), and oligomycin (5nM, 8h, *white squares*) treated cells were assayed for chymotrypsin-like activity with Suc-LLVY-AMC (*top graph*). Immunoblot analyses of each fraction probed with antibodies that react with Rpt6 (19S regulatory particle, *panels 1 and 3*) or α5, (core particle, *panels 2 and 4*). Proteins were precipitated with acetone from 450μl of each fraction. Similar results were obtained in triplicate experiments.

3.4.5. Mitochondrial dysfunction causes a selective decline in the levels of the Rpn10 subunit of the 19S particle that concurs with calpain but not caspase activation

(Hu Wang: antimycin and rotenone data) –

We considered that the decrease in 26S proteasome levels induced by oligomycin could be caused by a reduction in subunit levels. We thus investigated the effect of oligomycin on subunits of the 19S (Rpn2, Rpt5, Rpt6, and Rpn10) and 20S (α5 and β5) proteasome particles. Notably, from all of the proteasome subunits tested, only Rpn10 levels were reduced by oligomycin in a concentration (Fig. 18A, top row) and time (Fig. 18B, *top row*) dependent manner.

Since oligomycin triggers a loss of neuronal viability, we contemplated the possibility that apoptosis was induced and that the ensuing caspase activation was responsible for cleaving Rpn10, thus decreasing its levels. However, we did not observe cleavage of pro-caspase 3 (33kDa) to its active form (17kDa) in neurons treated with oligomycin (Fig. 18C, panel 1). Instead, pro-caspase 3 was processed to a ~29kDa fragment (Cl-caspase 3) and not to its active 17kDa form. The latter 17kDa fragment triggered by the endogenous product of inflammation prostaglandin J2 (J2), is shown for comparison in Fig. 18C (panel 1, last lane). J2 induces apoptosis in neurons (33).

We next investigated if calpain was activated upon mitochondrial dysfunction by assessing cleavage of one of its substrates, α-spectrin. Oligomycin-treatment clearly induced cleavage of α-spectrin (280kDa) to 145/150kDa fragments, which are indicative of calpain activation (Fig. 18C, *panel 2*). In

contrast, there was no detection of the 120kDa α-spectrin fragment, a marker of apoptotic cell death generated by caspase 3 processing of α-spectrin (242). For comparison, J2-induced cleavage of α-spectrin to the caspase-mediated 120kDa fragment is shown (Fig. 18C, panel 2, last lane). Oligomycin also induced the cleavage of another calpain substrate, the microtubule associated protein TAU (Fig. 18D, panels 1 and 2). TAU is a major component of neurofibrillary tangles in AD (243). Together, these results suggest that the selective decline in Rpn10 induced by mitochondrial dysfunction may be triggered by calpain-mediated processing. **FIGURE 18 (below and next page)**

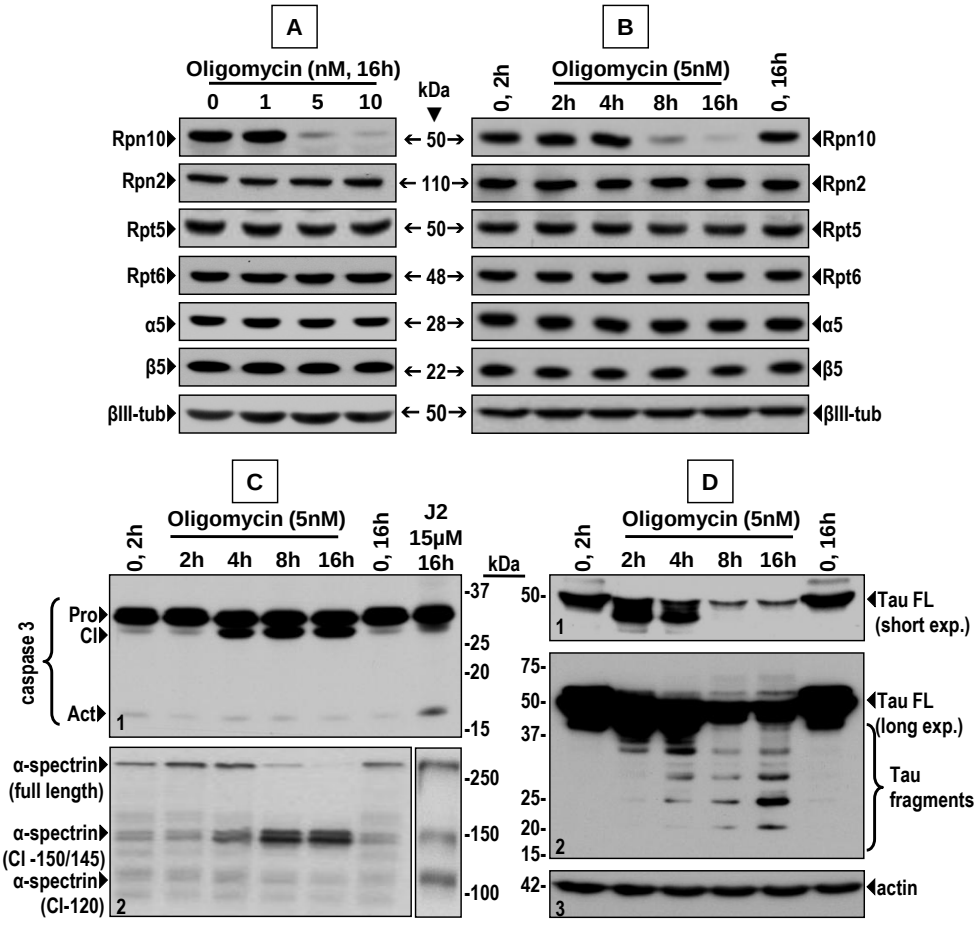

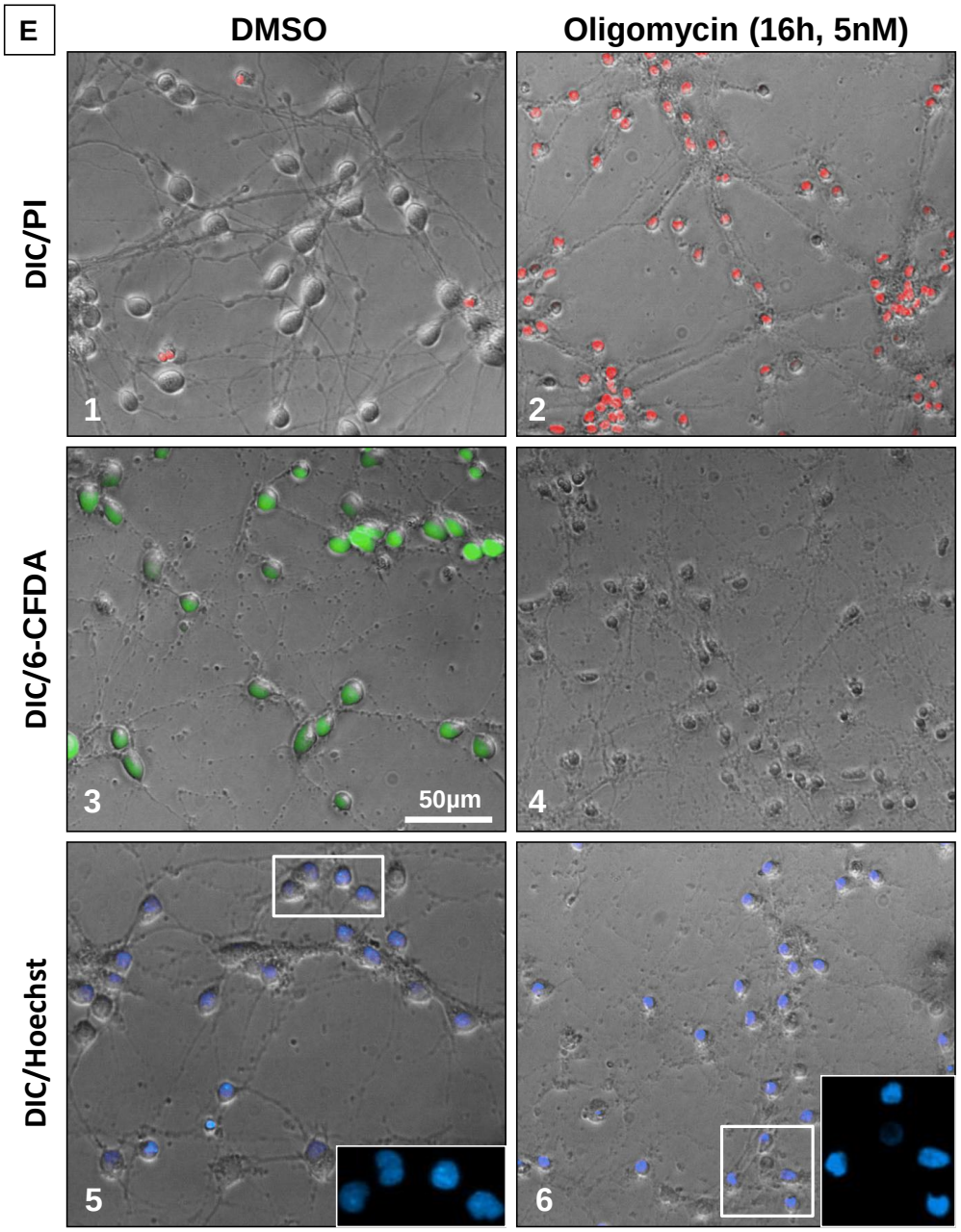

FIGURE 18. Effects of oligomycin on proteasome subunit levels (A and B), caspase 3 and α-spectrin (C), and TAU cleavage (D) in rat cerebral cortical neurons. Neurons were treated as indicated. Total lysates were analyzed by western blotting (30 µg of protein/lane) probed with the respective antibodies to detect in: **(A and B)** - proteasome subunits (19S particle: Rpn10, Rpn2, Rpt5 and Rpt6; 20S core: α5 and β5) and βIII-tubulin (loading control); **(C)** – caspase 3 (*panel 1*) and α-spectrin (*panel 2*); the effect of J2 is shown for comparison; **(D)** – TAU (*panels 1 and 2*) and actin (loading control, *panel 3*). Molecular mass markers in kDa are shown in the center (A and B), on the right (C) and on the left (D). Similar data were obtained in triplicate experiments. Pro (full length), Cl (cleaved) and Act (active) caspase 3; Tau FL, full length TAU. **(E)** Fluorescence staining with propidium iodide (PI, *panels 1 and 2*), 6-CFDA (*panels 3 and 4*), and Hoechst (*panels 5 and 6*) of neurons treated as indicated. In panels 5 and 6, the nuclei of the neurons within the white boxes are magnified and shown on the bottom right of each panel. DIC, differential interference contrast images. Similar results were obtained in triplicate experiments.

Fluorescence staining confirmed that oligomycin induces necrosis. Propidium iodide (PI) staining of oligomycin-treated neuronal cultures (Fig. 18E, panel 2) indicates necrotic cell death, as due to their extensive membrane damage, PI quickly moves into necrotic cells. The intact membrane of living cells (Fig. 18E, panel 1) and apoptotic cells prevents PI cell entry (244). Although apoptosis affects mainly the nucleus, in its later phases the plasma membrane becomes leaky and can also uptake PI (244). Staining with 6-carboxyfluorescein diacetate (6-CFDA) is used to detect living cells. When this non-fluorescent compound enters living cells, it is hydrolyzed by esterases generating 6-carboxyfluorescein that appears as green fluorescence (245). Thus, necrotic cells do not appear green (Fig. 18E, panel 4) while living cells do (Fig. 18E, panel 3). Nuclear morphology is shown with Hoechst staining (Fig. 18E, panels 5 and 6).

We established that antimycin mimics the effects of oligomycin on Rpn10, caspase 3, α-spectrin, and TAU cleavage (Fig. 19,next page). However, rotenone had only weak or undetectable effects on the cleavage of the latter proteins (Fig. 19). Since Rpn11, a deubiquitinating subunit, is linked to mitochondrial function (246), we investigated if its levels were altered by any of the three mitochondrial inhibitors. As shown in Fig. 19 (*panel 2*) no changes in Rpn11 were detected.

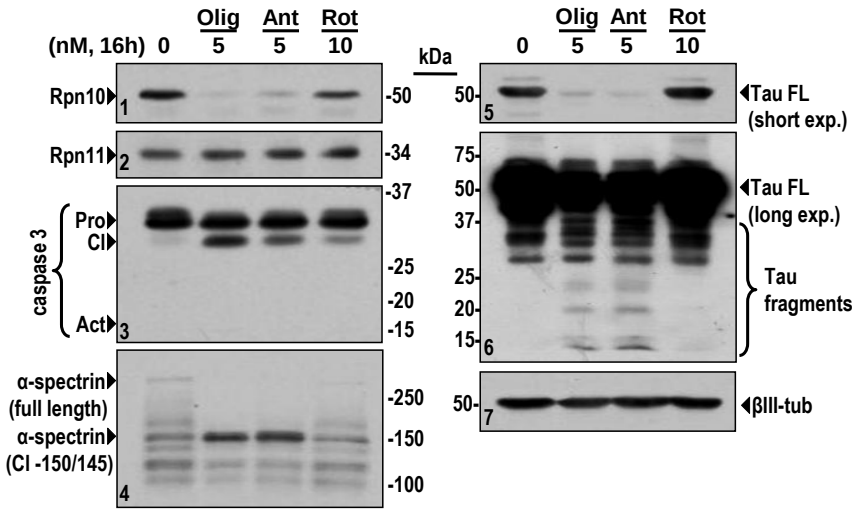

FIGURE 19. Effects of antimycin and rotenone on Rpn10 (*panel 1*), Rpn11 (*panel 2*), caspase 3 (*panel 3*), α-spectrin (*panel 4*), and TAU cleavage (*panels 5 & 6*) in rat cerebral cortical neurons. Neurons were treated for 16h with antimycin (Ant) or rotenone (Rot). Oligomycin (Olig) was included for comparison. Total lysates were analyzed by western blotting (30 μg of protein/lane) probed with the respective antibodies; βIII-tubulin (βIII-tub, loading control). Molecular mass markers in kDa are shown in the center. Similar data were obtained in triplicate experiments. Pro (full length), Cl (cleaved) and Act (active) caspase 3; Tau FL, full length TAU.

3.4.6. Upon mitochondrial impairment, Rpn10 is processed by calpain and not by proteasomes or lysosomes

(Hu Wang: Fig. 20B, C and D)–

Since oligomycin has the strongest effect, we only focused on this drug here. To sort out which proteolytic activity processes Rpn10 upon treatment with oligomycin, we pretreated neurons with inhibitors of the proteasome (Ep, epoxomicin), lysosome (CQ, chloroquine), and calpain [calpain inhibitor III (Cp3, Z-Val-Phe-CHO) and calpeptin (Cpt, Z-Leu-Nle-CHO)]. Only the calpain inhibitors (Fig. 20A, dashed box) prevented the decline in Rpn10 (panel 1). Furthermore, the calpain inhibitors blocked cleavage of pro-caspase 3 (panel 2), α-spectrin (panel 3), and TAU (panel

4). Pre-treatment with the calpain inhibitors also prevented the decline in 26S proteasome activity (Fig. 20B, panel 1) and assembly (Fig. 20B, panels 2 and 3) triggered by oligomycin. Surprisingly, Cp3 by itself inhibited 26S proteasome activity without triggering its disassembly, while Cpt stimulated the 20S proteasome. The two inhibitors *per se* did not alter proteasome levels by much, thus their individual effects on proteasome activity could be due to a secondary effect on the proteasome itself (for Cp3), and/or on a putative 20S proteasome activating factor regulated by calpain. Anyway, it is clear that the two calpain inhibitors prevented the negative effect of oligomycin on proteasomes.

The calpain inhibitors failed to prevent the decline in E1-activity (Fig. 20C) or the loss in viability induced by oligomycin (Fig. 20D). This is not surprising, since the calpain inhibitors target calpain, but not ATP depletion.

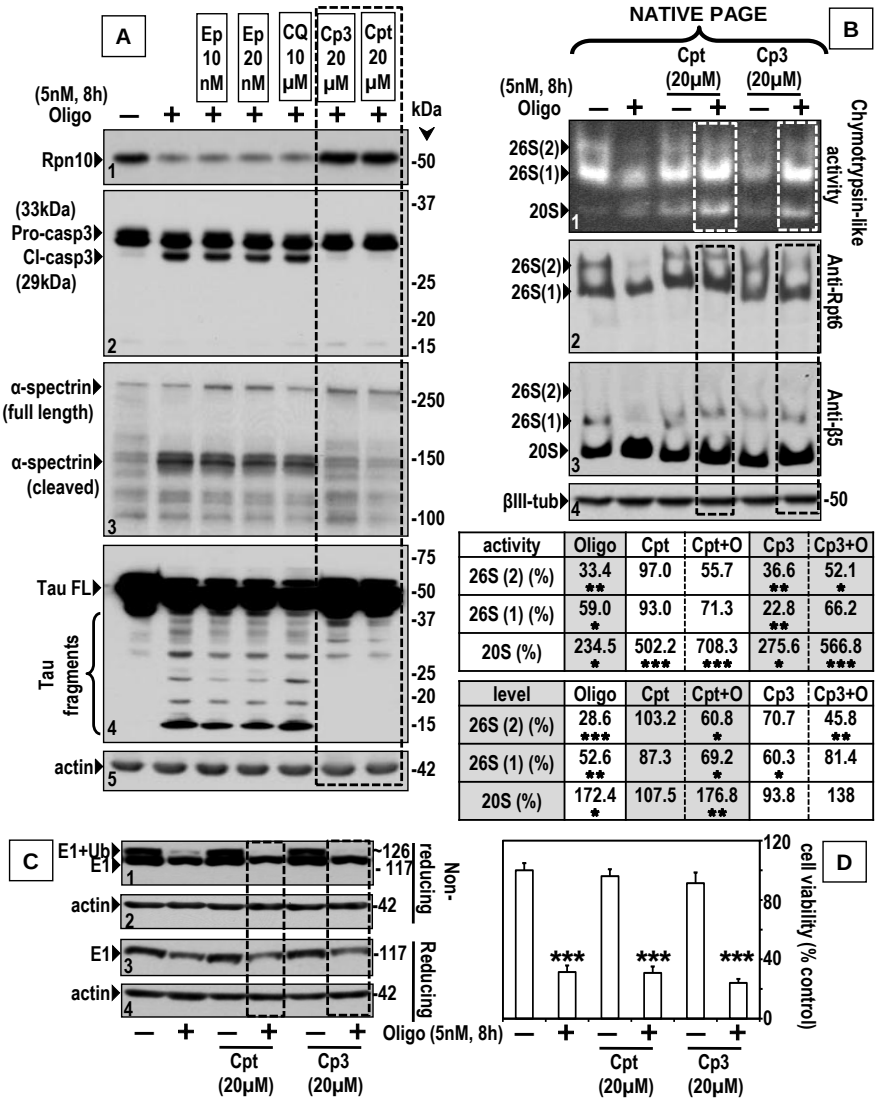

FIGURE 20. Calpain inhibitors but not proteasome or lysosomal inhibitors prevent/diminish the effects of oligomycin on: (A) Rpn10 (*panel 1*), caspase 3 (*panel 2*), α-spectrin (*panel 3*), and TAU (*panel 4*); (B) proteasome activity (*panel 1*) and levels (*panels 2 and 3*); but not on (C) E1-thiol ester, and (D) cell viability. Rat cerebral cortical neurons were pre-treated for 30min with epoxomicin (ep, proteasome inhibitor), chloroquine (CQ, lysosomal inhibitor), calpain inhibitor III (Cp3, Z-Val-Phe-CHO), calpeptin (Cpt, calpain inhibitor Z-Leu-Nle-CHO) where indicated, and then with oligomycin (Oligo). Total lysates were analyzed in: **(A and C)** - by western blotting (30 µg of protein/lane) probed with the respective antibodies using actin as loading control. In (A) panel 2, Pro (full length), Cl (cleaved) caspase 3; in panel 4, Tau FL, full length TAU. In (C) E1-ubiquitin (Ub) thiol ester (*upper bands*) and native E1 (*lower bands)* run under non-reducing conditions (*panels 1 and 2*), or reducing conditions with β-mercaptoethanol (*panels 3 and 4*). Molecular mass markers in kDa are shown on the right. Similar data were obtained in triplicate experiments. **(B)** – by the in-gel assay (30µg/sample) to assess 26S and 20S proteasome (*indicated on the left by arrows*) chymotrypsin-like activity (*panel 1*) and levels detected by immunoblotting with anti-Rpt6 (*panel 2*) and anti-β5 antibodies (*panel 3*). βIII-tubulin, loading control. Proteasome chymotrypsin-like activity and levels were semi-quantified by densitometry (*values in tables*). Percentages represent the ratio between data for each condition and control (DMSO) considered to be 100%. Values are means from at least three experiments. **(D)** Cell viability was assessed with the MTT assay. Percentages represent the ratio between the data for each condition and control (100%). Values indicate means and s.e. from 8 determinations per group. Asterisks identify values that are significantly different from control (* p<0.05; ** p<0.01; *** *p<0.001*).

3.4.7. Long-term (7 days) incubations with lower doses (one nM) of oligomycin mimicked the effects of acute (up to 16h) treatment with higher (5nM) oligomycin doses – In the previous experiments we investigated the effects of short-term (up to 16h) incubations with oligomycin (5nM). We also treated neurons with a low dose (one nM) of oligomycin for 7 days, to mimic the effect of chronic mitochondrial impairment. The same phenomena were observed upon the long 7 day treatment (Fig. 21): 26S proteasome activity (A, panel 1) and levels (B, panel 1), Ub-proteins (C), and ATP (D) all declined upon oligomycin treatment. To improve detection of the 20S proteasome, 0.04% SDS was added to the activity reaction buffer at the same time as the substrate. 20S proteasome activity (Fig. 21A, panel 2) and levels (Fig. 21B, panel 2) increased concurrently with the decline in 26S proteasomes.

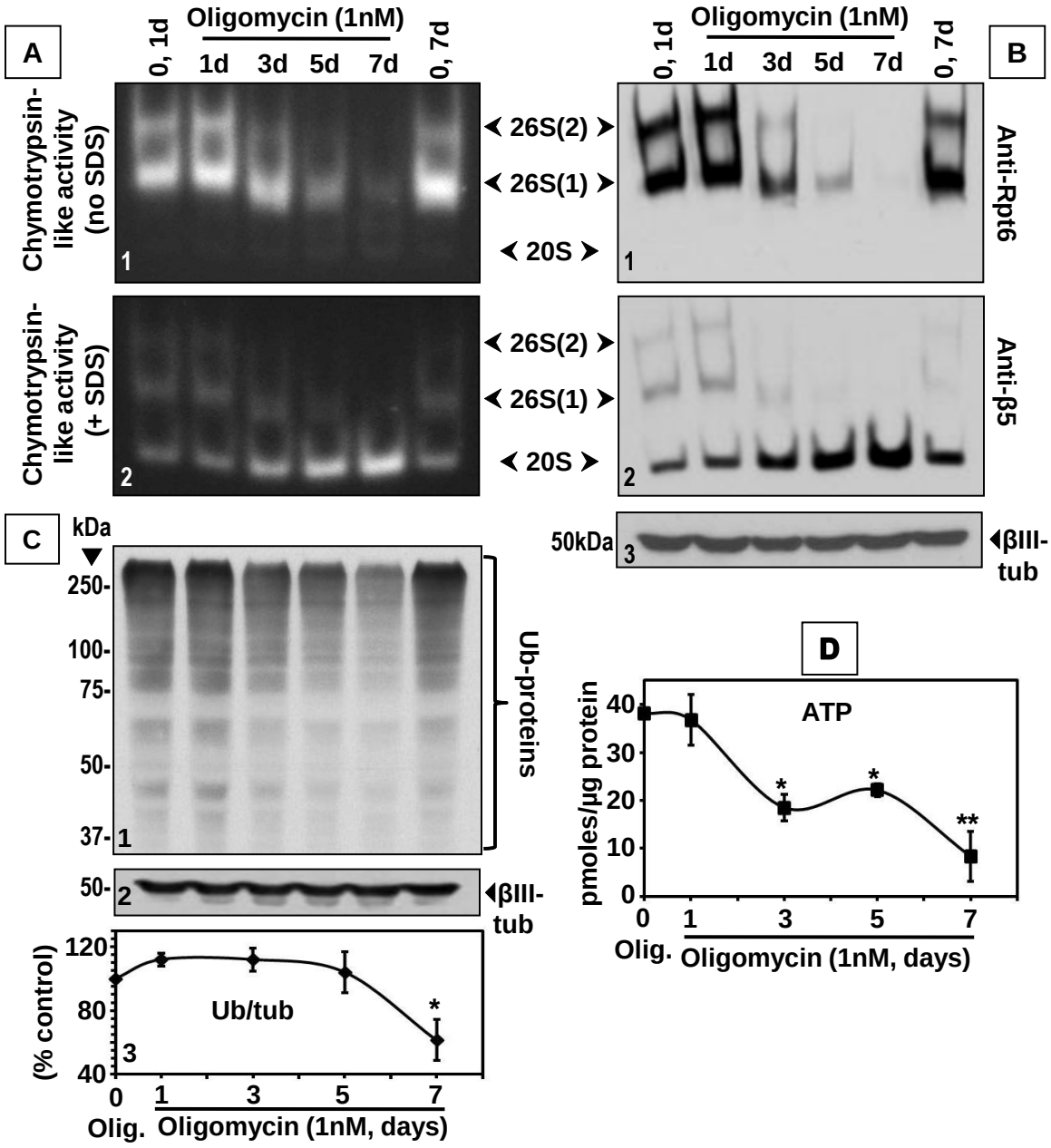

FIGURE 21. Effects of long-term incubations (up to 7 days) with oligomycin on rat cerebral cortical neurons. Neurons were treated with oligomycin (1nM) up to 7 days. Total lysates were analyzed by the in-gel assay (30μg/sample) to assess 26S and 20S proteasome **(A)** chymotrypsin-like activity (*panels 1 and 2*), and **(B)** levels detected by immunoblotting with anti-Rpt6 (*panel 1*), anti-β5 (*panel 2*) and anti-βIII-tubulin (βIII-tub, loading control) antibodies. Arrows in the middle indicate assembled 26S and 20S proteasomes. (**A**, *panel 2*) To improve detection of 20S proteasome activity, 0.04% SDS was added to the reaction buffer. In **(C)** lysates were analyzed by western blotting (30 μg of protein/lane) for ubiquitinated proteins (Ub-proteins). Molecular mass markers (kDa) are on the left. In **(D)** ATP steady state levels (pmoles/μg of protein) were assessed with the luciferin/luciferase system. Controls in **C** and **D** (0, Olig.) represent the average between one and 7 days without oligomycin. Values depict the mean and s.e. from at least three determinations. Asterisks identify values that are significantly different from control (* $p<0.05$; ** $p<0.01$).

3.5. DISCUSSION

In this study we characterize some of the mechanisms by which mitochondrial toxins (oligomycin, antimycin, and rotenone) affect the ubiquitin/proteasome pathway (UPP) in cortical neurons. It is clear that among the three drugs tested, rotenone caused the weakest changes on the UPP, as on ATP levels. In the first place, we show that mitochondrial impairment slows down the ubiquitination cascade by blocking its first step, i.e. by preventing ubiquitin-activation by the E1 enzyme. These results have implications for the sequence of events leading to chronic neurodegenerative diseases, such as AD, that are characterized by mitochondrial and UPP dysfunction. It is clear that these two phenomena are related in the course of AD. For therapeutic purposes, it would be important to determine which occurs upstream, UPP or mitochondrial impairment. On one hand, our data show that treatment with the three mitochondrial inhibitors blocks the ubiquitination cascade, thus diminishing the levels of ubiquitinated proteins instead of promoting their accumulation. On the other hand, it is well established that proteasome inhibition leads to accumulation of ubiquitinated proteins and affects mitochondrial function (247,248). Together these data support the notion that UPP impairment may precede mitochondrial dysfunction at least in the neurodegenerative process that leads to accumulation of ubiquitinated proteins.

In the second place, we demonstrate that mitochondrial impairment provokes the demise of 26S proteasomes in neurons. 26S proteasome dysfunction is caused by its disassembly that seems to be linked to selective processing of the Rpn10 subunit by calpain. Other proteasome subunits tested were not affected. Proteasome subunits Rpn2, Rpn10, and Rpt5 were reported to be cleaved in a caspase-mediated manner to facilitate the apoptotic program (249). Rpn10 is a subunit of the 19S regulatory particle that is a receptor for polyubiquitinated proteins (250,251), and was recently mapped to the apex of the 26S proteasome (252). We show now for the first time to our knowledge, that the decline in Rpn10 upon mitochondrial deficiency is due to calpain-dependent processing, as it is prevented by pre-treatment with calpain inhibitors and not by proteasome or lysosomal inhibitors. Calpains do not have a strict cleavage specificity, although some preferences for particular amino acid sequences, secondary structure (disordered regions) and PEST regions were suggested (200,201). To find a putative calpain cleavage site on Rpn10, we used two computational programs [http://ccd.biocuckoo.org/ (202) and http://calpain.org (203)]. We determined that a predicted calpain cleavage site on human Rpn10 is Ala360 (P1 position) within the following sequence: AIRNAMGSL***A***-SQAT.

Notably, an rpn10 mutant that binds the proteasome but not polyubiquitin chains rescued proteasome disassembly and loss of

viability in an *rpn11-1 rpn10Δ* lethal mutant (253). Another study showed that the levels of Rpn10 are diminished in old mice, while those of α5 remained unchanged. It was postulated that the decline in Rpn10 levels could be one of the major factors responsible for decreased proteasome function occurring with aging (254). These studies further support a critical requirement for Rpn10 in proteasome assembly.

Besides Rpn10, we observed calpain-mediated cleavage of two other proteins that are relevant to AD: caspase 3 and the microtubule associated protein TAU. Caspase 3 was cleaved to a fragment (29kDa) that seems to be associated with caspase inactivation (200). Calpain processing of caspase 3 to an inactive form could be a measure to prevent execution of the apoptotic pathway under conditions of ATP-deficit, as apoptosis is an energy-dependent death pathway (199). Calpain-activation is linked to ATP-depletion and necrosis, a cell death pathway characterized by a bioenergetic catastrophe (199). In fact, calpain-activation was shown to be induced by electron transport chain inhibitors, such as the ones used in our studies: rotenone, antimycin and oligomycin (255).

TAU is a major component of neurofibrillary tangles in AD and other tauopathies. TAU is reported to be cleaved by caspases and/or calpain depending on the pathological condition (256). Caspase 3-induced TAU cleavage at Asp 421 has a high tendency

for aggregation (243). Calpain-induced TAU fragments, including a typical "17 kDa" fragment, represents a marker for enhanced calpain activity in AD (257,258). We detected this typical 17kDa fragment in oligomycin- and antimycin-treated neurons, and observed preventive effects by calpain inhibitors. The dual vulnerability of TAU to calpain and caspases needs to be taken into consideration if preserving TAU integrity is considered as a therapeutic goal for AD and other tauopathies (256).

In the third place, we establish that mitochondrial toxins raise the activity and level of 20S proteasomes in neurons. It was proposed that 20S proteasomes in concert with immunoproteasomes degrade 70% to 80% of all oxidized proteins that are not aggregated (259,260). In addition, 26S proteasomes and the ubiquitination machinery are more vulnerable to oxidative damage than 20S proteasomes (261). Since we show that mitochondrial inhibitors cause a likely decline in $\Delta\Psi_m$ and elevate ROS, it is possible that 20S proteasomes are recruited under these conditions, to promote turnover of oxidized proteins, as these proteins may not be ubiquitinated (229,262). However, under mild conditions of oxidative stress, the UPP is up-regulated (224). Whether 26S or 20S proteasomes degrade oxidatively modified proteins remains to be confirmed.

In summary, our findings support a mechanism in neurons by which mitochondrial impairment causes a decline in the function

of the ubiquitin/proteasome pathway: the steps of the ubiquitin/proteasome pathway that are energy-dependent are down-regulated, i.e. ubiquitin-activation via E1 and 26S proteasome function. Concomitantly, 20S proteasome activity and levels are increased, possibly to promote protein degradation in a ubiquitin- and ATP-independent manner. Besides ATP-depletion, calpain activation promotes the switch from 26S to 20S proteasomes, as calpain processes the Rpn10 proteasome subunit. Rpn10 could act as a 26S proteasome gatekeeper to promote its disassembly when ATP is in short supply. Under low energy conditions, upgrading 20S proteasome levels and activity would ensure efficient protein degradation without energy expenditure. The reduction in ubiquitinated proteins and 26S proteasomes as well as the increase in 20S proteasomes in neurons was observed upon acute and long-term mitochondrial impairment. We postulate that under acute stress conditions, unregulated protein degradation as carried-out by 20S proteasomes may be sufficient to promote degradation of randomly unfolded oxidized proteins. However, regulated protein degradation by the ubiquitin/proteasome pathway is essential for long-term neuronal survival.

CHAPTER IV

MODEL AND CONCLUSIONS

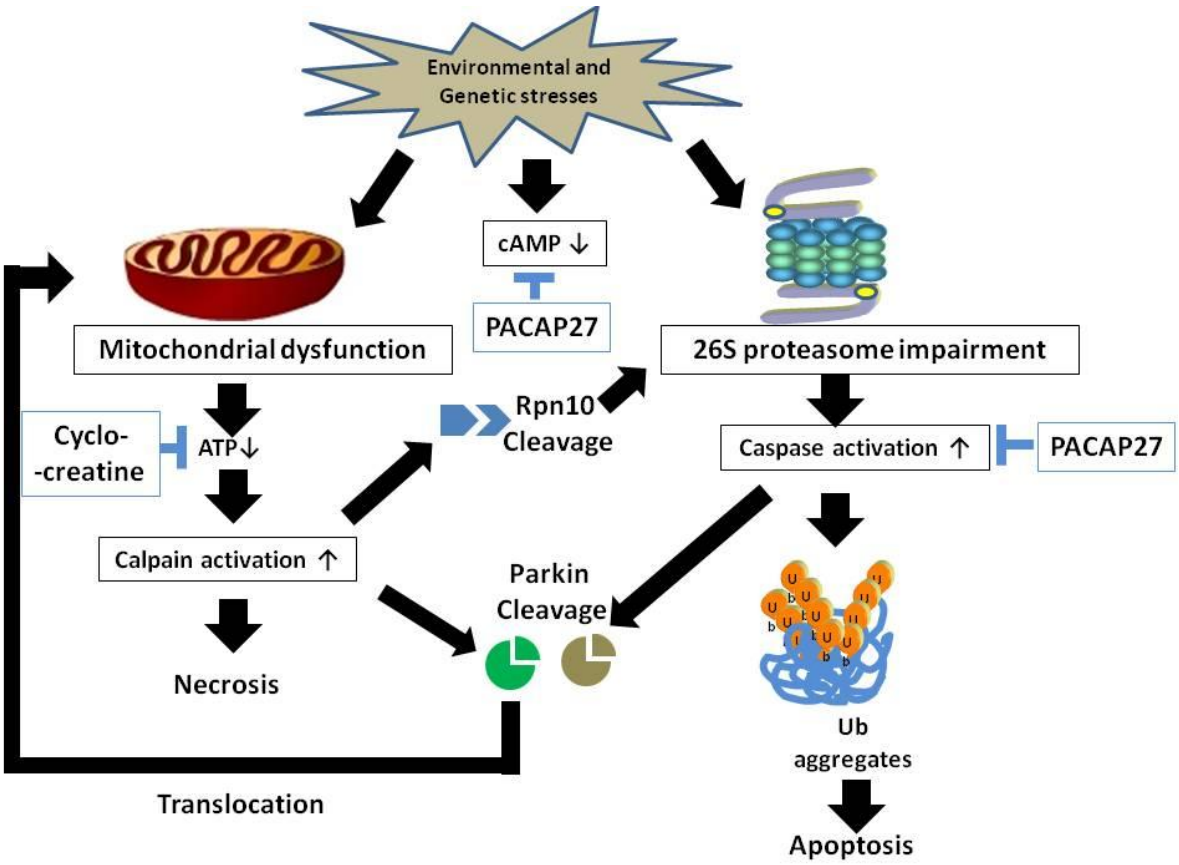

Neuroinflammation, mitochondrial impairment and UPP dysfunction, have long been individually attributed to be involved in the pathogenesis of PD. However emerging evidence suggests that PD is a multifactorial disorder (263,264). Few studies tried to integrate the relationship among these three pathological factors.

Our studies reveal that regardless of which of the factors neuroinflammation, mitochondrial impairment or proteasomal dysfunction cause neuronal damage resulting in caspase or calpain activation, they all lead to the cleavage of a common protein: Parkin. The newParkin identified upon mitochondrial

impairment translocates to mitochondria probably to regulate mitophagy. In addition to Parkin cleavage, our data reveal that calpain activation induced by mitochondrial impairment also cleaves Rpn10, resulting in the downregulation of 26S proteasomes with a concomitant increase in 20S proteasomes. As Parkin binds to the 26S proteasome via Rpn10 to deliver substrates for degradation, calpain-mediated Parkin cleavage could free newParkin for its translocation to mitochondria. Our data also establish that cyclocreatine preserves the integrity of full-length Parkin under conditions of ATP deficit induced by mitochondrial impairment. Furthermore, PACAP27 rescues midbrain neurons from caspase-cleavage of Parkin. Thus PACAP27 has neuroprotective potential against neuroinflammation and proteasomal inhibition in PD.

In conclusion, since PD is associated with multifaceted pathological mechanisms, we propose that to treat (stop/delay) the progression of neurodegeneration in PD, a combinatorial therapeutic approach that includes targeting necrosis (calpain activation) and apoptosis (caspase activation) is necessary.

CHAPTER V

FUTURE DIRECTIONS

We clearly show that both calpain and caspase activation lead to Parkin cleavage. This finding drives us to hypothesize that a common pathologic element among neuroinflammation, mitochondrial impairment and proteasomal dysfunction is Parkin cleavage.

Based on our data we propose the following future studies:

(1) Characterize calpain-cleavage sites in Parkin.

The caspase-cleavage site in Parkin is Asp126 (196). However, the calpain-cleavage site(s) in Parkin remains unclear. Based on our computational analysis with the two programs http://calpain.org] and [http://ccd.biocuckoo.org], we predict two calpain-cleavage sites in human/rat Parkin: Gln71 and Ala134. To verify this prediction, new experimental approaches including site-directed mutagenesis need to be carried-out:

1) *In vitro* cleavage assay: incubate purified calpain with purified Parkin Q71 mutant and Parkin A134 mutant *in vitro* and then, by western blotting analyze whether NewParkin is detected. If newParkin is not detected, this means that our prediction is correct.

2) *In vivo* cleavage assay: transfect SK-N-SH cells with the Parkin Q71 mutant or the Parkin A134 mutant. Under the same treatment conditions (Oligomycin 5nM for 16h), confirm whether NewParkin is still detected by western blot analysis. If

newParkin is not detected, this means that our prediction is correct.

(2) Verify Parkin phosphorylation sites that protect it from calpain-cleavage.

Since okadaic acid has high affinity for the inhibition of PP2A over PP1, and full-length phosphoParkin may be protected from calpain cleavage, it would be of interest to identify the phosphorylation sites in full-length Parkin. First, by using different protein kinase inhibitors reported to inhibit phosphorylation of Parkin *in vitro* (206) such as H89(PKA inhibitor), D4476 (casein kinase inhibitor), GF109203X (PKC inhibitor), it can established which kinase specifically phosphorylates full-length Parkin. Second, site-directed mutagenesis of Ser131 and Ser136, should be carried-out to determine if Parkin phosphorylation at these two sites influences calpain-cleavage of Parkin. *In vitro* incubations of purified calpain with Ser131 and Ser136 mutants of Parkin will further confirm this premise.

(3) Establish the impact of calpain-cleavage of Parkin on its function

We predict that Parkin is cleaved at its N-terminus to generate NewParkin. We show that NewParkin is mostly detected in

the mitochondrial enriched fraction. It is not known whether: (a) newParkin can still ubiquitinate its substrate to mediate their proteasomal degradation, and (b) newParkin promotes mitophagy.

Based on these considerations, the following experiments will verify the function of NewParkin:

a) Western blot analysis of Parkin "true" substrates such as AIMP2 and FBP-1, to establish their level of ubiquitination under conditions that promote the generation of NewParkin.
b) *In vitro* incubations of NewParkin with AIMP2 or FBP-1 in the presence of E1/E2, ubiquitin and ATP, followed by western blot analysis to provide direct evidence for the ubiquitination activity of NewParkin.
c) Western blot analysis for mitophagy markers will reveal whether overexpression of NewParkin in neurons promotes mitophagy.

(4) Validation of NewParkin in PD patients

Cleaved Parkin with a molecular weight similar that we predicted for newParkin, was identified in brains of PD patients. It is critical to confirm that NewParkin is detected in the brain of PD patients by western blot analysis. To validate newParkin, PD patient brain lysates and rat midbrain lysates

where newParkin is detected, should be compared.

Reference List

1. Byrd,R.A., Weissman,A.M. (2013) Compact Parkin only: insights into the structure of an autoinhibited ubiquitin ligase. *EMBO J.*.

2. Wauer,T., Komander,D. (2013) Structure of the human Parkin ligase domain in an autoinhibited state. *EMBO J.*.

3. Frank-Cannon,T.C., Alto,L.T., McAlpine,F.E., Tansey,M.G. (2009) Does neuroinflammation fan the flame in neurodegenerative diseases? *Mol. Neurodegener.*, **4**, 47.

4. Glass,C.K., Saijo,K., Winner,B., Marchetto,M.C., Gage,F.H. (2010) Mechanisms underlying inflammation in neurodegeneration. *Cell*, **140**, 918-934.

5. Exner,N., Lutz,A.K., Haass,C., Winklhofer,K.F. (2012) Mitochondrial dysfunction in Parkinson's disease: molecular mechanisms and pathophysiological consequences. *EMBO J*, **31**, 3038-3062.

6. Hauser,D.N., Hastings,T.G. (2013) Mitochondrial dysfunction and oxidative stress in Parkinson's disease and monogenic parkinsonism. *Neurobiol. Dis.*, **51**, 35-42.

7. Cook,C., Stetler,C., Petrucelli,L. (2012) Disruption of protein quality control in Parkinson's disease. *Cold Spring Harb. Perspect. Med.*, **2**, a009423.

8. Ebrahimi-Fakhari,D., Wahlster,L., McLean,P.J. (2012) Protein degradation pathways in Parkinson's disease: curse or blessing. *Acta Neuropathol.*, **124**, 153-172.

9. Dawson,T.M., Dawson,V.L. (2010) The role of parkin in familial and sporadic Parkinson's disease. *Mov Disord.*, **25 Suppl 1**, S32-S39.

10. Corti,O., Brice,A. (2013) Mitochondrial quality control turns out to be the principal suspect in parkin and PINK1-related autosomal recessive Parkinson's disease. *Curr. Opin. Neurobiol.*, **23**, 100-108.

11. Van,L., V, Berman,S.B. (2013) The interplay of neuronal mitochondrial dynamics and bioenergetics: implications for Parkinson's disease. *Neurobiol. Dis.*, **51**, 43-55.

12. Parkinson,J. (2002) An essay on the shaking palsy. 1817. *J. Neuropsychiatry Clin. Neurosci.*, **14**, 223-236.

13. Vilar,M., Chou,H.T., Luhrs,T., Maji,S.K., Riek-Loher,D., Verel,R., Manning,G., Stahlberg,H., Riek,R. (2008) The fold of alpha-synuclein fibrils. *Proc. Natl. Acad. Sci. U. S. A.*, **105**, 8637-8642.

14. Greffard,S., Verny,M., Bonnet,A.M., Seilhean,D., Hauw,J.J., Duyckaerts,C. (2010) A stable proportion of Lewy body bearing neurons in the substantia nigra suggests a model in which the Lewy body causes neuronal death. *Neurobiol. Aging.*, **31**, 99-103.

15. Allan,S.M., Rothwell,N.J. (2003) Inflammation in central nervous system injury. *Philos. Trans. R. Soc. Lond B Biol. Sci.*, **358**, 1669-1677.

16. Chung,Y.C., Ko,H.W., Bok,E., Park,E.S., Huh,S.H., Nam,J.H., Jin,B.K. (2010) The role of neuroinflammation on the pathogenesis of Parkinson's disease. *BMB. Rep.*, **43**, 225-232.

17. Walker,D.G., Lue,L.F. (2005) Investigations with cultured human microglia on pathogenic mechanisms of Alzheimer's disease and other neurodegenerative diseases. *J. Neurosci. Res.*, **81**, 412-425.

18. McGeer,P.L., McGeer,E.G. (2004) Inflammation and the degenerative diseases of aging. *Ann. N. Y. Acad. Sci.*, **1035**, 104-116.

19. Akiyama,H., Barger,S., Barnum,S., Bradt,B., Bauer,J., Cole,G.M., Cooper,N.R., Eikelenboom,P., Emmerling,M., Fiebich,B.L., *et al.* (2000) Inflammation and Alzheimer's disease. *Neurobiol. Aging*, **21**, 383-421.

20. Parachikova,A., Agadjanyan,M.G., Cribbs,D.H., Blurton-Jones,M., Perreau,V., Rogers,J., Beach,T.G., Cotman,C.W. (2007) Inflammatory changes parallel the early stages of Alzheimer disease. *Neurobiol. Aging*, **28**, 1821-1833.

21. Tan,Z.S., Beiser,A.S., Vasan,R.S., Roubenoff,R., Dinarello,C.A., Harris,T.B., Benjamin,E.J., Au,R., Kiel,D.P., Wolf,P.A., Seshadri,S. (2007) Inflammatory markers and the risk of Alzheimer disease: the Framingham Study. *Neurology*, **68**, 1902-1908.

22. Wyss-Coray,T. (2006) Inflammation in Alzheimer disease: driving force, bystander or beneficial response? *Nat. Med.*, **12**, 1005-1015.

23. Wyss-Coray,T., Mucke,L. (2002) Inflammation in neurodegenerative disease--a double-edged sword. *Neuron*, **35**, 419-432.

24. Scher,J.U., Pillinger,M.H. (2005) 15d-PGJ2: the anti-inflammatory prostaglandin? *Clin. Immunol.*, **114**, 100-109.

25. Liang,X., Wu,L., Hand,T., Andreasson,K. (2005) Prostaglandin D2 mediates neuronal protection via the DP1 receptor. *J. Neurochem.*, **92**, 477-486.

26. Musiek,E.S., Milne,G.L., McLaughlin,B., Morrow,J.D. (2005) Cyclopentenone eicosanoids as mediators of neurodegeneration: a pathogenic mechanism of oxidative stress-mediated and cyclooxygenase-mediated neurotoxicity. *Brain Pathol.*, **15**, 149-158.

27. Uchida,K., Shibata,T. (2008) 15-Deoxy-Delta(12,14)-prostaglandin J2: an electrophilic trigger of cellular responses. *Chem. Res. Toxicol.*, **21**, 138-144.

28. Li,Z., Melandri,F., Berdo,I., Jansen,M., Hunter,L., Wright,S., Valbrun,D., Figueiredo-Pereira,M.E. (2004) delta12-Prostaglandin J2 inhibits the ubiquitin hydrolase UCH-L1 and elicits ubiquitin–protein aggregation without proteasome inhibition. *Biochem. Biophys. Res. Commun.*, **319**, 1171-1180.

29. Ogburn,K.D., Figueiredo-Pereira,M.E. (2006) Cytoskeleton/endoplasmic reticulum collapse induced by prostaglandin J2 parallels centrosomal deposition of ubiquitinated protein aggregates. *J. Biol. Chem.*, **281**, 23274-23284.

30. Wang,Z., Aris,V.M., Ogburn,K.D., Soteropoulos,P., Figueiredo-Pereira,M.E. (2006) Prostaglandin J2 alters pro-survival and pro-death gene expression patterns and 26 S proteasome assembly in human neuroblastoma cells. *J. Biol. Chem.*, **281**, 21377-21386.

31. Koharudin,L.M., Liu,H., Di,M.R., Kodali,R.B., Graham,S.H., Gronenborn,A.M. (2010) Cyclopentenone prostaglandin-induced unfolding and aggregation of the Parkinson disease-

associated UCH-L1. *Proc. Natl. Acad. Sci. U. S. A*, **107**, 6835-6840.

32. Kondo,M., Oya-Ito,T., Kumagai,T., Osawa,T., Uchida,K. (2001) Cyclopentenone prostaglandins as potential inducers of intracellular oxidative stress. *J. Biol. Chem.*, **276**, 12076-12083.

33. Kondo,M., Shibata,T., Kumagai,T., Osawa,T., Shibata,N., Kobayashi,M., Sasaki,S., Iwata,M., Noguchi,N., Uchida,K. (2002) 15-Deoxy-Delta(12,14)-prostaglandin J(2): the endogenous electrophile that induces neuronal apoptosis. *Proc. Natl. Acad. Sci. U. S. A*, **99**, 7367-7372.

34. Martinez,B., Perez-Castillo,A., Santos,A. (2005) The mitochondrial respiratory complex I is a target for 15-deoxy-delta12,14-prostaglandin J2 action. *J Lipid Res.*, **46**, 736-743.

35. Ogburn,K.D., Bottiglieri,T., Wang,Z., Figueiredo-Pereira,M.E. (2006) Prostaglandin J2 reduces catechol-O-methyltransferase activity and enhances dopamine toxicity in neuronal cells. *Neurobiol. Dis.*, **22**, 294-301.

36. Li,Z., Jansen,M., Ogburn,K., Salvatierra,L., Hunter,L., Mathew,S., Figueiredo-Pereira,M.E. (2004) Neurotoxic prostaglandin J2 enhances cyclooxygenase-2 expression in neuronal cells through the p38MAPK pathway: a death wish? *J Neurosci. Res.*, **78**, 824-836.

37. Monneret,G., Li,H., Vasilescu,J., Rokach,J., Powell,W.S. (2002) 15-Deoxy-delta 12,14-prostaglandins D2 and J2 are potent activators of human eosinophils. *J. Immunol.*, **168**, 3563-3569.

38. Hata,A.N., Zent,R., Breyer,M.D., Breyer,R.M. (2003) Expression and molecular pharmacology of the mouse CRTH2 receptor. *J. Pharmacol. Exp. Ther.*, **306**, 463-470.

39. Liang,X., Wu,L., Wang,Q., Hand,T., Bilak,M., McCullough,L., Andreasson,K. (2007) Function of COX-2 and prostaglandins in neurological disease. *J. Mol. Neurosci.*, **33**, 94-99.

40. Liu,H., Li,W., Ahmad,M., Miller,T.M., Rose,M.E., Poloyac,S.M., Uechi,G., Balasubramani,M., Hickey,R.W., Graham,S.H. (2011) Modification of ubiquitin-C-terminal hydrolase-L1 by cyclopentenone prostaglandins exacerbates hypoxic injury. *Neurobiol. Dis.*, **41**, 318-328.

41. Liu,H., Li,W., Ahmad,M., Rose,M.E., Miller,T.M., Yu,M., Chen,J., Pascoe,J.L., Poloyac,S.M., Hickey,R.W., Graham,S.H. (2013) Increased Generation of Cyclopentenone Prostaglandins after Brain Ischemia and Their Role in Aggregation of Ubiquitinated Proteins in Neurons. *Neurotox. Res.*.

42. Kunz,T., Marklund,N., Hillered,L., Oliw,E.H. (2002) Cyclooxygenase-2, prostaglandin synthases, and prostaglandin H2 metabolism in traumatic brain injury in the rat. *J. Neurotrauma*, **19**, 1051-1064.

43. Hickey,R.W., Adelson,P.D., Johnnides,M.J., Davis,D.S., Yu,Z., Rose,M.E., Chang,Y.F., Graham,S.H. (2007) Cyclooxygenase-2 activity following traumatic brain injury in the developing rat. *Pediatr. Res.*, **62**, 271-276.

44. Becker,C., Jick,S.S., Meier,C.R. (2010) Risk of stroke in patients with idiopathic Parkinson disease. *Parkinsonism. Relat Disord.*, **16**, 31-35.

45. Uchida,H., Yokoyama,H., Kimoto,H., Kato,H., Araki,T. (2010) Long-term changes in the ipsilateral substantia nigra after transient focal cerebral ischaemia in rats. *Int. J Exp. Pathol.*, **91**, 256-266.

46. Rodriguez-Grande,B., Blackabey,V., Gittens,B., Pinteaux,E., Denes,A. (2013) Loss of substance P and inflammation precede delayed neurodegeneration in the substantia nigra after cerebral ischemia. *Brain Behav. Immun.*, **29**, 51-61.

47. Hutson,C.B., Lazo,C.R., Mortazavi,F., Giza,C.C., Hovda,D., Chesselet,M.F. (2011) Traumatic brain injury in adult rats causes progressive nigrostriatal dopaminergic cell loss and enhanced vulnerability to the pesticide paraquat. *J Neurotrauma*, **28**, 1783-1801.

48. Burke,J.F., Stulc,J.L., Skolarus,L.E., Sears,E.D., Zahuranec,D.B., Morgenstern,L.B. (2013) Traumatic brain injury may be an independent risk factor for stroke. *Neurology*.

49. Pierre,S.R., Lemmens,M.A., Figueiredo-Pereira,M.E. (2009) Subchronic infusion of the product of inflammation prostaglandin J2 models sporadic Parkinson's disease in mice. *J. Neuroinflammation.*, **6**, 18.

50. Aoki,T., Narumiya,S. (2012) Prostaglandins and chronic inflammation. *Trends Pharmacol. Sci.*, **33**, 304-311.

51. Subra,C., Grand,D., Laulagnier,K., Stella,A., Lambeau,G., Paillasse,M., De,M.P., Monsarrat,B., Perret,B., Silvente-Poirot,S., *et al.* (2010) Exosomes account for vesicle-mediated transcellular transport of activatable phospholipases and prostaglandins. *J. Lipid Res.*, **51**, 2105-2120.

52. Schneider,A., Simons,M. (2013) Exosomes: vesicular carriers for intercellular communication in neurodegenerative disorders. *Cell Tissue Res.*, **352**, 33-47.

53. Schlossmacher,M.G., Frosch,M.P., Gai,W.P., Medina,M., Sharma,N., Forno,L., Ochiishi,T., Shimura,H., Sharon,R., Hattori,N., *et al.* (2002) Parkin localizes to the Lewy bodies of Parkinson disease and dementia with Lewy bodies. *Am. J. Pathol.*, **160**, 1655-1667.

54. Goldberg,A.L. (2003) Protein degradation and protection against misfolded or damaged proteins. *Nature.*, **426**, 895-899.

55. Gorman,A.M. (2008) Neuronal cell death in neurodegenerative diseases: recurring themes around protein handling. *J. Cell Mol. Med.*, **12**, 2263-2280.

56. Lucking,C.B., Durr,A., Bonifati,V., Vaughan,J., De,M.G., Gasser,T., Harhangi,B.S., Meco,G., Denefle,P., Wood,N.W., *et al.* (2000) Association between early-onset Parkinson's disease and mutations in the parkin gene. *N. Engl. J. Med.*, **342**, 1560-1567.

57. Foroud,T., Uniacke,S.K., Liu,L., Pankratz,N., Rudolph,A., Halter,C., Shults,C., Marder,K., Conneally,P.M., Nichols,W.C. (2003) Heterozygosity for a mutation in the parkin gene leads to later onset Parkinson disease. *Neurology.*, **60**, 796-801.

58. Maraganore,D.M., Lesnick,T.G., Elbaz,A., Chartier-Harlin,M.C., Gasser,T., Kruger,R., Hattori,N., Mellick,G.D., Quattrone,A., Satoh,J., *et al.* (2004) UCHL1 is a Parkinson's disease susceptibility gene. *Ann. Neurol.*, **55**, 512-521.

59. McNaught,K.S., Belizaire,R., Isacson,O., Jenner,P., Olanow,C.W. (2003) Altered proteasomal function in sporadic Parkinson's disease. *Exp. Neurol.*, **179**, 38-46.

60. McNaught,K.S., Jenner,P. (2001) Proteasomal function is impaired in substantia nigra in Parkinson's disease. *Neurosci. Lett.*, **%19;297**, 191-194.

61. Tofaris,G.K., Razzaq,A., Ghetti,B., Lilley,K.S., Spillantini,M.G. (2003) Ubiquitination of alpha-synuclein in Lewy bodies is a pathological event not associated with impairment of proteasome function. *J. Biol. Chem.*, **278**, 44405-44411.

62. Furukawa,Y., Vigouroux,S., Wong,H., Guttman,M., Rajput,A.H., Ang,L., Briand,M., Kish,S.J., Briand,Y. (2002) Brain proteasomal function in sporadic Parkinson's disease and related disorders. *Ann. Neurol.*, **51**, 779-782.

63. McNaught,K.S., Belizaire,R., Isacson,O., Jenner,P., Olanow,C.W. (2003) Altered proteasomal function in sporadic Parkinson's disease. *Exp. Neurol.*, **179**, 38-46.

64. McNaught,K.S., Belizaire,R., Isacson,O., Jenner,P., Olanow,C.W. (2003) Altered proteasomal function in sporadic Parkinson's disease. *Exp. Neurol.*, **179**, 38-46.

65. McNaught,K.S., Perl,D.P., Brownell,A.L., Olanow,C.W. (2004) Systemic exposure to proteasome inhibitors causes a progressive model of Parkinson's disease. *Ann. Neurol.*, **56**, 149-162.

66. Matsui,H., Ito,H., Taniguchi,Y., Inoue,H., Takeda,S., Takahashi,R. (2010) Proteasome inhibition in medaka brain induces the features of Parkinson disease. *J. Neurochem.*.

67. Xie,W., Li,X., Li,C., Zhu,W., Jankovic,J., Le,W. (2010) Proteasome inhibition modeling nigral neuron degeneration in Parkinson's disease. *J. Neurochem.*.

68. Langston,J.W., Ballard,P., Tetrud,J.W., Irwin,I. (1983) Chronic Parkinsonism in humans due to a product of meperidine-analog synthesis. *Science*, **219**, 979-980.

69. Schapira,A.H., Cooper,J.M., Dexter,D., Clark,J.B., Jenner,P., Marsden,C.D. (1990) Mitochondrial complex I deficiency in Parkinson's disease. *J. Neurochem.*, **54**, 823-827.

70. Pan-Montojo,F., Anichtchik,O., Dening,Y., Knels,L., Pursche,S., Jung,R., Jackson,S., Gille,G., Spillantini,M.G., Reichmann,H., Funk,R.H. (2010) Progression of Parkinson's disease pathology is reproduced by intragastric administration of rotenone in mice. *PLoS. One.*, **5**, e8762.

71. Beal,M.F. (2003) Mitochondria, oxidative damage, and inflammation in Parkinson's disease. *Ann. N. Y. Acad. Sci.*, **991**, 120-131.

72. de Moura,M.B., dos Santos,L.S., Van,H.B. (2010) Mitochondrial dysfunction in neurodegenerative diseases and cancer. *Environ. Mol. Mutagen.*, **51**, 391-405.

73. Winklhofer,K.F., Haass,C. (2010) Mitochondrial dysfunction in Parkinson's disease. *Biochim. Biophys. Acta*, **1802**, 29-44.

74. Devi,L., Raghavendran,V., Prabhu,B.M., Avadhani,N.G., Anandatheerthavarada,H.K. (2008) Mitochondrial import and accumulation of alpha-synuclein impair complex I in human dopaminergic neuronal cultures and Parkinson disease brain. *J. Biol. Chem.*, **283**, 9089-9100.

75. Moreira,P.I., Zhu,X., Wang,X., Lee,H.G., Nunomura,A., Petersen,R.B., Perry,G., Smith,M.A. (2010) Mitochondria: a therapeutic target in neurodegeneration. *Biochim. Biophys. Acta*, **1802**, 212-220.

76. Whitworth,A.J., Pallanck,L.J. (2009) The PINK1/Parkin pathway: a mitochondrial quality control system? *J. Bioenerg. Biomembr.*, **41**, 499-503.

77. Winklhofer,K.F., Haass,C. (2010) Mitochondrial dysfunction in Parkinson's disease. *Biochim. Biophys. Acta*, **1802**, 29-44.

78. Matsumine,H., Saito,M., Shimoda-Matsubayashi,S., Tanaka,H., Ishikawa,A., Nakagawa-Hattori,Y., Yokochi,M., Kobayashi,T., Igarashi,S., Takano,H., *et al.* (1997) Localization of a gene for an autosomal recessive form of juvenile Parkinsonism to chromosome 6q25.2-27. *Am. J. Hum. Genet.*, **60**, 588-596.

79. Kitada,T., Asakawa,S., Hattori,N., Matsumine,H., Yamamura,Y., Minoshima,S., Yokochi,M., Mizuno,Y., Shimizu,N. (1998) Mutations in the parkin gene cause autosomal recessive juvenile parkinsonism. *Nature*, **392**, 605-608.

80. Lucking,C.B., Durr,A., Bonifati,V., Vaughan,J., De,M.G., Gasser,T., Harhangi,B.S., Meco,G., Denefle,P., Wood,N.W., *et al.* (2000) Association between early-onset Parkinson's disease and mutations in the parkin gene. *N. Engl. J. Med.*, **342**, 1560-1567.

81. Chaudhary,S., Behari,M., Dihana,M., Swaminath,P.V., Govindappa,S.T., Jayaram,S., Goyal,V., Maitra,A., Muthane,U.B., Juyal,R.C., Thelma,B.K. (2006) Parkin mutations in familial and sporadic Parkinson's disease among Indians. *Parkinsonism. Relat Disord.*, **12**, 239-245.

82. Wang,C., Ma,H., Feng,X., Xie,S., Chan,P. (2010) Parkin dosage mutations in patients with early-onset sporadic and familial Parkinson's disease in Chinese: an independent pathogenic role. *Brain Res.*, **1358**, 30-38.

83. Schlossmacher,M.G., Frosch,M.P., Gai,W.P., Medina,M., Sharma,N., Forno,L., Ochiishi,T., Shimura,H., Sharon,R., Hattori,N., *et al.* (2002) Parkin localizes to the Lewy bodies of Parkinson disease and dementia with Lewy bodies. *Am. J. Pathol.*, **160**, 1655-1667.

84. Poorkaj,P., Moses,L., Montimurro,J.S., Nutt,J.G., Schellenberg,G.D., Payami,H. (2005) Parkin mutation dosage and the phenomenon of anticipation: a molecular genetic study of familial parkinsonism. *BMC. Neurol.*, **5**, 4.

85. Pavese,N., Moore,R.Y., Scherfler,C., Khan,N.L., Hotton,G., Quinn,N.P., Bhatia,K.P., Wood,N.W., Brooks,D.J., Lees,A.J., Piccini,P. (2010) In vivo assessment of brain monoamine systems in parkin gene carriers: a PET study. *Exp. Neurol.*, **222**, 120-124.

86. Hart,M.P., Xu,A. (2009) Mice expressing mutant parkin exhibit hallmark features of Parkinson's disease. *J. Neurosci.*, **29**, 7392-7394.

87. Schlossmacher,M.G., Frosch,M.P., Gai,W.P., Medina,M., Sharma,N., Forno,L., Ochiishi,T., Shimura,H., Sharon,R., Hattori,N., *et al.* (2002) Parkin localizes to the Lewy bodies of Parkinson disease and dementia with Lewy bodies. *Am. J. Pathol.*, **160**, 1655-1667.

88. Shimura,H., Hattori,N., Kubo,S., Yoshikawa,M., Kitada,T., Matsumine,H., Asakawa,S., Minoshima,S., Yamamura,Y., Shimizu,N., Mizuno,Y. (1999) Immunohistochemical and subcellular localization of Parkin protein: absence of

protein in autosomal recessive juvenile parkinsonism patients. *Ann. Neurol.*, **45**, 668-672.

89. Hristova,V.A., Beasley,S.A., Rylett,R.J., Shaw,G.S. (2009) Identification of a novel Zn2+-binding domain in the autosomal recessive juvenile Parkinson-related E3 ligase parkin. *J. Biol. Chem.*, **284**, 14978-14986.

90. Sakata,E., Yamaguchi,Y., Kurimoto,E., Kikuchi,J., Yokoyama,S., Yamada,S., Kawahara,H., Yokosawa,H., Hattori,N., Mizuno,Y., *et al.* (2003) Parkin binds the Rpn10 subunit of 26S proteasomes through its ubiquitin-like domain. *EMBO Rep.*, **4**, 301-306.

91. Hristova,V.A., Beasley,S.A., Rylett,R.J., Shaw,G.S. (2009) Identification of a novel Zn2+-binding domain in the autosomal recessive juvenile Parkinson-related E3 ligase parkin. *J. Biol. Chem.*, **284**, 14978-14986.

92. Rankin,C.A., Roy,A., Zhang,Y., Richter,M. (2011) Parkin, A Top Level Manager in the Cell's Sanitation Department. *Open. Biochem. J.*, **5**, 9-26.

93. Hristova,V.A., Beasley,S.A., Rylett,R.J., Shaw,G.S. (2009) Identification of a novel Zn2+-binding domain in the autosomal recessive juvenile Parkinson-related E3 ligase parkin. *J. Biol. Chem.*, **284**, 14978-14986.

94. Cookson,M.R. (2003) Parkin's substrates and the pathways leading to neuronal damage. *Neuromolecular. Med.*, **3**, 1-13.

95. Gu,W.J., Abbas,N., Lagunes,M.Z., Parent,A., Pradier,L., Bohme,G.A., Agid,Y., Hirsch,E.C., Raisman-Vozari,R., Brice,A. (2000) Cloning of rat parkin cDNA and distribution of parkin in rat brain. *J. Neurochem.*, **74**, 1773-1776.

96. Meng,F., Yao,D., Shi,Y., Kabakoff,J., Wu,W., Reicher,J., Ma,Y., Moosmann,B., Masliah,E., Lipton,S.A., Gu,Z. (2011) Oxidation of the cysteine-rich regions of parkin perturbs its E3 ligase activity and contributes to protein aggregation. *Mol. Neurodegener.*, **6**, 34.

97. Wong,E.S., Tan,J.M., Wang,C., Zhang,Z., Tay,S.P., Zaiden,N., Ko,H.S., Dawson,V.L., Dawson,T.M., Lim,K.L. (2007) Relative sensitivity of parkin and other cysteine-containing enzymes to stress-induced solubility alterations. *J. Biol. Chem.*, **282**, 12310-12318.

98. Vandiver,M.S., Paul,B.D., Xu,R., Karuppagounder,S., Rao,F., Snowman,A.M., Ko,H.S., Lee,Y.I., Dawson,V.L., Dawson,T.M., *et al.* (2013) Sulfhydration mediates neuroprotective actions of parkin. *Nat. Commun.*, **4**, 1626.

99. Zheng,X., Hunter,T. (2013) Parkin mitochondrial translocation is achieved through a novel catalytic activity coupled mechanism. *Cell Res.*.

100. Dagata,V., Cavallaro,S. (2004) Parkin transcript variants in rat and human brain. *Neurochem. Res.*, **29**, 1715-1724.

101. Humbert,J., Beyer,K., Carrato,C., Mate,J.L., Ferrer,I., Ariza,A. (2007) Parkin and synphilin-1 isoform expression changes in Lewy body diseases. *Neurobiol. Dis.*, **26**, 681-687.

102. Beyer,K., Domingo-Sabat,M., Humbert,J., Carrato,C., Ferrer,I., Ariza,A. (2008) Differential expression of alpha-synuclein, parkin, and synphilin-1 isoforms in Lewy body disease. *Neurogenetics.*, **9**, 163-172.

103. Huynh,D.P., Dy,M., Nguyen,D., Kiehl,T.R., Pulst,S.M. (2001) Differential expression and tissue distribution of parkin isoforms during mouse development. *Brain Res. Dev. Brain Res.*, **130**, 173-181.

104. Kahns,S., Lykkebo,S., Jakobsen,L.D., Nielsen,M.S., Jensen,P.H. (2002) Caspase-mediated parkin cleavage in apoptotic cell death. *J. Biol. Chem.*, **277**, 15303-15308.

105. Vande,W.L., Lamkanfi,M., Vandenabeele,P. (2008) The mitochondrial serine protease HtrA2/Omi: an overview. *Cell Death Differ.*, **15**, 453-460.

106. Park,H.M., Kim,G.Y., Nam,M.K., Seong,G.H., Han,C., Chung,K.C., Kang,S., Rhim,H. (2009) The serine protease HtrA2/Omi cleaves Parkin and irreversibly inactivates its E3 ubiquitin ligase activity. *Biochem. Biophys. Res. Commun.*, **387**, 537-542.

107. Shimura,H., Hattori,N., Kubo,S., Yoshikawa,M., Kitada,T., Matsumine,H., Asakawa,S., Minoshima,S., Yamamura,Y., Shimizu,N., Mizuno,Y. (1999) Immunohistochemical and subcellular localization of Parkin protein: absence of protein in autosomal recessive juvenile parkinsonism patients. *Ann. Neurol.*, **45**, 668-672.

108. Zarate-Lagunes,M., Gu,W.J., Blanchard,V., Francois,C., Muriel,M.P., Mouatt-Prigent,A., Bonici,B., Parent,A., Hartmann,A., Yelnik,J., *et al.* (2001) Parkin immunoreactivity in the brain of human and non-human primates: an immunohistochemical analysis in normal conditions and in Parkinsonian syndromes. *J. Comp Neurol.*, **432**, 184-196.

109. Gu,W.J., Abbas,N., Lagunes,M.Z., Parent,A., Pradier,L., Bohme,G.A., Agid,Y., Hirsch,E.C., Raisman-Vozari,R., Brice,A. (2000) Cloning of rat parkin cDNA and distribution of parkin in rat brain. *J. Neurochem.*, **74**, 1773-1776.

110. Huynh,D.P., Dy,M., Nguyen,D., Kiehl,T.R., Pulst,S.M. (2001) Differential expression and tissue distribution of parkin isoforms during mouse development. *Brain Res. Dev. Brain Res.*, **130**, 173-181.

111. Horowitz,J.M., Myers,J., Stachowiak,M.K., Torres,G. (1999) Identification and distribution of Parkin in rat brain. *Neuroreport*, **10**, 3393-3397.

112. Schlossmacher,M.G., Frosch,M.P., Gai,W.P., Medina,M., Sharma,N., Forno,L., Ochiishi,T., Shimura,H., Sharon,R., Hattori,N., *et al.* (2002) Parkin localizes to the Lewy bodies of Parkinson disease and dementia with Lewy bodies. *Am. J. Pathol.*, **160**, 1655-1667.

113. Stichel,C.C., Augustin,M., Kuhn,K., Zhu,X.R., Engels,P., Ullmer,C., Lubbert,H. (2000) Parkin expression in the adult mouse brain. *Eur. J. Neurosci.*, **12**, 4181-4194.

114. Huynh,D.P., Dy,M., Nguyen,D., Kiehl,T.R., Pulst,S.M. (2001) Differential expression and tissue distribution of parkin isoforms during mouse development. *Brain Res. Dev. Brain Res.*, **130**, 173-181.

115. Schlossmacher,M.G., Frosch,M.P., Gai,W.P., Medina,M., Sharma,N., Forno,L., Ochiishi,T., Shimura,H., Sharon,R., Hattori,N., *et al.* (2002) Parkin localizes to the Lewy bodies of Parkinson disease and dementia with Lewy bodies. *Am. J. Pathol.*, **160**, 1655-1667.

116. Shimura,H., Hattori,N., Kubo,S., Yoshikawa,M., Kitada,T., Matsumine,H., Asakawa,S., Minoshima,S., Yamamura,Y., Shimizu,N., Mizuno,Y. (1999) Immunohistochemical and subcellular localization of Parkin

protein: absence of protein in autosomal recessive juvenile parkinsonism patients. *Ann. Neurol.*, **45**, 668-672.

117. Huynh,D.P., Dy,M., Nguyen,D., Kiehl,T.R., Pulst,S.M. (2001) Differential expression and tissue distribution of parkin isoforms during mouse development. *Brain Res. Dev. Brain Res.*, **130**, 173-181.

118. Schlossmacher,M.G., Frosch,M.P., Gai,W.P., Medina,M., Sharma,N., Forno,L., Ochiishi,T., Shimura,H., Sharon,R., Hattori,N., *et al.* (2002) Parkin localizes to the Lewy bodies of Parkinson disease and dementia with Lewy bodies. *Am. J. Pathol.*, **160**, 1655-1667.

119. Shimura,H., Hattori,N., Kubo,S., Yoshikawa,M., Kitada,T., Matsumine,H., Asakawa,S., Minoshima,S., Yamamura,Y., Shimizu,N., Mizuno,Y. (1999) Immunohistochemical and subcellular localization of Parkin protein: absence of protein in autosomal recessive juvenile parkinsonism patients. *Ann. Neurol.*, **45**, 668-672.

120. Ledesma,M.D., Galvan,C., Hellias,B., Dotti,C., Jensen,P.H. (2002) Astrocytic but not neuronal increased expression and redistribution of parkin during unfolded protein stress. *J. Neurochem.*, **83**, 1431-1440.

121. Zhao,J., Ren,Y., Jiang,Q., Feng,J. (2003) Parkin is recruited to the centrosome in response to inhibition of proteasomes. *J. Cell Sci.*, **116**, 4011-4019.

122. Kao,S.Y. (2009) DNA damage induces nuclear translocation of parkin. *J. Biomed. Sci.*, **16**, 67.

123. Narendra,D., Tanaka,A., Suen,D.F., Youle,R.J. (2008) Parkin is recruited selectively to impaired mitochondria and promotes their autophagy. *J. Cell Biol.*, **183**, 795-803.

124. Matsuda,N., Tanaka,K. (2010) Uncovering the roles of PINK1 and parkin in mitophagy. *Autophagy.*, **6**, 952-954.

125. Narendra,D., Tanaka,A., Suen,D.F., Youle,R.J. (2008) Parkin is recruited selectively to impaired mitochondria and promotes their autophagy. *J. Cell Biol.*, **183**, 795-803.

126. Geisler,S., Holmstrom,K.M., Skujat,D., Fiesel,F.C., Rothfuss,O.C., Kahle,P.J., Springer,W. (2010) PINK1/Parkin-mediated mitophagy is dependent on VDAC1 and p62/SQSTM1. *Nat. Cell Biol.*, **12**, 119-131.

127. Cai,Q., Zakaria,H.M., Simone,A., Sheng,Z.H. (2012) Spatial parkin translocation and degradation of damaged mitochondria via mitophagy in live cortical neurons. *Curr. Biol.*, **22**, 545-552.

128. Koyano,F., Okatsu,K., Ishigaki,S., Fujioka,Y., Kimura,M., Sobue,G., Tanaka,K., Matsuda,N. (2013) The principal PINK1 and Parkin cellular events triggered in response to dissipation of mitochondrial membrane potential occur in primary neurons. *Genes Cells*.

129. Van,L., V, Arnold,B., Cassady,S.J., Chu,C.T., Burton,E.A., Berman,S.B. (2011) Bioenergetics of neurons inhibit the translocation response of Parkin following rapid mitochondrial depolarization. *Hum. Mol. Genet.*, **20**, 927-940.

130. Sterky,F.H., Lee,S., Wibom,R., Olson,L., Larsson,N.G. (2011) Impaired mitochondrial transport and Parkin-independent degeneration of respiratory chain-deficient dopamine neurons in vivo. *Proc. Natl. Acad. Sci. U. S. A*, **108**, 12937-12942.

131. Joselin,A.P., Hewitt,S.J., Callaghan,S.M., Kim,R.H., Chung,Y.H., Mak,T.W., Shen,J., Slack,R.S., Park,D.S. (2012) ROS-dependent regulation of Parkin and DJ-1 localization during oxidative stress in neurons. *Hum. Mol. Genet.*, **21**, 4888-4903.

132. Moore,D.J. (2006) Parkin: a multifaceted ubiquitin ligase. *Biochem. Soc. Trans.*, **34**, 749-753.

133. Corti,O., Hampe,C., Koutnikova,H., Darios,F., Jacquier,S., Prigent,A., Robinson,J.C., Pradier,L., Ruberg,M., Mirande,M., *et al.* (2003) The p38 subunit of the aminoacyl-tRNA synthetase complex is a Parkin substrate: linking protein biosynthesis and neurodegeneration. *Hum. Mol. Genet.*, **12**, 1427-1437.

134. Ko,H.S., Kim,S.W., Sriram,S.R., Dawson,V.L., Dawson,T.M. (2006) Identification of far upstream element-binding protein-1 as an authentic Parkin substrate. *J. Biol. Chem.*, **281**, 16193-16196.

135. Wang,H.Q., Imai,Y., Inoue,H., Kataoka,A., Iita,S., Nukina,N., Takahashi,R. (2008) Pael-R transgenic mice crossed with parkin deficient mice displayed progressive

and selective catecholaminergic neuronal loss. *J. Neurochem.*, **107**, 171-185.

136. Ren,Y., Zhao,J., Feng,J. (2003) Parkin binds to alpha/beta tubulin and increases their ubiquitination and degradation. *J. Neurosci.*, **23**, 3316-3324.

137. Rawal,N., Corti,O., Sacchetti,P., rdilla-Osorio,H., Sehat,B., Brice,A., Arenas,E. (2009) Parkin protects dopaminergic neurons from excessive Wnt/beta-catenin signaling. *Biochem. Biophys. Res. Commun.*, **388**, 473-478.

138. Staropoli,J.F., McDermott,C., Martinat,C., Schulman,B., Demireva,E., Abeliovich,A. (2003) Parkin is a component of an SCF-like ubiquitin ligase complex and protects postmitotic neurons from kainate excitotoxicity. *Neuron*, **37**, 735-749.

139. Um,J.W., Min,D.S., Rhim,H., Kim,J., Paik,S.R., Chung,K.C. (2006) Parkin ubiquitinates and promotes the degradation of RanBP2. *J. Biol. Chem.*, **281**, 3595-3603.

140. Chan,N.C., Salazar,A.M., Pham,A.H., Sweredoski,M.J., Kolawa,N.J., Graham,R.L., Hess,S., Chan,D.C. (2011) Broad activation of the ubiquitin-proteasome system by Parkin is critical for mitophagy. *Hum. Mol. Genet.*, **20**, 1726-1737.

141. Heo,J.M., Rutter,J. (2011) Ubiquitin-dependent mitochondrial protein degradation. *Int. J. Biochem. Cell Biol.*, **43**, 1422-1426.

142. Rana,A., Rera,M., Walker,D.W. (2013) Parkin overexpression during aging reduces proteotoxicity, alters mitochondrial dynamics, and extends lifespan. *Proc. Natl. Acad. Sci. U. S. A*, **110**, 8638-8643.

143. Roth,J.A., Singleton,S., Feng,J., Garrick,M., Paradkar,P.N. (2010) Parkin regulates metal transport via proteasomal degradation of the 1B isoforms of divalent metal transporter 1. *J. Neurochem.*, **113**, 454-464.

144. Um,J.W., Im,E., Lee,H.J., Min,B., Yoo,L., Yoo,J., Lubbert,H., Stichel-Gunkel,C., Cho,H.S., Yoon,J.B., Chung,K.C. (2010) Parkin directly modulates 26S proteasome activity. *J Neurosci.*, **30**, 11805-11814.

145. ves da,C.C., Checler,F. (2012) Parkin: much more than a simple ubiquitin ligase. *Neurodegener. Dis.*, **10**, 49-51.

146. Lee,K., Lee,M.H., Kang,Y.W., Rhee,K.J., Kim,T.U., Kim,Y.S. (2012) Parkin induces apoptotic cell death in TNF-alpha-treated cervical cancer cells. *BMB. Rep.*, **45**, 526-531.

147. Kim,K.Y., Stevens,M.V., Akter,M.H., Rusk,S.E., Huang,R.J., Cohen,A., Noguchi,A., Springer,D., Bocharov,A.V., Eggerman,T.L., *et al.* (2011) Parkin is a lipid-responsive regulator of fat uptake in mice and mutant human cells. *J. Clin. Invest*, **121**, 3701-3712.

148. Hasegawa,T., Treis,A., Patenge,N., Fiesel,F.C., Springer,W., Kahle,P.J. (2008) Parkin protects against tyrosinase-mediated dopamine neurotoxicity by suppressing stress-activated protein kinase pathways. *J. Neurochem.*, **105**, 1700-1715.

149. Vercammen,L., Van der,P.A., Vaudano,E., Gijsbers,R., Debyser,Z., Van den,H.C., Baekelandt,V. (2006) Parkin protects against neurotoxicity in the 6-hydroxydopamine rat model for Parkinson's disease. *Mol. Ther.*, **14**, 716-723.

150. Benskey,M., Lee,K.Y., Parikh,K., Lookingland,K.J., Goudreau,J.L. (2013) Sustained resistance to acute MPTP toxicity by hypothalamic dopamine neurons following chronic neurotoxicant exposure is associated with sustained up-regulation of parkin protein. *Neurotoxicology*, **37**, 144-153.

151. Khandelwal,P.J., Dumanis,S.B., Feng,L.R., Maguire-Zeiss,K., Rebeck,G., Lashuel,H.A., Moussa,C.E. (2010) Parkinson-related parkin reduces alpha-Synuclein phosphorylation in a gene transfer model. *Mol. Neurodegener.*, **5**, 47.

152. Vaudry,D., Falluel-Morel,A., Bourgault,S., Basille,M., Burel,D., Wurtz,O., Fournier,A., Chow,B.K., Hashimoto,H., Galas,L., Vaudry,H. (2009) Pituitary adenylate cyclase-activating polypeptide and its receptors: 20 years after the discovery. *Pharmacol. Rev.*, **61**, 283-357.

153. Shneider,Y., Shtrauss,Y., Yadid,G., Pinhasov,A. (2010) Differential expression of PACAP receptors in postnatal rat brain. *Neuropeptides*, **44**, 509-514.

154. Eiden,L.E., Samal,B., Gerdin,M.J., Mustafa,T., Vaudry,D., Stroth,N. (2008) Discovery of pituitary adenylate cyclase-activating polypeptide-regulated genes through microarray analyses in cell culture and in vivo. *Ann. N. Y. Acad. Sci.*, **1144**, 6-20.

155. Gasperini,L., Piubelli,C., Carboni,L. (2012) Proteomics of rat hypothalamus, hippocampus and pre-frontal/frontal cortex after central administration of the neuropeptide PACAP. *Mol. Biol Rep.*, **39**, 2921-2935.

156. Holighaus,Y., Weihe,E., Eiden,L.E. (2012) STC1 induction by PACAP is mediated through cAMP and ERK1/2 but not PKA in cultured cortical neurons. *J Mol. Neurosci.*, **46**, 75-87.

157. Nakamachi,T., Li,M., Shioda,S., Arimura,A. (2006) Signaling involved in pituitary adenylate cyclase-activating polypeptide-stimulated ADNP expression. *Peptides*, **27**, 1859-1864.

158. Reglodi,D., Kiss,P., Lubics,A., Tamas,A. (2011) Review on the Protective Effects of PACAP in Models of Neurodegenerative Diseases In vitro and In vivo. *Curr. Pharm. Des*, **17**, 962-972.

159. Deguil,J., Chavant,F., Lafay-Chebassier,C., Perault-Pochat,M.C., Fauconneau,B., Pain,S. (2010) Neuroprotective effect of PACAP on translational control alteration and cognitive decline in MPTP parkinsonian mice. *Neurotox. Res.*, **17**, 142-155.

160. Reglodi,D., Lubics,A., Kiss,P., Lengvari,I., Gaszner,B., Toth,G., Hegyi,O., Tamas,A. (2006) Effect of PACAP in 6-OHDA-induced injury of the substantia nigra in intact young and ovariectomized female rats. *Neuropeptides*, **40**, 265-274.

161. Watson,M.B., Nobuta,H., Abad,C., Lee,S.K., Bala,N., Zhu,C., Richter,F., Chesselet,M.F., Waschek,J.A. (2013) PACAP deficiency sensitizes nigrostriatal dopaminergic neurons to paraquat-induced damage and modulates central and peripheral inflammatory activation in mice. *Neuroscience*, **240**, 277-286.

162. Watson,M.B., Nobuta,H., Abad,C., Lee,S.K., Bala,N., Zhu,C., Richter,F., Chesselet,M.F., Waschek,J.A. (2013) PACAP deficiency sensitizes nigrostriatal dopaminergic neurons to paraquat-induced damage and modulates central and peripheral inflammatory activation in mice. *Neuroscience*, **240**, 277-286.

163. Brown,D., Tamas,A., Reglodi,D., Tizabi,Y. (2013) PACAP Protects Against Salsolinol-Induced Toxicity in

Dopaminergic SH-SY5Y Cells: Implication for Parkinson's Disease. *J. Mol. Neurosci.*, **50**, 600-607.

164. Deguil,J., Jailloux,D., Page,G., Fauconneau,B., Houeto,J.L., Philippe,M., Muller,J.M., Pain,S. (2007) Neuroprotective effects of pituitary adenylate cyclase-activating polypeptide (PACAP) in MPP+-induced alteration of translational control in Neuro-2a neuroblastoma cells. *J. Neurosci. Res.*, **85**, 2017-2025.

165. Takei,N., Skoglosa,Y., Lindholm,D. (1998) Neurotrophic and neuroprotective effects of pituitary adenylate cyclase-activating polypeptide (PACAP) on mesencephalic dopaminergic neurons. *J. Neurosci. Res.*, **54**, 698-706.

166. Wang,G., Qi,C., Fan,G.H., Zhou,H.Y., Chen,S.D. (2005) PACAP protects neuronal differentiated PC12 cells against the neurotoxicity induced by a mitochondrial complex I inhibitor, rotenone. *FEBS Lett.*, **579**, 4005-4011.

167. Rayport,S., Sulzer,D., Shi,W.X., Sawasdikosol,S., Monaco,J., Batson,D., Rajendran,G. (1992) Identified postnatal mesolimbic dopamine neurons in culture: morphology and electrophysiology. *J. Neurosci.*, **12**, 4264-4280.

168. Jiang,Q., Yan,Z., Feng,J. (2006) Neurotrophic factors stabilize microtubules and protect against rotenone toxicity on dopaminergic neurons. *J Biol Chem*, **281**, 29391-29400.

169. Brewer,G.J., Torricelli,J.R., Evege,E.K., Price,P.J. (1993) Optimized survival of hippocampal neurons in B27-supplemented Neurobasal, a new serum-free medium combination. *J. Neurosci. Res.*, **35**, 567-576.

170. Nam,Y., Brewer,G.J., Wheeler,B.C. (2007) Development of astroglial cells in patterned neuronal cultures. *J Biomater. Sci. Polym. Ed*, **18**, 1091-1100.

171. Mosmann,T. (1983) Rapid colorimetric assay for cellular growth and survival: application to proliferation and cytotoxicity assays. *J Immunol Methods*, **65**, 55-63.

172. Myeku,N., Metcalfe,M.J., Huang,Q., Figueiredo-Pereira,M. (2011) Assessment of proteasome impairment and accumulation/aggregation of ubiquitinated proteins in neuronal cultures. *Methods Mol. Biol.*, **793**, 273-296.

173. Liu,Y., Schubert,D.R. (2009) The specificity of neuroprotection by antioxidants. *J Biomed. Sci.*, **16**, 98.

174. Meng,L., Mohan,R., Kwok,B.H., Elofsson,M., Sin,N., Crews,C.M. (1999) Epoxomicin, a potent and selective proteasome inhibitor, exhibits in vivo antiinflammatory activity. *Proc. Natl. Acad Sci U. S. A*, **96**, 10403-10408.

175. Groll,M., Kim,K.B., Kairies,N., Huber,R., Crews,C.M. (2000) Crystal structure of epoxomicin:20S proteasome reveals a molecular basis of α',β'-epoxomicin proteasome inhibitors. *J. Am. Chem. Soc.*, **122**, 1237-1238.

176. Kahns,S., Lykkebo,S., Jakobsen,L.D., Nielsen,M.S., Jensen,P.H. (2002) Caspase-mediated parkin cleavage in apoptotic cell death. *J. Biol. Chem.*, **277**, 15303-15308.

177. Degli,E.M. (1998) Inhibitors of NADH-ubiquinone reductase: an overview. *Biochim. Biophys. Acta*, **1364**, 222-235.

178. Betarbet,R., Sherer,T.B., MacKenzie,G., Garcia-Osuna,M., Panov,A.V., Greenamyre,J.T. (2000) Chronic systemic pesticide exposure reproduces features of Parkinson's disease. *Nat. Neurosci.*, **3**, 1301-1306.

179. Van,L., V, Arnold,B., Cassady,S.J., Chu,C.T., Burton,E.A., Berman,S.B. (2011) Bioenergetics of neurons inhibit the translocation response of Parkin following rapid mitochondrial depolarization. *Hum. Mol. Genet.*, **20**, 927-940.

180. Endo,A., Matsumoto,M., Inada,T., Yamamoto,A., Nakayama,K.I., Kitamura,N., Komada,M. (2009) Nucleolar structure and function are regulated by the deubiquitylating enzyme USP36. *J. Cell Sci.*, **122**, 678-686.

181. Hachiya,N., Mihara,K., Suda,K., Horst,M., Schatz,G., Lithgow,T. (1995) Reconstitution of the initial steps of mitochondrial protein import. *Nature*, **376**, 705-709.

182. Shoshan-Barmatz,V., De,P., V, Zweckstetter,M., Raviv,Z., Keinan,N., Arbel,N. (2010) VDAC, a multi-functional mitochondrial protein regulating cell life and death. *Mol. Aspects Med.*, **31**, 227-285.

183. Bose,S., Weikl,T., Bugl,H., Buchner,J. (1996) Chaperone function of Hsp90-associated proteins. *Science*, **274**, 1715-1717.

184. Huang,Q., Wang,H., Perry,S.W., Figueiredo-Pereira,M.E. (2013) Negative regulation of 26S proteasome stability via calpain-mediated cleavage of Rpn10 subunit upon mitochondrial dysfunction in neurons. *J Biol Chem*, **288**, 12161-12174.

185. Turrens,J.F. (2003) Mitochondrial formation of reactive oxygen species. *J. Physiol*, **552**, 335-344.

186. Liu,Y., Schubert,D.R. (2009) The specificity of neuroprotection by antioxidants. *J. Biomed. Sci.*, **16**, 98.

187. Stadtman,E.R., Berlett,B.S. (1998) Reactive oxygen-mediated protein oxidation in aging and disease. *Drug Metab Rev*, **30**, 225-243.

188. Schipper,H.M. (2004) Heme oxygenase-1: transducer of pathological brain iron sequestration under oxidative stress. *Ann. N. Y. Acad. Sci.*, **1012**, 84-93.

189. Akude,E., Zherebitskaya,E., Chowdhury,S.K., Smith,D.R., Dobrowsky,R.T., Fernyhough,P. (2011) Diminished superoxide generation is associated with respiratory chain dysfunction and changes in the mitochondrial proteome of sensory neurons from diabetic rats. *Diabetes*, **60**, 288-297.

190. Azzu,V., Parker,N., Brand,M.D. (2008) High membrane potential promotes alkenal-induced mitochondrial uncoupling and influences adenine nucleotide translocase conformation. *Biochem. J.*, **413**, 323-332.

191. Huang,H., Wang,H., Figueiredo-Pereira,M.E. (2013) Regulating the Ubiquitin/Proteasome Pathway Via cAMP-signaling: Neuroprotective Potential. *Cell Biochem. Biophys.*.

192. Metcalfe,M.J., Huang,Q., Figueiredo-Pereira,M.E. (2012) Coordination between proteasome impairment and caspase activation leading to TAU pathology: neuroprotection by cAMP. *Cell Death Dis.*, **3**, e326.

193. Ellington,W.R. (2001) Evolution and physiological roles of phosphagen systems. *Annu. Rev. Physiol*, **63**, 289-325.

194. Kurosawa,Y., Degrauw,T.J., Lindquist,D.M., Blanco,V.M., Pyne-Geithman,G.J., Daikoku,T., Chambers,J.B., Benoit,S.C., Clark,J.F. (2012) Cyclocreatine treatment improves cognition in mice with creatine transporter deficiency. *J Clin. Invest*, **122**, 2837-2846.

195. Kahns,S., Lykkebo,S., Jakobsen,L.D., Nielsen,M.S., Jensen,P.H. (2002) Caspase-mediated parkin cleavage in apoptotic cell death. *J Biol Chem*, **277**, 15303-15308.

196. Kahns,S., Kalai,M., Jakobsen,L.D., Clark,B.F., Vandenabeele,P., Jensen,P.H. (2003) Caspase-1 and caspase-8 cleave and inactivate cellular parkin. *J. Biol. Chem.*, **278**, 23376-23380.

197. Thorpe,J.A., Christian,P.A., Schwarze,S.R. (2008) Proteasome inhibition blocks caspase-8 degradation and sensitizes prostate cancer cells to death receptor-mediated apoptosis. *Prostate*, **68**, 200-209.

198. Laussmann,M.A., Passante,E., Hellwig,C.T., Tomiczek,B., Flanagan,L., Prehn,J.H., Huber,H.J., Rehm,M. (2012) Proteasome inhibition can impair caspase-8 activation upon submaximal stimulation of apoptotic tumor necrosis factor-related apoptosis inducing ligand (TRAIL) signaling. *J Biol Chem*, **287**, 14402-14411.

199. Zong,W.X., Thompson,C.B. (2006) Necrotic death as a cell fate. *Genes Dev.*, **20**, 1-15.

200. Orrenius,S., Zhivotovsky,B., Nicotera,P. (2003) Regulation of cell death: the calcium-apoptosis link. *Nat. Rev. Mol. Cell Biol*, **4**, 552-565.

201. Sorimachi,H., Ono,Y. (2012) Regulation and physiological roles of the calpain system in muscular disorders. *Cardiovasc. Res.*, **96**, 11-22.

202. Liu,Z., Cao,J., Gao,X., Ma,Q., Ren,J., Xue,Y. (2011) GPS-CCD: a novel computational program for the prediction of calpain cleavage sites. *PLoS. ONE.*, **6**, e19001.

203. DuVerle,D.A., Ono,Y., Sorimachi,H., Mamitsuka,H. (2011) Calpain cleavage prediction using multiple kernel learning. *PLoS. ONE.*, **6**, e19035.

204. Dagata,V., Cavallaro,S. (2004) Parkin transcript variants in rat and human brain. *Neurochem. Res.*, **29**, 1715-1724.

205. Mizuno,Y., Asakawa,S., Suzuki,T., Hattori,N., Minoshima,S., Chiba,T., Yoshino,H., Shimizu,N., Tanaka,K. (2003) In Pulst,S.-M. (ed.), *Genetics of movement disorders*. Elsevier Science, San Diego, pp. 305-314.

206. Yamamoto,A., Friedlein,A., Imai,Y., Takahashi,R., Kahle,P.J., Haass,C. (2005) Parkin phosphorylation and modulation of its E3 ubiquitin ligase activity. *J. Biol. Chem.*, **280**, 3390-3399.

207. Boudreau,R.T., Hoskin,D.W. (2005) The use of okadaic acid to elucidate the intracellular role(s) of protein phosphatase 2A: lessons from the mast cell model system. *Int. Immunopharmacol.*, **5**, 1507-1518.

208. Gong,C.X., Lidsky,T., Wegiel,J., Zuck,L., Grundke-Iqbal,I., Iqbal,K. (2000) Phosphorylation of microtubule-associated protein tau is regulated by protein phosphatase 2A in mammalian brain. Implications for neurofibrillary degeneration in Alzheimer's disease. *J. Biol. Chem.*, **275**, 5535-5544.

209. Perier,C., Bove,J., Vila,M. (2012) Mitochondria and programmed cell death in Parkinson's disease: apoptosis and beyond. *Antioxid. Redox. Signal.*, **16**, 883-895.

210. Schlossmacher,M.G., Frosch,M.P., Gai,W.P., Medina,M., Sharma,N., Forno,L., Ochiishi,T., Shimura,H., Sharon,R., Hattori,N., *et al.* (2002) Parkin localizes to the Lewy bodies of Parkinson disease and dementia with Lewy bodies. *Am. J. Pathol.*, **160**, 1655-1667.

211. Shimura,H., Hattori,N., Kubo,S., Yoshikawa,M., Kitada,T., Matsumine,H., Asakawa,S., Minoshima,S., Yamamura,Y., Shimizu,N., Mizuno,Y. (1999) Immunohistochemical and subcellular localization of Parkin protein: absence of protein in autosomal recessive juvenile parkinsonism patients. *Ann Neurol*, **45**, 668-672.

212. Beal,M.F. (2011) Neuroprotective effects of creatine. *Amino. Acids*, **40**, 1305-1313.

213. Livnat-Levanon,N., Glickman,M.H. (2011) Ubiquitin-proteasome system and mitochondria - reciprocity. *Biochim. Biophys. Acta*, **1809**, 80-87.

214. Ding,Q., Dimayuga,E., Keller,J.N. (2006) Proteasome regulation of oxidative stress in aging and age-related diseases of the CNS. *Antioxid. Redox. Signal.*, **8**, 163-172.

215. Stranahan,A.M., Mattson,M.P. (2012) Recruiting adaptive cellular stress responses for successful brain ageing. *Nat. Rev. Neurosci.*, **13**, 209-216.

216. Reddy,P.H. (2007) Mitochondrial dysfunction in aging and Alzheimer's disease: strategies to protect neurons. *Antioxid. Redox. Signal.*, **9**, 1647-1658.

217. Beal,M.F. (2005) Mitochondria take center stage in aging and neurodegeneration. *Ann. Neurol.*, **58**, 495-505.

218. Bedford,L., Paine,S., Rezvani,N., Mee,M., Lowe,J., Mayer,R.J. (2009) The UPS and autophagy in chronic neurodegenerative disease: six of one and half a dozen of the other--or not? *Autophagy.*, **5**, 224-227.

219. Nicholls,D.G. (2008) Oxidative stress and energy crises in neuronal dysfunction. *Ann. N. Y. Acad. Sci.*, **1147**, 53-60.

220. Mosconi,L., Pupi,A., De Leon,M.J. (2008) Brain glucose hypometabolism and oxidative stress in preclinical Alzheimer's disease. *Ann. N. Y. Acad. Sci.*, **1147**, 180-195.

221. Hoyer,S. (1992) Oxidative energy metabolism in Alzheimer brain. Studies in early-onset and late-onset cases. *Mol. Chem. Neuropathol.*, **16**, 207-224.

222. Liu,C.W., Li,X., Thompson,D., Wooding,K., Chang,T.L., Tang,Z., Yu,H., Thomas,P.J., DeMartino,G.N. (2006) ATP binding and ATP hydrolysis play distinct roles in the function of 26S proteasome. *Mol. Cell*, **24**, 39-50.

223. Zhu,X., Perry,G., Smith,M.A., Wang,X. (2012) Abnormal Mitochondrial Dynamics in the Pathogenesis of Alzheimer's Disease. *J. Alzheimers. Dis.*.

224. Shang,F., Taylor,A. (2011) Ubiquitin-proteasome pathway and cellular responses to oxidative stress. *Free Radic. Biol. Med.*, **51**, 5-16.

225. Shringarpure,R., Grune,T., Mehlhase,J., Davies,K.J. (2003) Ubiquitin conjugation is not required for the degradation of oxidized proteins by proteasome. *J. Biol. Chem.*, **278**, 311-318.

226. Shang,F., Nowell,T.R., Jr., Taylor,A. (2001) Removal of oxidatively damaged proteins from lens cells by the ubiquitin-proteasome pathway. *Exp. Eye Res.*, **73**, 229-238.

227. Lin,M.T., Beal,M.F. (2006) Mitochondrial dysfunction and oxidative stress in neurodegenerative diseases. *Nature*, **443**, 787-795.

228. Dasuri,K., Ebenezer,P.J., Zhang,L., Fernandez-Kim,S.O., Uranga,R.M., Gavilan,E., Di,B.A., Keller,J.N. (2010) Selective vulnerability of neurons to acute toxicity after proteasome inhibitor treatment: implications for oxidative stress and insolubility of newly synthesized proteins. *Free Radic. Biol. Med.*, **49**, 1290-1297.

229. Grune,T., Jung,T., Merker,K., Davies,K.J. (2004) Decreased proteolysis caused by protein aggregates, inclusion bodies, plaques, lipofuscin, ceroid, and 'aggresomes' during oxidative stress, aging, and disease. *Int. J. Biochem. Cell Biol.*, **36**, 2519-2530.

230. Aiken,C.T., Kaake,R.M., Wang,X., Huang,L. (2011) Oxidative stress-mediated regulation of proteasome complexes. *Mol. Cell Proteomics.*, **10**, R110.

231. Grimm,S., Hoehn,A., Davies,K.J., Grune,T. (2011) Protein oxidative modifications in the ageing brain: consequence for the onset of neurodegenerative disease. *Free Radic. Res.*, **45**, 73-88.

232. Jha,N., Kumar,M.J., Boonplueang,R., Andersen,J.K. (2002) Glutathione decreases in dopaminergic PC12 cells interfere with the ubiquitin protein degradation pathway: relevance for Parkinson's disease? *J Neurochem.*, **80**, 555-561.

233. Huang,L.S., Cobessi,D., Tung,E.Y., Berry,E.A. (2005) Binding of the respiratory chain inhibitor antimycin to the mitochondrial bc1 complex: a new crystal structure reveals an altered intramolecular hydrogen-bonding pattern. *J. Mol. Biol.*, **351**, 573-597.

234. Berridge,M.V., Tan,A.S. (1993) Characterization of the cellular reduction of 3-(4,5-dimethylthiazol-2-yl)-2,5-diphenyltetrazolium bromide (MTT): subcellular localization, substrate dependence, and involvement of mitochondrial electron transport in MTT reduction. *Arch. Biochem. Biophys.*, **303**, 474-482.

235. Liu,Y., Peterson,D.A., Kimura,H., Schubert,D. (1997) Mechanism of cellular 3-(4,5-dimethylthiazol-2-yl)-2,5-diphenyltetrazolium bromide (MTT) reduction. *J. Neurochem.*, **69**, 581-593.

236. Rego,A.C., Vesce,S., Nicholls,D.G. (2001) The mechanism of mitochondrial membrane potential retention following release of cytochrome c in apoptotic GT1-7 neural cells. *Cell Death. Differ.*, **8**, 995-1003.

237. Oddo,S. (2008) The ubiquitin-proteasome system in Alzheimer's disease. *J. Cell Mol. Med.*, **12**, 363-373.

238. Shibata,T., Yamada,T., Kondo,M., Tanahashi,N., Tanaka,K., Nakamura,H., Masutani,H., Yodoi,J., Uchida,K. (2003) An endogenous electrophile that modulates the regulatory mechanism of protein turnover: inhibitory effects of 15-deoxy-delta(12,14)-prostaglandin J2 on proteasome. *Biochemistry*, **42**, 13960-13968.

239. Jahngen-Hodge,J., Obin,M.S., Gong,X., Shang,F., Nowell,T.R.J., Gong,J., Abasi,H., Blumberg,J., Taylor,A. (1997) Regulation of ubiquitin-conjugating enzymes by glutathione following oxidative stress. *J Biol Chem*, **272**, 28218-28226.

240. Eytan,E., Ganoth,D., Armon,T., Hershko,A. (1989) ATP-dependent incorporation of 20S protease into the 26S complex that degrades proteins conjugated to ubiquitin. *Proc Natl Acad Sci U S A*, **86**, 7751-7755.

241. Goldberg,A.L. (2007) Functions of the proteasome: from protein degradation and immune surveillance to cancer therapy. *Biochem. Soc. Trans.*, **35**, 12-17.

242. Wang,K.K. (2000) Calpain and caspase: can you tell the difference? *Trends Neurosci.*, **23**, 20-26.

243. Binder,L.I., Guillozet-Bongaarts,A.L., Garcia-Sierra,F., Berry,R.W. (2005) Tau, tangles, and Alzheimer's disease. *Biochim. Biophys. Acta*, **1739**, 216-223.

244. Vitale,M., Zamai,L., Mazzotti,G., Cataldi,A., Falcieri,E. (1993) Differential kinetics of propidium iodide uptake in apoptotic and necrotic thymocytes. *Histochemistry*, **100**, 223-229.

245. Breeuwer,P., Drocourt,J.L., Bunschoten,N., Zwietering,M.H., Rombouts,F.M., Abee,T. (1995) Characterization of uptake and hydrolysis of fluorescein diacetate and carboxyfluorescein diacetate by intracellular esterases in Saccharomyces cerevisiae, which result in accumulation of fluorescent product. *Appl. Environ. Microbiol.*, **61**, 1614-1619.

246. Rinaldi,T., Ricordy,R., Bolotin-Fukuhara,M., Frontali,L. (2002) Mitochondrial effects of the pleiotropic proteasomal mutation mpr1/rpn11: uncoupling from cell cycle defects in extragenic revertants. *Gene*, **286**, 43-51.

247. Sullivan,P.G., Dragicevic,N.B., Deng,J.H., Bai,Y., Dimayuga,E., Ding,Q., Chen,Q., Bruce-Keller,A.J., Keller,J.N. (2004) Proteasome inhibition alters neural mitochondrial homeostasis and mitochondria turnover. *J. Biol. Chem.*, **279**, 20699-20707.

248. Papa,L., Rockwell,P. (2008) Persistent mitochondrial dysfunction and oxidative stress hinder neuronal cell recovery from reversible proteasome inhibition. *Apoptosis.*, **13**, 588-599.

249. Sun,X.M., Butterworth,M., MacFarlane,M., Dubiel,W., Ciechanover,A., Cohen,G.M. (2004) Caspase activation inhibits proteasome function during apoptosis. *Mol. Cell*, **14**, 81-93.

250. Glickman,M.H., Rubin,D.M., Coux,O., Wefes,I., Pfeifer,G., Cjeka,Z., Baumeister,W., Fried,V.A., Finley,D. (1998) A subcomplex of the proteasome regulatory particle required for ubiquitin-conjugate degradation and related to the COP9-signalosome and eIF3. *Cell*, **94**, 615-623.

251. Verma,R., Oania,R., Graumann,J., Deshaies,R.J. (2004) Multiubiquitin chain receptors define a layer of substrate selectivity in the ubiquitin-proteasome system. *Cell*, **118**, 99-110.

252. Sakata,E., Bohn,S., Mihalache,O., Kiss,P., Beck,F., Nagy,I., Nickell,S., Tanaka,K., Saeki,Y., Forster,F., Baumeister,W. (2012) Localization of the proteasomal

ubiquitin receptors Rpn10 and Rpn13 by electron cryomicroscopy. *Proc. Natl. Acad. Sci. U. S. A*, **109**, 1479-1484.

253. Chandra,A., Chen,L., Madura,K. (2010) Synthetic lethality of rpn11-1 rpn10Delta is linked to altered proteasome assembly and activity. *Curr. Genet.*, **56**, 543-557.

254. Huber,N., Sakai,N., Eismann,T., Shin,T., Kuboki,S., Blanchard,J., Schuster,R., Edwards,M.J., Wong,H.R., Lentsch,A.B. (2009) Age-related decrease in proteasome expression contributes to defective nuclear factor-kappaB activation during hepatic ischemia/reperfusion. *Hepatology*, **49**, 1718-1728.

255. Shell,J.R., Lawrence,D.S. (2012) Proteolytic regulation of the mitochondrial cAMP-dependent protein kinase. *Biochemistry*, **51**, 2258-2264.

256. Liu,M.C., Kobeissy,F., Zheng,W., Zhang,Z., Hayes,R.L., Wang,K.K. (2011) Dual vulnerability of tau to calpains and caspase-3 proteolysis under neurotoxic and neurodegenerative conditions. *ASN. Neuro.*, **3**, e00051.

257. Garg,S., Timm,T., Mandelkow,E.M., Mandelkow,E., Wang,Y. (2011) Cleavage of Tau by calpain in Alzheimer's disease: the quest for the toxic 17 kD fragment. *Neurobiol. Aging.*, **32**, 1-14.

258. Ferreira,A., Bigio,E.H. (2011) Calpain-mediated tau cleavage: a mechanism leading to neurodegeneration shared by multiple tauopathies. *Mol. Med.*, **17**, 676-685.

259. Pacifici,R.E., Salo,D.C., Davies,K.J. (1989) Macroxyproteinase (M.O.P.): a 670 kDa proteinase complex that degrades oxidatively denatured proteins in red blood cells [published erratum appears in Free Radic Biol Med 1990;8(2):211-2]. *Free Radic Biol Med*, **7**, 521-536.

260. Pickering,A.M., Koop,A.L., Teoh,C.Y., Ermak,G., Grune,T., Davies,K.J. (2010) The immunoproteasome, the 20S proteasome and the PA28alphabeta proteasome regulator are oxidative-stress-adaptive proteolytic complexes. *Biochem J*, **432**, 585-594.

261. Reinheckel,T., Sitte,N., Ullrich,O., Kuckelkorn,U., Davies,K.J., Grune,T. (1998) Comparative resistance of the

20S and 26S proteasome to oxidative stress. *Biochem J*, **335 (Pt 3)**, 637-642.

262. Kastle,M., Grune,T. (2011) Proteins bearing oxidation-induced carbonyl groups are not preferentially ubiquitinated. *Biochimie*, **93**, 1076-1079.

263. Jain,S., Wood,N.W., Healy,D.G. (2005) Molecular genetic pathways in Parkinson's disease: a review. *Clin. Sci. (Lond)*, **109**, 355-364.

264. Przedborski,S. (2005) Pathogenesis of nigral cell death in Parkinson's disease. *Parkinsonism. Relat Disord.*, **11 Suppl 1**, S3-S7.